Vibrational Spectroscopic Detection of Beta- and Gamma-Turns in Synthetic and Natural Peptides and Proteins

Elemér Vass,[†] Miklós Hollósi,*[,†] Françoise Besson,[‡] and René Buchet[‡]

Department of Organic Chemistry, Eötvös Loránd University, H-1518 Budapest 112, P.O. Box 32, Hungary, and Université Claude Bernard—Lyon I, U. F. R. Chimie Biochimie, 69622 Villeurbanne, Cedex, France

Received May 6, 2002

Contents

1. Introduction

The final goal of functional genomics is to determine the biological role for all of the genes in a cell. At present, the genome-scale prediction of protein function is based primarily on the recognition of sequence homology using various sequence similarity analyzing tools. With this approach, the prediction of "function" is based on homology with proteins of known function, irrespective of any knowledge of 3D structure.[1,2] In general, the missing link between sequence and function is the knowledge of the detailed 3D structure.

There are four levels of protein structure. The first level is the sequence or primary structure which can be derived today easily from the polynucleotide sequence that codes the consecutive amino acid residues in a polypeptide chain. The next level, the secondary structure or conformation, refers to the arrangement of the backbone of the polypeptide chain (Figure 1). Examples of regular arrangement are the α-helix, β-sheet, and turns. The folding of segments of secondary structures into a compact molecule is called the tertiary structure. Proteins composed of more than one polypeptide chain which are arranged in a regular manner also show a fourth level of organization, the quaternary structure.

Protein structural families in several databases are organized according to both evolutionary relationship and common folding arrangements. Most structure classifications of proteins are based on domain similarities. The ~12 000 protein chains deposited in the Brookhaven Protein Data Bank (PDB) give rise to about 16 000 domains. The number of fold groups, currently recognized as similar, is at around 700. Ten highly populated fold groups, associated with three or more functions, were described as superfolds. Structural classification is based on the content of the main types of periodic secondary structures, the α-helix, and the β-sheet. Four classes are distinguished: mainly α, mainly β, mixed $\alpha\beta$, and low secondary structure. It is the mixed $\alpha\beta$ class which contains the greatest number of homologous families.[3]

Today predictive methods[4] serve to bridge the gap between the size of the protein sequence databases and structure databases. There are roughly 10 times more entries in non-redundant protein sequence databases than in the structure database PDB. After the success of the human genom project and with the rapid increase in the number of deciphered genoms, structure prediction is expected to become an indispensable tool of the analysis and identification of unknown proteins.[5] The most complex and technically demanding task is the tertiary structure predic-

* To whom correspondence should be addressed.
[†] Eötvös Loránd University.
[‡] Université Claude Bernard—Lyon I.

10.1021/cr000100n CCC: $44.00
Published on Web 04/16/2003

Elemér Vass was born in Târgu-Mureş, Romania, in 1965. He studied chemistry at the Faculty of Chemistry and Chemical Engineering of the Babeş-Bolyai University of Cluj, Romania, where he graduated as a chemical engineer in 1990. In the same year he moved to Budapest, Hungary, where he joined the organic sulfur chemistry group of Professor Árpád Kucsman at the Department of Organic Chemistry of the Eötvös Loránd University. Between 1990 and 1997 he studied, under the guidance of Prof. Ferenc Ruff, the mechanism of hydrolysis reaction of spiro-λ^4-sulfanes with O-S(IV)-O and N-S(IV)-O axial bond systems, receiving a Ph.D. degree in 1997. Since 1994 he has collaborated with the chiroptical spectroscopy group of Prof. Miklós Hollósi, and his research has focused on the FTIR and CD spectroscopic investigation of H-bonded folded polypeptide structures, especially β- and γ-turns occurring in small and midsize cyclic and linear peptides and peptide derivatives, resulting in more than 20 publications in this field. His recent interests also include molecular modeling. Today he is assistant professor at the Department of Organic Chemistry of the Eötvös Loránd University, giving lectures on IR and UV spectroscopy and coordinating special laboratory courses on organic spectroscopy for chemistry students.

Françoise Besson was born in 1951 in Mâcon, France. She received her B.Sc. degree in chemistry (1973) from the University of Dijon and her Ph.D. degree (1977) under the supervision of Professor Georges Michel from the University of Lyon I. She began her academic career in 1979 as a CNRS researcher in the Laboratoire de Biochimie Microbienne, University of Lyon I. Her research interests were the isolation of new natural cyclic lipopeptides from *Bacillus subtilis*. Five antifungal compounds containing β-amino fatty acid were isolated, and their conformational analysis showed that they are stabilized by turns. She is currently investigating the organization of natural and biomimetic lipid raft membranes in the Laboratoire de Physico-chimie Biologique, University of Lyon I.

tion. It is well-known that while sequence may specify conformation, the same conformation may be specified by multiple sequences. Thus, similarities between proteins may not necessarily be detected through traditional sequence-based methods. Deducing the relationship between sequence and structure is at the root of the "protein-folding problem".[6]

Miklós Hollósi was born in Budapest, Hungary, in 1941. He studied chemistry at the Faculty of Natural Sciences of Eötvös Loránd University (ELU) in Budapest. After receiving a Ph.D. in organic chemistry under the supervision of Prof. Viktor Bruckner in 1967, he joined the Department of Organic Chemsitry of ELU. Since 1990 he has been Professor and, since 1993, head of the Department of Organic Chemistry of ELU. In 1971–72 he conducted postdoctoral studies under the direction of Professor Theodor Wieland in Max-Planck-Institut für Medizinische Forschung Abteilung Naturstoff Chemie in Heidelberg, Germany. As a visiting research associate, he worked in the Graduate Department of Biochemistry of Brandeis University, Waltham, MA, with Professor Gerald D. Fasman in 1983 and 1986. He spent a year as a visiting professor at the Wistar Institute, Philadelphia. He is a member of the European and American Peptide Societies. He received the Award of ELU (1990) and the Award of the Hungarian Academy of Sciences (1996). He became a Doctor of Chemical Sciences (D.Sc.) in 1990 and a member of the Hungarian Academy of Sciences in 1998. He started his scientific carrier as a synthetic chemist dealing with the synthesis of cyclopeptides, glycopeptides, phosphopeptides, and thiopeptides. After 1975 he became interested in chiroptical spectroscopy and the conformational analysis of peptides and proteins. He developed a combined CD and FTIR spectroscopic method for the conformational screening of flexible polypeptides. At ELU he lectures on natural products chemistry, stereochemistry, chiroptical spectroscopy and structural biology. Since 1991 he has been head of the Chiroptical and Vibrational Spectroscopic Laboratory of ELU.

René Buchet graduated in 1986 from the University of Montreal (Ph.D. in chemistry) under the supervision of Professor Camille Sandorfy. After a postdoctoral stay from 1986 to 1987 at the University of Alabama in Birmingham with Professor Dan W. Urry, he joined the Professor Anthony Martonosi's group at the Health Science Center of SUNY, Syracuse, NY, where he was Research Assistant Professor from 1987 to 1990. He then was a research scientist in Professor Urs Peter Fringeli's group at the ETH, Zürich. Finally in 1992, he went to the University of Lyon I, where he is currently a professor of Biochemistry. His research interests are molecular spectroscopy and conformations of membrane proteins.

In addition to the α-helix and β-sheet structures, the third group of ordered or regular secondary structures of proteins is turns. β-Turns (β-bends,

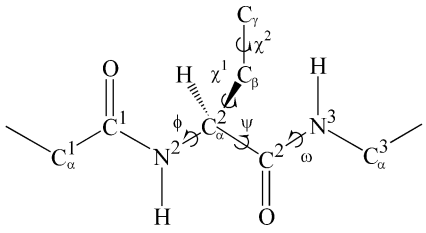

Figure 1. Torsion angles (ϕ, ψ, ω, and χ) defining the backbone and side-chain conformation of an amino acid residue.

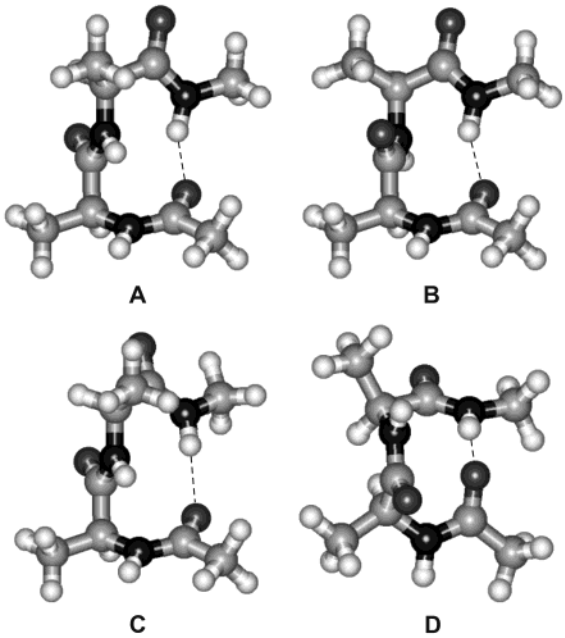

Figure 2. β-Turns type I (A), type II (B), type III (C), and type VIa (D) featuring a 1←4 (C_{10}) intramolecular H-bond. For standard torsion angles, see Table 1.

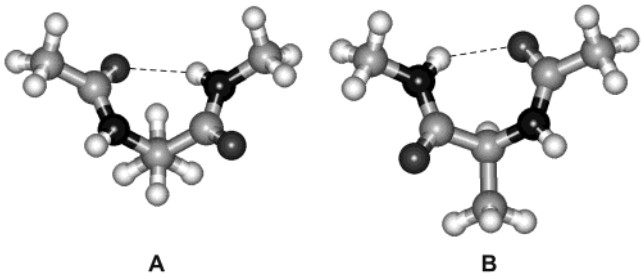

Figure 3. Classic (A) and inverse (B) γ-turns with a 1←3 (C_7^{ax} or C_7^{eq}) intramolecular H-bond. For standard torsion angles, see Table 1.

reverse turns) form the most abundant and best-characterized group of folded secondary structures.[7] They comprise four amino acid residues connected by three amide groups. About three-quarter of tight turns feature a 1←4 (C_{10}) H-bonding between the backbone CO(i) and NH(i + 3) groups (Figure 2). γ-Turns containing only three amino acid residues have been identified by X-ray crystallographic studies.[8] The 1←3 (C_7) H-bonding present in many γ-turns is formed between the backbone CO(i) and NH(i+2) groups (Figure 3). Recent X-ray diffraction analysis has revealed the existence of α-turns, another group of folded polypeptide conformations containing five amino acid residues with one intramolecular H-bonding (IHB).[9] Less frequently occurring secondary structural motifs of proteins are bulges[7] and loops.[10] More details concerning folded polypeptide conformations will be presented in section 4.

Circular dichroism (CD) spectroscopy, the most widely used chiroptical method, has an extreme sensitivity toward protein secondary structures.[11] CD spectroscopy was the first method which delivered reliable data on the secondary structure of proteins in solution, in the first place on the ratio of the α-helix and β-sheet conformations.[12] On the basis of comparative X-ray crystallographic and spectroscopic studies on models, the two major families of β-turns, type I/III and type II, have different chiral contributions.[13] The chiral characterization of γ- and α-turns and other less frequently occurring folded structures (turns featuring a cis amide bond, loops, etc.) awaits further studies.

Vibrational spectroscopy is the method of choice for detecting and characterizing H-bonded polypeptide conformations. The amide group gives rise to several strong IR bands, the fine structure of which depends on the various types of H-bonded secondary structures and their relative amounts.[14]

In recent years, intensive efforts have been made to develop peptidomimetics that display more favorable pharmacological properties than their biologically active peptide prototypes. The most promising approach of the design and synthesis of peptidomimetics is the imitation of certain secondary structures, in the first place turns.[15] Biophysical investigations are necessary to compare the conformation of the mimetic with that of the parent peptide and to monitor the conformational stability of the mimetic in different biological environments.

This review is aimed at summarizing the main forms of application of vibrational spectroscopy for conformational characterization of peptides and proteins with special emphasis on the detection of H-bondings in turns. The focus of many reviews[14] was the characterization of overall protein structure by FTIR spectroscopy. The limitations and advantages of approaches based on curve-fitting analysis of bands or pattern recognition have been described[14] and will not be commented here. Our work covering the period between ∼1990 and 2002 summarizes the basic knowledge of vibrational spectroscopy and its forms of application for proteins, peptides, and their derivatives.

2. Classification of Protein Secondary Structures

Our knowledge on protein secondary structures is based on the X-ray structure of an increasing number of proteins.[7,16] The most stable and frequent types of regular, periodic secondary structures are the α-helix and the parallel and antiparallel β-pleated sheets. The 3_{10}-helix is rare: it occurs in short helical segments at the end of α-helices rather than in the interior of long helical segments. The formation of 3_{10}-helix is favored by α-amino isobutyric acid (Aib) residues.[17] The hypothetic γ-helix of Pauling has not been detected in proteins; the occurrence of other (distorted) helical structures is not frequent either.

Table 1. Ordered (Regular) Polypeptide Secondary Structures

	torsion angles (deg)		
	ϕ (deg)	ψ (deg)	ref
	Periodic		
α-helix (right-handed 3.6_{13}-helix)	−48	−57[a]	*i*
	−45	−55[b]	*i*
3_{10}-helix[c]	−60	−30	*j*
β-pleated sheet (β-strand or β-structure)			*k*
parallel	−139	135	
antiparallel	−119	113	
polyproline II (left-handed extended helix, PPII)	−78	149	*k*
	Aperiodic		
β-turn[d], type I	−60	$-30\ (i+1)\ \tau^{h} = 45$	24, 65
	−90	$0\ (i+2)$	
β-turn[d], type II	−60	$120\ (i+1)\ \tau = 1$	
	80	$0\ (i+2)$	
β-turn, type III	−60	$-30\ (i+1)\ \tau = 65$	24, 65
	−60	$-30\ (i+2)$	
β-turn, type VIa[e]	−60	$120\ (i+1)\ \tau = -4$	24, 65
	−90	$0\ (i+2)$	
β-turn, type VIb[e]	−120	$120\ (i+1)\ \tau = -7$	24, 65
	−60	$0\ (i+2)$	
β-turns, other types[f]			66
γ-turn, inverse[g]	−70 to −85	60 to 70 $(i+1)$	8
γ-turn, classic[g]	70 to 85	−60 to −70 $(i+1)$	8

[a] Pauling and Corey helix. [b] Standard α-helix. [c] Repeats of type III β-turns. [d] Standard β-turns; types I′−III′ turns have a mirror image backbone conformation with oppositely signed torsion angles. [e] With a cis peptide bond between residues $i+1$ and $i+2$. [f] Open or distorted β-turns. [g] Periodicity cannot be defined. [h] For the definition of τ, see ref 70. [i] Manning, M. C.; Illangasekare, M.; Woody, R. W. *Biophys. Chem.* **1988**, *31*, 77. [j] Dyson, H. J.; Wright, P. E. *Ann. Rev. Biophys. Biochem. Chem.* **1991**, *20*, 519. [k] Stern, L. K.; Brown, J. H.; Jardeczky, T. S.; et al. *Nature* **1994**, *368*, 215.

Another abundant structure is the β-turn (β-bend, reverse turn), which has many types (section 4).[7,18] On the basis of X-ray crystallography, γ- and α-turns also have a significant frequency of occurrence in globular proteins.[8,9]

The fourth group of protein secondary structures is the unordered or random coil conformation. The existence of truly unordered structure is questioned now by both solid state and in solution studies on native proteins. In protein crystals, regions which cannot be classified as helices, β-sheet structures, or turns are rare. Several lines of evidence suggest that the "random coil", at least locally, is a left-handed helix having a structure similar to the poly(proline) II (PPII) conformation of the polypeptide chains in collagen and related proteins.[11,19] However, many of the PPII regions of proteins do not contain proline residue(s). Thus, the left-handed extended helix represents another general form of helical structures of proteins.

The polypeptide backbone of protein chains can be characterized by the average values of the ϕ and ψ torsion angles (Figure 1).[7] Standard torsion angles of the periodic and aperiodic ordered secondary structures are given in Table 1. However, the torsion angles of secondary structures in real proteins are far from the standard values. Thus, sometimes even the assignment of protein secondary structure is problematic. At present there are two objective algorithms for assigning protein secondary structure from X-ray diffraction data. The algorithm developed by Levitt and Greer is based on patterns of backbone H-bondings, inter-C^{α} distances and inter-C^{α} torsion angles.[20] The algorithm using "relaxed" criteria usually predicts higher content of secondary structures than that by crystallographers. Kabsch and Sander used a set of "restricted" criteria for the pattern recognition process.[21] With different criteria, assignment procedures will result in different contents of secondary structures for the same set of X-ray diffraction data.

In addition to the most abundant standard helical and β-pleated sheetlike structures listed in Table 1, recent high-resolution X-ray diffraction studies have revealed the existence of a variety of distorted secondary structures such as bent helices, twisted β-strands, or β-sheets, etc. Deviations from the periodicity of the ϕ and ψ torsion angles may be due to environmental reasons, as in the case of transmembrane helices, or to sequential reasons. Repeats of certain segments in the polypeptide chain frequently give rise to secondary superstructures, a well-characterized example of which is the repeating β-sheet/β-turn conformation. Multiple (or repeating) β-turns were identified and characterized previously.[22] Continuous turns have been added to the family of secondary superstructures recently.[23] Continuous turns comprise individual γ-turns or β-turns or both that are situated immediately one after the other along the polypeptide chain. They were identified from a representative data set of 3D protein crystal structures. The continuous turns frequently observed in proteins were $\gamma\beta$, $\beta\gamma$, $\gamma\gamma$, and $\beta\beta$.

In some cases hydrophobic residues spaced at intervals of three and four residues allow two α-helices to form compact multistranded coiled-coil structures, an important element in structural proteins such as keratin and myosin. Furthermore, many proteins consist of several domains which may be regarded as the folding units of globular proteins. Frequently occurring domains (FODs) or superfolds are elements of the tertiary structure, while coiled-coils represent regular quaternary structures.

3. Methods of Conformational Analysis of Proteins and Peptides

This section gives a short summary of new techniques or improvements in the field of biophysical methods with special emphasis on their applicability for detecting and characterizing turn structures in peptides and proteins. For the vibrational spectroscopy of peptides and proteins, see section 5.

3.1. Circular Dichroism Spectroscopy

Circular dichroism (CD) spectroscopy has played a pioneering role in secondary structural analysis of polypeptides.[11,24−26] Greenfield and Fasman first proposed a quantitative method of determining protein secondary structure from CD spectra of a synthetic polypeptide, $(Lys)_n$, which can adopt three conformations under different conditions.[27] The other approach is the determination of basis spectra for a combination of secondary structures from the CD spectra of proteins of known 3D structure.[26]

Until the mid 1970s, the contribution of β-turns to the overall CD of proteins had been neglected. It was Woody who calculated the CD spectra of a wide range of β-turns, using the matrix method.[28] A variety of CD spectral types (class A−D) were predicted, but most turns in the type I and type II regions (Table 1) were calculated to give a spectrum like that (class B) observed experimentally for type II β-turns. This early theoretic prediction has proved to be correct for type II turns but not for type I. From the mid-1970s, a great number of β-turn models have been synthesized in different laboratories. Many of them, in the first place the cyclic ones, were also characterized by X-ray crystallography, NMR, vibrational spectroscopy, molecular mechanics, or molecular dynamics calculations. CD studies on the cyclic models *cyclo*(Xxx-Pro-Yyy)[24b,25] **1** (Chart 1), *cyclo*[Ala-Xxx-NH-$(CH_2)_5$-CO][29] **2**, and *cyclo*[Gly-Pro-Xxx-Gly-NH-$(CH_2)_4$-CO][13,30] **3** have revealed that models with a well-established type II β-turn give a spectrum that resembles the β-sheet spectrum, but is shifted to the red by 5−10 nm (class B). Contrary to this, the CD spectrum of the type I β-turn is similar to that of the α-helix, but the positive band at short wavelengths is weaker in the turn spectrum. The contradiction between theory and experiment was resolved by more recent theoretical calculations applying the Applequist model.[31] These calculations resulted in good description of the ππ* region of the CD spectrum: that is, the exciton "helical" (class C) CD feature of type I β-turns is in agreement with model studies.[13]

Methods using data sets of proteins with known X-ray crystallographic structure generally decompose the CD spectra into four components (α-helix, β-sheet, unordered, and turns).[32,33] Model peptides including repeating polypeptides have been suggested first to represent the CD of the different types of β-turns. A term for the β-turn (net β-turn) was first used by Chang et al.[34]

In the case of many cyclic **1**−**9** and some linear peptides, inspection of the CD spectra or deconvolution techniques using well-selected reference spectra give qualitative and semiquantitative data on the presence and "amount" (number) of the two families of β-turns. However, in the CD spectra of proteins, the contribution of β-turns is generally superimposed by the much stronger chiroptical contribution of the α-helix and β-sheet conformation.

Chart 1

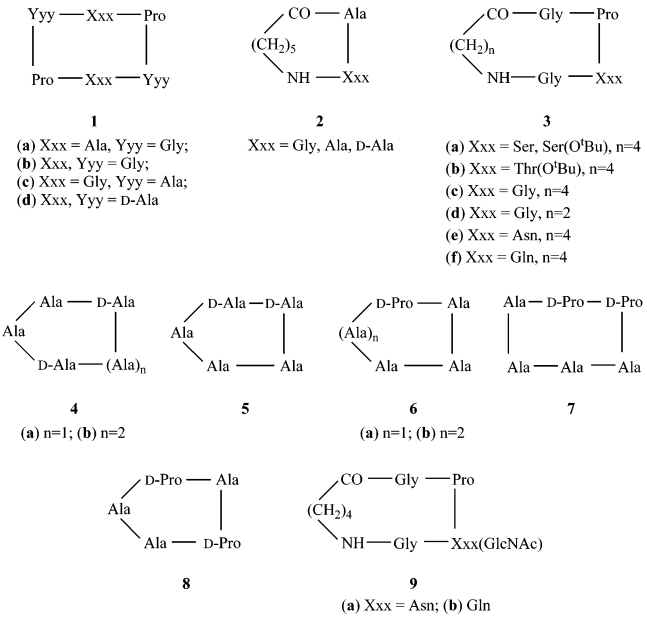

Protein secondary structural prediction became very popular by the end of the 1970s.[4] The combination of secondary structural prediction with CD curve deconvolution allows to obtain good estimates of secondary structure content of proteins.

CD is the simplest experimental tool for checking the correct folding of new proteins produced by recombinant DNA technique and for characterizing the conformational propensities and flexibility of small and midsize synthetic peptides.

3.2. X-Ray Crystallography

X-ray crystallography gives a picture at or near to atomic resolution on proteins and protein complexes of growing size and complexity. Before the mid-1990s, only a few macromolecular structures were available at high (<1.2 Å) resolution. Synchrotron sources,[35,36] efficient 2D detectors, and cryogenic freezing are vital for collecting data at atomic resolution. Protein crystals contain about 50% water, which means that the protein experiences an environment not very different from that in vivo.

Fiber diffraction is the only practical method of structure determination at the molecular level for naturally filamentous systems[37] such as DNA and complex assemblies,[38] including filamentous viruses and cytoskeletal filaments. X-ray holography[39] completes the arsenal of modern crystallographic techniques.

The number of soluble proteins with known X-ray structure exceeded 12 000 by the end of 2001. Contrary to this, only about two dozen are integral membrane proteins. This fact is disappointing if we consider that, for example, close to 40% of the 6000 gene products encoded by the genom of baker's yeast are expected to be integral membrane proteins.

Membrane proteins are difficult to crystallize. Another source of difficulties in reaching atomic resolution is radiation damage.[40]

X-ray crystallography has played a pioneering role in detecting and characterizing turn structures. Because of their conformational rigidity, cyclic peptides have been the most favored objects of X-ray crystallographic analysis.[24,25,41] This method allows not only the classification of turns but also the analysis of their distortions in cyclic models. X-ray structures at atomic resolution provide us with information on the turn type also in the case of small and midsize (<∼30 kD) proteins.

One of the biggest challenges facing X-ray crystallography is the structure determination of linear peptides. The first problem is the low tendency of linear peptides to crystallize. Further difficulties may arise from the presence of more than one conformation and, in particular, from crystal disorder. All this explains that our crystallography-based knowledge of the conformational and folding preferences of linear peptides is rather limited.

3.3. Nuclear Magnetic Resonance Spectroscopy

Nuclear magnetic resonance (NMR) spectroscopy is the most powerful method for studying the steric structure of all kinds of polypeptides (from small peptides to protein complexes) in solution. During the past decade, tremendous growth has taken place in the field of NMR spectroscopy.[42]

PDB contained more than 5600 structures of proteins determined by NMR in February 2002. The size distribution of these deposits shows that most of the proteins are in the 2−25 kD range and only few have molecular weights above 25 kD. Using the NMR techniques TROSY (transverse relaxation-optimized spectroscopy) and CRINEPT (cross-correlated relaxation-enhanced polarization transfer) in combination with suitable ^{2}H, ^{13}C, ^{15}N isotop labeling schemes, the size limit for the observation of NMR signals in solution has been extended severalfold. The application of these new techniques allows to measure high-quality NMR spectra of proteins with molecular sizes beyond 100 kDa.[43−45]

Heteronuclear NMR spin relaxation spectroscopy constitutes a powerful experimental approach for characterizing conformational dynamics of proteins in solution on picosecond/nanosecond and microsecond/millisecond time scales.[46]

High-resolution NMR spectroscopy of biomolecules is made possible by the existence of chemical shift dispersion, but the interpretation of shift tensors in terms of structure and dynamics is often difficult.[47]

The ability to apply NMR spectroscopy to both liquid- and solid-phase samples provides the opportunity for structure determination of proteins in several membrane environments.[48] Solid-state NMR (SSNMR) spectroscopy does not rely on rapid molecular reorientation for line narrowing, and therefore, it is well suited for peptides and proteins immobilized in phospholipid bilayers.[49] One of the SSNMR methods takes advantage of the favorable spectroscopic properties exhibited by uniaxially oriented samples. The other approach utilizes unoriented bilayer samples and relies on magic-angle spinning (MAS) methods for spectral resolution and for the measurement of distances via homonuclear or heteronuclear dipolar interactions.[50]

NMR spectroscopy is successfully applied for detecting and characterizing turn structures of polypeptides and proteins in solution. Similarly to X-ray crystallography, NMR has been targeted first on cyclic peptides.[13,24,25,51] Using NMR-based constraints, molecular mechanics (MM) or molecular dynamics (MD) calculations resulted in a high-resolution picture on the overall conformation of a cyclic peptide or a mixture of its conformers.[52] Contrary to X-ray crystallography, NMR experiments do not deliver sufficient information for revealing minor distortions of the standard turn structures. The most demanding task is the structure elucidation of flexible small and midsize linear peptides. Temperature-dependence studies in nonaqueous and aqueous solutions are the method of choice for monitoring conformational preferences and the dynamics of conformational transitions.

3.4. Electron Microscopy

The field of electron microscopy is experiencing a revolutionary progress because near-atomic resolution has been achieved for a number of important biological systems.[53] Today structure determinations around 20 Å are ubiquitous, those in the range of 6−9 Å are growing and those near 3 Å are becoming frequent.

Two-dimensional crystals have proved to be the most suitable for obtaining high-resolution information by electron microscopy.[54] Data at 7 Å resolution were first reported for bacteriorhodopsin. Thanks to technical and computational improvements, the structure of this molecule is known today at a 3.0 Å resolution. Electron microscopy of two-dimensional crystals has been applied primarily to membrane proteins, in which the native membrane is naturally conducive to forming planar sheets.

Due to its relatively low resolution, electron microscopy is not the method of choice today for detecting and characterizing turns. However, several electron microscopic studies of important proteins such as the H^{+}ATPase, Ca^{2+}ATPase, core protein of the hepatitis B virus or the larger papillomavirus capsid have been published since 1997 at 6−9 Å resolutions sufficient to reveal folded elements of their secondary structure.[53]

3.5. Special Techniques

Special techniques, such as small-angle scattering,[55] scanning force microscopy,[56] femtosecond laser spectroscopy,[57] and site directed spin labeling,[58] complete the arsenal of biologists in the study of complex biosystems. These techniques are often most powerful when used as a complementary tool with other structure-elucidating methods. However, the resolving power of these methods is not high enough to detect and characterize turns in proteins.

It is very difficult to determine the positions of hydrogen atoms in protein molecules using X-rays

alone. In contrast, it is well known that neutron diffraction provides an experimental tool for directly locating H-atoms. Recently Niimura and co-workers succeeded in collecting neutron diffraction data from a tetragonal hen egg-white lysozyme crystal.[59] Applying Laue diffractometry with a neutron imaging plate, the positions of 960 H atoms and 157 bound water molecules have been determined. Neutron diffraction has the potential of giving a high-resolution picture on H-atoms involved in H-bonding of folded secondary structures.

Fluorescence microscopy is an ubiquitous part of modern biology due to recent advances in immunolabeling and in situ hybridization and due to the advent of the green fluorescent protein.[60] However, like all forms of optical imaging, it is a subject to physical limits on its resolving power.

Volumetric studies can characterize the properties of molecules as a function of solution conditions, including the role of solvation. Volumetric data are uniquely sensitive to the hydration properties of nucleic acids and proteins. They provide complementary information to other techniques for defining the nature of the forces that control intra- and intermolecular recognition events modulating biomolecular processes.[61]

3.6. Methods for Exploring Early Events in Protein Folding

Due to the enormous number of degrees of freedom available to a polypeptide chain, the speed of conformational transitions and the structural complexity of the native state, protein folding is among the most complex biological processes, and it continues to fascinate theoretical and experimental biophysicists alike. The earliest conformational events related to folding, such as the formation of isolated helical segments, reverse turns, and β-hairpins, occur within microseconds or less. However, even small proteins require orders of magnitude more time in which to complete the process of folding.[62a] Thus, one of the most urgent problems in protein folding is to understand the relationship between the dynamic properties of elementary conformational events and the rate-limiting kinetic barrier in folding.[62b]

Rapid mixing, the most common method for initiating protein folding or unfolding, relies on turbulent mixing to achieve a rapid change in solvent conditions (denaturant concentration, pH, etc.). Quenched-flow or freeze-quench experiments can be coupled with many other analytical techniques, such as NMR, electron paramagnetic resonance, electrospray ionization mass spectrometry, and so on.[62c] Temperature-jump methods make use of the observation that the native structure of a protein is generally stable over only a limited temperature range and unfolding can occur at both higher and lower temperatures. The microsecond time scale can be accessed by conventional methods. More recently, IR laser methods have been developed in order to extend the time resolution into the 10 ns range. Protein folding transitions are dependent not only on temperature and solvent composition, but also on pressure (pressure-jump methods). Protein folding or unfolding can also be initiated by photochemical events (photochemical trigger).

Recent technical advances ("microfabricated devices"), ultrarapid mixing and temperature-jump techniques, in conjunction with improved detection methods,[62c] have resulted in better understanding of early structural events ("burst phase") in protein folding.

4. Turns: Definition and Classification

Turns are aperiodic or nonrepetitive motif elements of the secondary structure of proteins. Among them, β-turns and γ-turns have been studied in details. (In this review, the term "turn" is used for tight turns.[7] For related structural elements such as bulges, loops, etc., see refs 7 and 10.) α-Turns, the third group of turns, have been characterized and classified on the basis of careful analysis of X-ray crystallographic data on 190 proteins.[9] Turns play an important role from both structural and functional points of views. First, they mediate folding of the polypeptide chain into a compact globular or other tertiary structure. Second, turns usually occur on the environment-exposed surface region of proteins, and therefore, they are likely involved in cellular and molecular recognition processes and in interactions between peptide and nonpeptide substrates and receptors.[24a,25,63] However, the recognition event is not necessarily a consequence of the turn conformation. It may simply be the result of a favorable side-chain clustering which facilitates intermolecular interaction. Turns may also serve as templates for designing new molecules such as drugs, pesticides, and antigens.

According to X-ray crystallographic data on an increasing number of proteins, β-turns are the most frequent type of tight turns, which account for 25−30% of the total number of residues of the molecule.[7,13,25,63,64] β-Turns comprise four amino acid residues connected by three amide groups (Figure 2). The earliest definition and classification of β-turns by Venkatachalam[65] were based upon the presence of a 1←4 (C_{10}) H-bonding. Lewis et al. found[66] that about one-fourth of β-turns do not possess the intramolecular H-bonding (IHB) stipulated by Venkatachalam.

The other well-established subtype of tight folded structures is the γ-turns, comprising only three amino acid residues connected by two peptide groups (Figure 3). The 1←3 (C_7) IHB for a γ-turn is formed between the backbone CO(i) and NH($i + 2$) groups.[8] The possible ϕ and ψ torsion angles for H-bonded γ-turns were calculated by Némethy and Printz.[67]

The third subtype of tight turns is α-turns comprising five amino acid residues and all have an IHB.[9] Because of their lower occurrence in proteins, α-turns have received less attention than β-or γ-turns.

The classification of H-bonded β-turns is based on the ϕ and ψ torsion angles of the second ($i + 1$) and third ($i + 2$) residues involved in the turn (Table 1). Open β-turns featuring no IHB are defined by the distance, d_β, between $C^\alpha(i)-C^\alpha(i+3)$. In a β-turn d_β is less than 7 Å, and the residues involved are not constituents of an α-helix. Angularity criteria are also used to define and classify β-turns.[68−70] The angular-

ity value, τ (also called twisting parameter), is the torsion angle determined by the coordinates of the C_i, C_{i+1}, C_{i+2}, and C_{i+3} backbone atoms. According to a modified angularity criterion, τ should be in the $-90° \leq \tau \leq 90°$ range for β-turns. A recent classification using τ values is based on ab initio calculations.[70]

There are two types of γ-turns: inverse and classic γ-turns (Figure 3). γ-Turns with a strong 1←3 H-bonding are rather rare in proteins.[71] Milner-White examined 54 proteins whose structures have been determined to a resolution of ≤0.2 nm.[8] Omitting the criteria of strong H-bonds, both types of γ-turns were found to be abundant in proteins. Weakly H-bonded inverse γ-turns were shown to occur in the middle of strands of β-sheets. In this situation, they contain the H-bond system expected in a 2.2_7 helix. Classic γ-turns are generally associated with chain reversals in proteins.[8]

An intraturn H-bonding can be formed in each of the nine α-turn types. Except for type I-α_c featuring a cis peptide bond between residues $i + 1$ and $i + 2$, all the other types have trans amide bonds.[9] From 356 α-turns found in 190 proteins (221 chains), 238 (67%) are of type I-α_{RS}.

5. Infrared Spectra of Peptides and Proteins Containing β-Turns

5.1. Methodology

From methodological points of view, polypeptides, which are below the size limit of proteins, can be divided into two groups. Midsize peptides comprise more than ~10, while small peptides less than approximately 10 amino acid residues. Insulin, having two chains interconnected by disulfide bridges, comprises 53 amino acid residues and represents the borderline between midsize peptides and proteins. Above this size polypeptides, in general, have a well-defined tertiary structure even in dilute aqueous buffer solutions and can be characterized in detail by NMR spectroscopy.[43] The interpretation of NMR data for flexible small and midsize peptides must be carried out with caution. NMR is a slow method with a time scale of seconds to hundreds of seconds. Hence, conformational interconversions not requiring peptide bond rotations will result in averaged NMR parameters, the interpretation of which is of little value in terms of a single component of conformer mixtures.

From the variety of fast time-scale methods, CD spectroscopy was first used for conformational characterization of midsize peptides.[13,24,25,26] Vibrational spectroscopy [infrared (IR) and Raman] was applied from the late 1960s as a complementary approach to CD in determining polypeptide and protein secondary structures.[14,72] Like CD, vibrational spectroscopy has a fast time scale (10^{-13} s). Amide vibrations are highly sensitive to H-bonding. Amide A (NH stretching, between ~3450 and ~3300 cm^{-1}) and amide I (carbonyl stretching coupled with in-plane NH bending and CN stretching modes, around 1695−1610 cm^{-1}) bands are shifted to lower wavenumber during the formation of hydrogen bonds, while amide II (NH bending and CN stretching, around 1575−1480 cm^{-1}) band shifts to higher wavenumber. For example, a change in hydrogen bonding distance of only 0.002 Å shifts the wavenumber of the amide A band of a polypeptide by approximately 1 cm^{-1}.[73] This shift is well within the limits of detection of most IR and Raman instruments.[73] Free and hydrogen-bonded species can be visualized as separate bands in the vibrational spectra in contrast to NMR spectra where only time-averaged structures are revealed. The amide I or amide II bands appear in H_2O buffer, while the corresponding bands in D_2O buffer are termed amide I′ and amide II′, respectively. The information obtained from IR and Raman spectra may be of global type such as the secondary structure composition of a polypeptide,[14] or it can be highly specific such as alteration of individual hydrogen bonds or chemical bonds.[74] Thus vibrational techniques are of great help in not only detecting turns but also quantitating their distortions. The most intense band in the IR spectrum, the amide I band, consists of a series of overlapped component bands which occur as a result of the secondary structures present in polypeptides. The analysis of the amide I band permits to determine the secondary structures of polypeptides or proteins.[14,74−76] In the case of Raman spectra, amide I and amide III (IR inactive, CN stretching, and NH bending, around 1320−1220 cm^{-1}) bands can be used to determine the secondary structures of polypeptides.[75a,77] The experimental and theoretical basis of IR and Raman band assignments for the secondary structures of polypeptides and proteins containing random-coil, α-helix, and β-sheet structures are well established and were discussed in several IR[14,74−76] and Raman[75a,77] reviews. Although the band assignment of β-turn structures, based on theoretical[14,75] and experimental results,[13,14,78−80] is widely used, the identification of β-turn structures is not straightforward. To support the diagnostic value of vibrational spectroscopy in detecting turns, infrared evidence characteristic of β-turns will be presented in subsequent sections. There are five distinctive features more or less firmly established: (i) β-Turns absorb not only in the 1690−1660 cm^{-1} region (weakly solvated or shielded amide backbone) but also in the 1645−1635 cm^{-1} infrared region (IHB amide groups). (ii) Usually, relative intensities of β-turn bands ($I_{1690-1660}$:$I_{1645-1635}$ = 2:1−3:2) are different from those of β-sheets ($I_{1690-1660}$:$I_{1640-1620}$ = 1:10−1:8). (iii) Halogenated solvents stabilize helix-like structures, including turns and destabilize β-sheets, permitting better discrimination of the β-sheet from turn structures. (iv) Proton donor solvents (H_2O or TFE) solvate differently amide groups involved in turns. They tend to promote the formation of bifurcated H-bonds (one carbonyl group accepting two hydrogens) or H-bonds between amide groups and solvent molecules, shifting the amide I bands to lower wavenumbers. Proton acceptor solvents (in the first place DMSO used in NMR spectroscopy) tend to break H-bonds between the carbonyl and NH groups of peptide backbone but allow inverse bifurcation (two acceptor and one donor), causing a shift to higher wavenumbers. (v) The IHB amide carbonyl of γ-turns absorbs at low-wavenumber

range, around 1635−1620 cm^{-1}, while that of β-turns between 1645 and 1635 cm^{-1}.

The joint use of spectroscopic methods such as CD, Raman, and VCD is useful to confirm the presence of turn structures.

5.2. Detection of β-Turns in Small Peptides

Small peptides are useful structural models. They can be easily synthesized and characterized by several spectroscopic methods. In addition, detailed molecular mechanics or molecular dynamics calculations can be performed to assist in turn-to-sequence assignments. Generally, IR bands appearing between 1690 and 1660 cm^{-1} in the spectrum of polypeptides in D_2O or H_2O have been assigned to β-turns.[14,75] This spectral region comprises absorptions of weakly solvated or shielded amide carbonyls which are not involved in H-bonds. A β-turn comprises three amide groups from which the first one accepts the 1←4 IHB occurring in many well-defined β-turns (Figure 2). The other two amide groups point outward and experience an environment that, in the case of in solution spectra, is basically determined by the side chains of residues in the $i + 1$ and $i + 2$ position and the nature of the solvent. Consequently, the position of amide I band of the first acceptor carbonyl (around 1645−1635 cm^{-1}) should differ from that of the other two amide groups (1690−1660 cm^{-1}). On the basis of their relative populations and assuming that each band reflects distinct population of carbonyl groups, the relative amide I intensity $I_{1690-1660}$:$I_{1645-1635}$ should be near 2:1. Proton donor solvents may shift the amide I band of the first acceptor carbonyl to lower wavenumbers below 1635 cm^{-1}.

IR spectra on many cyclic **3**−**9**, **36a** (section 5.4), and linear peptides **10**−**13** (Tables 2 and 3 and Chart 2) have given support to the proposal that the characteristic acceptor amide I band of H-bonded type I and II β-turns appears near 1640 cm^{-1} in D_2O, $CHCl_3$, and DMSO[79,81] (see also section 5.4). For example the intensity ratio of the high-wavenumber bands to the 1642 cm^{-1} one in the spectrum of **3** is close to 3:2, reflecting three free and two associated carbonyl groups (Figure 4A). In halogenated alcohols (e.g., TFE) the acceptor band may be shifted below 1635 cm^{-1}.[79] Under favorable structural and solvational conditions, the population of H-bonded β-turns is high enough even in small linear peptides[13,79] to give rise to a β-turn band of well-defined position and intensity. Indeed, β-turns in small peptides containing Pro residues may absorb not only above ∼1660 cm^{-1} but also in the 1628−1632 cm^{-1} region.[79] The amide A region (Table 2) indicates populations of free (characterized by the 3460−3410 cm^{-1} band) and hydrogen-bonded (characterized by the 3380−3300 cm^{-1} bands) NH groups of peptide backbone.

3_{10} helices are repeats of type III β-turns having a C═O···H−N geometry similar to that in type I β-turns. The assignment to 3_{10}-helix of a 1660−1662 cm^{-1} component band is based on the structure of α-amino isobutyric acid (Aib) peptides determined by X-ray crystallography.[17] On the basis of experimental evidence from electron diffraction photographs and Raman and polarized IR spectra, the 3_{10} helix is the preferred conformation of poly(Aib)$_n$.[17b] The amide I band of poly(Aib)$_n$ in a 3_{10}-helical structure was calculated to absorb at 1665 cm^{-1} while type III β-turns at 1686 and 1646 ± 3 cm^{-1}.[82]

IR spectra of a series of protected Aib peptides were reported.[17b,83] The IR spectra of **14**−**20** showed an amide I band between 1666 and 1662 cm^{-1}, which was assigned to the C_{10} IHB system of the 3_{10}-helix.[17b] This-wavenumber range, together with the position of the amide II at 1533−31 cm^{-1}, agrees well with the calculated wavenumbers of Krimm and Bandekar for the 3_{10}-helix.[75a] The two minor components of the amide I band detectable in the spectra of **14** (n = 8−10) peptides at 1646−1644 and 1681−1679 cm^{-1} were assigned to type III β-turns and/or free carbonyls, respectively. IR spectra of peptides **17** (n = 3−5), **20** (n = 2, 4), and **21** show a major amide I component at 1641−39 cm^{-1}. This dominant low-wavenumber amide I band was attributed to the Aib−Pro (or Dpg−Pro) amide bond.[83a] The interactions between amides were assumed to be more significant than the differences between secondary and tertiary amides or the effects of H-bondings of different strength. Contrary to this, in the FTIR spectrum of Ala-based linear peptides **22** (Chart 3), suggested to form 3_{10} rather than α-helix, the dominant amide I′ band had a maximum at 1637 cm^{-1}.[84a] However, FTIR and vibrational circular dichroism spectroscopic studies have demonstrated that the Ala-rich peptides in D_2O adopt a hydrated α-helical conformation with frayed ends,[84b−d] and the amount of fraying increases with temperature and shorter length. For a theoretical analysis of the impact of α-methyl substitution on experimental IR and vibrational circular dichroism (VCD) spectra, see section 10 and ref 83b.

To conclude, due to their high conformational freedom, there are only few small linear peptides having well established β-turn structures. So far the experimental evidence collected here indicates that not only the 1690−1660 cm^{-1} but also the 1645−1635 cm^{-1} region (bands strongly contributed by the carbonyl of acceptor amides) is characteristic of β-turns. It has been shown that in small (<∼10 residues) cyclic peptides which cannot adopt α-helical or β-sheet conformations, the 1645−35 cm^{-1} band is diagnostic of the presence of H-bonded β-turns (section 5.4).

5.3. Detection of β-Turns in Midsize Peptides

Midsize peptides represent a group of polypeptides with great biological importance.[13,15,25] Peptide hormones, epitopic peptides, signal peptides, enzyme inhibitors, neuropeptides, etc., as well as their synthetic analogues and fragments, belong to this group of peptides. An understanding of their functions requires knowledge of their steric structure and conformational mobility under different conditions. In the case of proteins, containing only a limited number of H-bonded β-turns, the IR bands of β-turns are likely overlapped by the much stronger component bands associated to other types of structures such as random coil, α-helix, and antiparallel β-sheets. However, in midsize peptides, the β-turns are ex-

Table 2. FTIR Spectroscopic Studies on Selected Small and Midsize Peptides with Established β-Turn Conformation

peptide	other methods used	type of folded stucture	frequency used for assignment (cm^{-1})[a] amide A	amide I	ref
Ac-Pro-Pro-NH_2, Ac-Pro-Pro-$NHCH_3$	^1H, ^{13}C NMR	βVI-turn (cis Pro-Pro bond)	3335, 3322	1634, 1632	78e
Ac-Pro-D-Pro-NH_2, Ac-Pro-D-Pro-$NHCH_3$		βII-turn	3335, 3330	1634, 1628	
Ac-Pro-Pro-$NHCH_3$	^1H NMR	βI-turn	3460	1659, 1634	78b
Ac-Pro-D-Pro-$NHCH_3$		βII-turn	3460	1661, 1628	
Piv-Pro-Ser-$NHCH_3$,	X-ray cryst., ^1H NMR, CD	βI-turn	3460−50 (free)	−	78a
Piv-Pro-D-SerNHCH$_3$	^1H NMR, CD	βII-turn	3380−40		
opiate peptides **10-13**	sequence-dependence, modeling	βII-turn in ProGly peptides	−	1639−33(TFE) ~1640 ($CHCl_3$)	79
Leu^5-enkephalin (YGGFL) and ^{13}C or ^{17}O-labeled derivatives (at Gly^2 or Gly^3)	^{17}O NMR		−	1670(69) (CH_3CN/DMSO 4:1) 1655(46) (D_2O)	80f
peptides representing the processing site of pro-oxytocin/ neurophysin precursor (OT/Np) **26a,b**	^1H NMR, CD	Two β-turns	−	>1660, 1627(24) (TFE or DMSO) 1642, 1608, 1585 (D_2O)	80a
pro-OT/Np peptide **26c**	^1H NMR, CD	β-turns, description of the methods (FSD, CF, Nth derivative spectra)	−	>1660 (DMSO or DMSO/D_2O) 1627−23,[b] 1609−03 (D_2O)	80b
Peptides (14-18-mers) from the N-terminal domain of pro-OT/Np **26a-d**	^1H NMR, CD	βI, βII H→D exchange; FSD, CF, Nth derivative spectra	−	>1660 (DMSO or DMSO/D_2O)	80c
26e	^1H NMR, CD	βI, βII	−	1648−37, 1630−25	
δ-sleep-inducing peptide **24**	^1H NMR, CD, fluorescence, modeling	two βI-turns	−	1648, 1637 (buffer and TFE)	93
calcitonin gen-related peptide sequences **27**	^1H NMR (NOESY), receptor binding assay	βII-turn centered at Pro	−	1672−70	80e
hemagglutinin fragments **23**	CD, sequence-dependence	β-turns (together with β-sheet)	−	~1635 (TFE)	90a
elastin peptides and depsipeptides **28**	^1H NMR, CD	βI-turn and γ-turn in equilibrium at PG residues	3452−16 (free) 3343−01 (IHB)	1681−66 β-turn, β-sheet 1645−34 β-sheet ($CDCl_3$)	92
peptides **29** representing the protein core epitope from gastrointestinal mucin (MUC2)	CD, sequence-dependence, inhibition radioisotopic immunoglobulin assay	β-turn γ-turn	− −	1646−34 1632−28 (TFE)	91
galanins **25a−c**	^1H NMR, CD	β-turn band and deformation band of water traces	−	1637	94
vasopressin peptides **30** and β-Asp and β-D-Asp analogues	^1H NMR, CD, sequence and pD dependence, modeling	β-turn or γ-turn	−	1647	95
natriuretic peptides **32**	CD, comparative studies on related peptides, receptor binding assay	β-turn/β-sheet	−	1672−70 1637−35	96
snake curaremimetic toxin **31**	CD	β-turn β-turn/β-sheet	−	1696−94 1668 1637	98

[a] In CH_2Cl_2, other solvent used in parentheses. [b] Weak band. Abbreviations: FSD, Fourier self-deconvolution, CF, curve-fitting.

pected to give a detectable contribution to the IR spectra.

Furthermore, midsize peptides produced by solid-phase peptide synthesis are often present in the form of trifluoroacetate salts as a result of the final purification by HPLC using trifluoroacetic acid-containing eluents. This counterion gives an IR band around 1673 cm^{-1}.[85] Thus, disregarding the presence of trifluoroacetate and identification of β-turns on the basis of high-wavenumber amide I band(s) alone may be a source of conformational artifacts. The consideration of both the high-wavenumber (>1660 cm^{-1}) and low-wavenumber (1645−35 cm^{-1}) amide I regions may help to avoid misinterpretation of the IR spectra of trifluoroacetate salts and to estimate relative β-turn contents which are compatible with CD data and secondary structure prediction.

Halogenated alcohols have been suggested to mimic the microenvironment established by apolar proteins or membranes. Addition of TFE or HFIP (hexafluoro-2-propanol) to an aqueous solution of midsize peptides leads to a general shift of the conformational equilibria toward an increased amount (or predominance) of intra-H-bonded structures or structural

Table 3. Characteristic Wavenumbers of Selected Cyclic Peptides Featuring β- and/or γ-Turn Structures

peptide	FTIR approach	other methods used	type of folded structure	characteristic amide I wavenumbers/ cm^{-1}	ref
3a	FSD	X-ray cryst., ^1H NMR (DMSO), CD (TFE)	βI(III)-turn	1683−79, ∼1665, 1645−42 (CH_3CN)[a] 1673, ∼1665sh, 1642 ($CHCl_3$)[b]	81
3b	FSD	X-ray cryst., ^1H NMR (DMSO), CD (TFE)	βI(III)- and γ-turn or bifurcation	1656sh, 1640, 1622 (D_2O)	81
3c	FSD	^1H NMR (DMSO), CD (TFE, H_2O)	βII-turn (main conformer)	1673, 1660sh, 1642 (DMSO)	81
3d	FSD	CD (TFE, H_2O)	βII- and γ-turn or bifurcation	1655, 1641sh, 1621 (D_2O)	81
3e	FSD	^1H NMR (DMSO), CD (TFE, H_2O)	βII(I)- and γ-turns, bifurcation	1677, 1662, 1640, 1627, 1604 (TFE) 1693, 1684, 1667, 1641 (DMSO)	103
3f	FSD	^1H NMR (DMSO), CD (TFE, H_2O)	βII- and γ-turns, bifurcation	1674, 1664, 1643, 1627, 1603 (TFE) 1694, 1676, 1667, 1658, 1642 (DMSO)	103
cyclo(aAaA$_2$) **4a**	curve-fitting	CD (TFE), NMR (DMSO)	βII′ + γ-turns, inverse bifurcation	1685m, 1669s, 1646s (TFE) 1687w, 1669s, 1648m (DMSO)	101
cyclo(aA$_2$aA$_2$) **4b**	curve-fitting	CD (TFE), NMR (DMSO)	two βII′-turns, inverse bifurcation	1682m, 1671m, 1653s, 1636s (TFE) 1689w, 1677s, 1652s, 1632w (DMSO)	101
cyclo(a$_2$A$_3$) **5**	curve-fitting	CD (TFE), NMR (DMSO)	βII + γ-turns, inverse bifurcation	1685m, 1667s, 1653w, 1641m, 1628 (TFE) 1682m, 1665s, 1648m, 1633m, 1621w (DMSO)	101
cyclo(pA$_4$) **6a**	curve-fitting	CD (TFE), NMR (DMSO)	βII′-turn, bifurcation	1694w, 1679m, 1666w, 1651m, 1628m, 1612m (TFE) 1687m, 1671m, 1657s, 1629m (DMSO)	101
cyclo(pA$_5$) **6b**	curve-fitting	CD (TFE), NMR (DMSO)	βII′ + βII-turns, γ-turn	1691w, 1678m, 1670m, 1656m, 1633s, 1615w (TFE) 1689m, 1675m, 1659s, 1636s (DMSO)	101
cyclo(p$_2$A$_4$) **7**	curve-fitting	CD (TFE), NMR (DMSO)	βI′ + βII′-turns, γ-turn	1699w, 1677m, 1671w, 1654m, 1635m, 1616m (TFE) 1684m, 1669m, 1656m, 1639s (DMSO)	101
cyclo(pApA$_2$) **8**	curve-fitting	CD (TFE), NMR (DMSO)	βII′ + γ-turns	1677m, 1655m, 1636m, 1618s (TFE) 1689m, 1679m, 1660m, 1633m, 1623w (DMSO)	101
cyclosporins A,C and D **42a−c**	FSD	NMR ($CDCl_3$) and X-ray for **42a**	γ-turn	∼1625 (CCl_4, $CDCl_3$, weakened in CH_3CN, missing in DMSO and D_2O-CH_3CN 1:1 mixture)	193
cyclosporin H **42d**	FSD		γ-turn	∼1616m (CCl_4, weakened in $CDCl_3$, missing in DMSO and D_2O-CH_3CN 1:1 mixture)	193
33a	FSD		β-turn, γ-turn, bifurcation (in D_2O)	1686, 1676, 1648, 1631, 1621 (CH_3CN) 1670, 1641, 1595 (D_2O)	100
33b	FSD		β-turn and/or γ-turn, bifurcation (in D_2O)	1695, 1676, 1662, 1632 (CH_3CN) 1666, 1636, 1602 (D_2O) 1673, 1641, 1600 (TFE)	100
33c	FSD		β-turn	1691, 1677, 1630 (CH_3CN)	100
33d	FSD		β-turn, bifurcation (in D_2O)	1683, 1667, 1635 (CH_3CN) 1674, 1641, 1606 (D_2O)	100
36a	FSD	NMR (TFE/H_2O, DMSO), CD (TFE)	βII-turn	1674sh, 1661, 1647, 1627 (90% TFE/D_2O) 1670, 1660sh, 1640 (DMSO) 1670, 1659, 1640, 1621 (D_2O)	80d

[a] Amide A bands in CH_3CN at ∼3410 cm^{-1} (free) and ∼3340 cm^{-1} (IHB). [b] Amide A bands in $CHCl_3$ at ∼3435 cm^{-1} (free) and ∼3335 cm^{-1} (IHB). Abbreviations: FSD, Fourier self-deconvolutions; s, strong, m, medium, w, weak, sh, shoulder.

domains.[86] The CD spectra in TFE of many midsize peptides have a helix-like (class C) band pattern.[13,87] This type of CD spectrum may be correlated with a variety of secondary structures (3_{10} conformation, repeats of type I, III, or II′ turns, or even a small amount of α-helix). CD spectroscopy alone does not allow to distinguish between α- or 3_{10}-helix and turns. In the IR spectrum in TFE the α-helix region (1660−1650 cm^{-1}) is clearly separated from the acceptor region (1645−1635 cm^{-1}) of β-turns. Fortunately, the β-sheet or β-strand conformation, giving rise to an amide I band between 1640 and 1620 cm^{-1}, is not stabilized by fluorinated alcohols. Accordingly, the joint application of CD and IR spectroscopy has a unique power to detect β-turns in midsize peptides. Comparative experiments are recommended in halogenated alcohols, water, and their mixtures to map the conformational space which is allowed for a given sequence. The CD/FTIR approach was applied for detection of turns in glycosylated[88] and phosphorylated[89] peptides. The tendency of epitopic peptides to adopt turn conformation was also probed by CD and FTIR spectroscopy.[90,91] The effect of micelles[90b] and metal ions[89a] upon chain folding was also monitored.

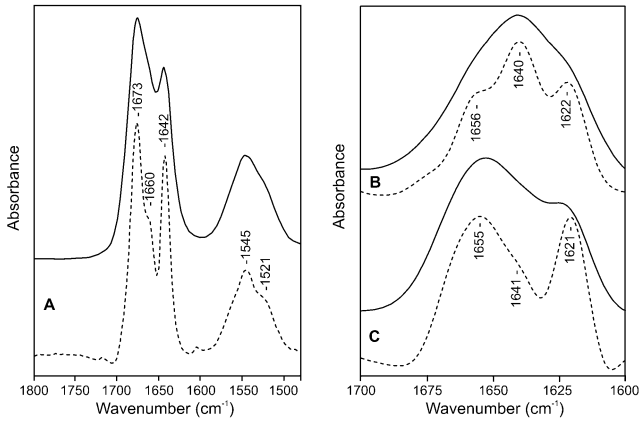

Figure 4. FTIR spectra of **3** [Xxx = Gly, $n = 4$] in DMSO (A), **3** [Xxx = Thr(O^{t}Bu), $n = 4$] (B), and **3** [Xxx = Thr(O^{t}Bu), $n = 2$] (C) in D_2O. [Amide I and amide II regions (A); amide I region (B and C). Broken traces are the band-narrowed (FSD) spectra.] Adapted with permisson from ref 81, *Biopolymers*, copyright 1993 John Wiley & Sons, Inc.

Chart 2

Boc-TyrProGlyPheLeu-OH	Boc-TyrProGlyPheLeuThr-OH	Boc-TyrGlyProPheLeu-OH
10	**11**	**12**
Boc-TyrProPheLeu-OH	Cbz-(Aib)$_n$-O^{t}Bu	Cbz-(AibAla)$_n$-OMe
13	**14** n=3-10	**15** n=1-5
Cbz-Ala-(AibAla)$_n$-OMe	*p*-Br-Cbz-(ProAib)$_n$-OMe	Cbz-(ProAib)$_n$-OMe
16 n=1-5	**17** n=2-5	**18** n=1-4
Ac-(ProAib)$_4$-OMe	*p*-Br-Cbz-Aib-(ProAib)$_n$-OMe	For-MetDpgPro-OH
19	**20** n=1-5	**21** Dpg = dipropylglycine

Chart 3

Ac-C*AAAKAAAAKAAAAKA-NH$_2$
Ac-AAAAKAAC*AKAAAAKA-NH$_2$
Ac-AAAC*KC*AAAKAAAAKA-NH$_2$
Ac-AAAC*KAC*AAKAAAAKA-NH$_2$
Ac-AAAC*KAAC*AKAAAAKA-NH$_2$

22

C* = nitroxide-labelled Cys

(**a**) VTGLRNIPSIQSRGLFGAIAGFIEG
(**b**) GLFGAIAGFIEG
(**c**) VTGLRNIPSIQS
(**d**) VTGLRNIPSIQSR

23

WAGGDASGE

(**a**) GWTLNSAGYLLGPHAIDNHRSFHDKYGLA-NH$_2$
(**b**) GWTLNSAGYLLGPHAVGNHRSFSDKNGLTS-OH
(**c**) GWTLNSAGYLLGPHAIDNHRSFSDKHGLT-NH$_2$

24 **25**

(**a**) LGGKRAVLDLDVR-HH$_2$
(**b**) PLGGKRAVLDLDVR-NH$_2$
(**c**) LGGKRAVL-NH$_2$
(**d**) PLGGKRAVL-NH$_2$
(**e**) CYIQNCPLGGKRAVLDLDVR-NH$_2$

26

(**a**) FVPTDVGAFAF-NH$_2$
(**b**) FVPTNVGAFAF-NH$_2$
(**c**) TDVGPFAF-NH$_2$
(**d**) FVPTDVGPFAF-NH$_2$

27

P$_1$-VPGXG-P$_2$ (VPGXG)$_n$
P$_1$-VAPGXG-P$_2$ (VAPGXG)$_n$

28

X = V or S-α-hydroxy-isovaleric acid,
P$_1$ = Ac or Boc, P$_2$ = Bzl or NHMe

(**a**) TPTPTPTGTQTPTT-NH$_2$
(**b**) TGTQTPTT-OH
(**c**) QTPTT-OH
(**d**) TPTPT-OH
(**e**) TPTPTGTQ-OH
(**f**) TPTGTQ-OH
(**g**) TGTQ-OH

29

A comparison of the CD and FTIR spectroscopic behavior of peptide fragments **23**, representing the intersubunit region of influenza virus hemagglutinin,

Chart 4

(**a**) GGGCYFQDCPKG-NH$_2$
(**b**) GGGCYFQ$^{\beta}$DCPKG-NH$_2$

30

(**a**) G$_3$-[D5, K8]vasopressin
(**b**) G$_3$-[βD5, K8]vasopressin

CYKKVWRDHRGTIIERGC-NH$_2$

31

snake curaremimetic disulphide cyclized fragment

(**a**) SLRRSSCFGGRIDRIGAQSGLGCNSFRY
(**b**) SLRRSSCFGGRMDRIGAQSGLGCNSFRY
(**c**) AAGPRSLRRSSCFGGRIDRIGAQSGLGCNSFRY

32

natriuretic peptides
(**a**) α-rat ANF(99-126)
(**b**) α-human ANF(99-126)
(**c**) β-rat ANF(92-126)

allowed to localize β-turns in the N-terminal part of the molecule.[90a]

Table 2 shows selected examples of small[78] and midsize[79,80,83,90−94] peptides as well as macrocyclic disulfides[95−99] characterized by IR and other spectroscopic methods. 2D NMR spectra of δ-sleep inducing peptide[93] **24** indicated the presence of β-turns. Buffer/TFE difference CD spectra suggested the presence of type II rather type I β-turn(s), while the IR spectrum showed a band at 1637 cm^{-1}.

The assignment of the β-turn band at around 1640 cm^{-1}, near to the random coil (unordered) amide I′ region, is not always straightforward. For example, galanins **25**, which contain α-helix based on CD and NMR spectra, show a band at 1637 cm^{-1} in the IR spectrum in TFE that is indicative of either β-turns or H-bonding between the C═O groups with TFE or water present in TFE.[94] Peptides **26** representing the dibasic proteolytic processing site of pro-oxytocin/neurophysin were monitored by CD, FTIR, 1D, and 2D NMR methods.[80] In DMSO, the second derivative patterns did not show significant component bands below 1660 cm^{-1}. This is what is expected: DMSO is a strong acceptor for hydrogen bonds; it disrupts the IHB of β-turns.[80a] Contrary to this, low-wavenumber components were observed in D_2O between 1650 and 1600 cm^{-1}.[80a]

CD and FTIR spectroscopic studies were performed on cyclic disulfides built up from ∼10 or more than 10 residues. Vasopressin derivatives **30** (Chart 4) adopt β-turns according to FTIR spectroscopy.[95] Considering the internal mobility, cyclic disulfides comprising more than 10 amino acid residues are situated conformationally between the five- to eight-membered cyclic and midsize linear peptides. An example of macrocyclic disulfides is the family of natriuretic peptides **32**.[96] According to CD spectra, these peptides exist in two conformational states, β-sheet and β-turns in 20−60% HFIP/water solution. IR spectra in D_2O of natriuretic peptides **32a**,**c** revealed two amide I′ bands at 1670 and 1647 cm^{-1} and 1672 and 1650 cm^{-1}. These bands were assigned to antiparallel β-sheets/β-turns. The IR spectrum of an octadecapeptide fragment of a snake curaremimetic toxin **31**, cyclized through a disulfide bridge, was measured in the solid state (dry film) and in D_2O or deuterated TFE solution (hydrated film).[98] In the IR spectra measured in dry and hydrated films, bands at 1627 or 1623 and 1674 or 1668 cm^{-1} were

associated with antiparallel β-sheet, while those at 1696, 1694, and 1637 cm^{-1} with turns. The contribution of turns to the ~1670 cm^{-1} band was also discussed.

The IR spectra of insulin and S-thiomethyl derivatives of its A and B chains as well as despentapeptide (26−30) B and desoctapeptide (23−30) B chain analogues indicated a component band between 1692 and 1681 cm^{-1}, which was assigned to β-turns.[99] In addition to the α-helix band (1650 cm^{-1}) and 3_{10}-helix band (1660 cm^{-1}), a band located around 1633−1630 cm^{-1} was associated with "irregular helix".

In conclusion, for the midsize peptides, two distinctive regions located around 1690−1660 and 1645−1635 cm^{-1} are characteristic of β-turns; however, their IR spectra are often overlapped with contributions of other types of secondary structures. Therefore, it is advisable to use whenever possible the CD/FTIR method[13] or perform vibrational optical activity measurements (section 10) for detecting turns.

5.4. Cyclic Peptides: Classical Models of β-Turns

Cyclic peptides have played a distinguished role in the characterization of folded polypeptide structures. The most favored representatives of cyclic model peptides are cyclic hexamers which can be regarded as "doubled" β-turns. NMR spectroscopy was used for detailed conformational studies on cyclic peptides in solution from the late 1970s.[13,25,51] Models with a C_2 symmetric constitution were selected first. The position of the turn was pinpointed by introducing an amino acid residue (in many cases proline) having a high frequency of occurrence in turns.

Mantsch and co-workers measured the infrared spectra (Table 3) of a selection of cyclic peptides of the general formula *cyclo*[^{1}Gly-^{2}Pro-^{3}Xxx-^{4}Gly-NH-$(CH_2)_n$-CO] **3**, in different solvents.[81] Their steric structures were characterized by X-ray crystallography and/or NMR spectroscopy.[30] The unique structural feature of these models is the presence of five amide C═O and only four N−H groups. The samples were dissolved in acetonitrile, chloroform, DMSO, chloroethanol, TFE, and D_2O. Their IR spectra usually showed two amide I bands: a broader and stronger one above 1660 cm^{-1} and a weaker one between 1645 and 1635 cm^{-1} (Figure 4). For samples in D_2O, a third band was observed near 1620 cm^{-1}. In the majority of spectra, the intensity ratio of the high-wavenumber band and the 1640 ± 5 cm^{-1} band was close to 3:2. The structural data inferred from NMR and X-ray diffraction analysis allowed associating the 1640 ± 5 cm^{-1} component band to H-bonded C═O groups of two β-turns occurring in the models. The high-wavenumber asymmetric band (Figure 4) belongs to solvent-exposed, weakly solvated C═O groups.

In the spectra of models with a shorter bridge ($n = 2$ in the general formula), the intensity of the low-wavenumber band is weaker, indicating that in peptides having a smaller 16-membered ring, there is only one strong intramolecular H-bonded β-turn, in agreement with spectroscopic data and molecular dynamics calculations. The FTIR spectra of the cyclic models **33**[100] (Chart 5) are indicative of the presence

Chart 5

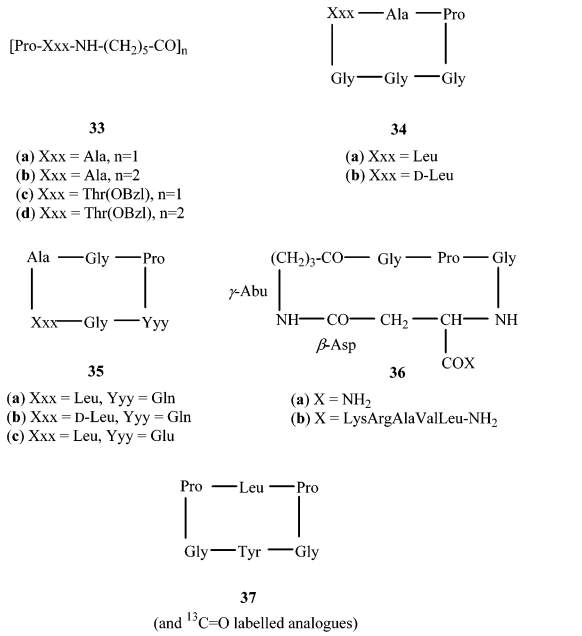

of more than one dominant β- or γ-turn conformer (section 7.2).

Infrared spectroscopic studies on a variety of cyclic peptides **3**−**9** and **34**−**37**, with different ring size and amino acid composition supported the assignment of the 1640 ± 5 cm^{-1} band to the amide group(s) of H-bonded β-turns.[101a] Of particular interest is a series of cyclic penta- and hexapeptide models **4**−**8** whose steric structure has been inferred from 2D NMR experiments and restrained MD simulations.[101b] The incorporation of D-Ala or D-Pro was expected to stabilize type I′ or II′ β-turns (mirror image of type I or II turns). NMR spectra were measured in DMSO;[101b] therefore, FTIR measurements were performed in the same solvent and also in the structure-promoting solvent TFE. The comparison of the NMR and infrared spectra was assisted by the temperature coefficient data ($\Delta\delta/\Delta T$) in DMSO of the NH groups involved in turn structures. The turn band was always found in the FSD IR spectra of models with one or two NMR-based type I′, II, or II′ β-turns (Table 3). However, its position in the TFE spectra was sometimes shifted to lower (1635−1630 cm^{-1}) wavenumber values as a sign of probable bifurcation (two donor NHs and one acceptor C═O) or solvation of the C═O of the IHB acceptor amide (section 8). On the other hand, an amide I component band shifted to higher (1655−1645 cm^{-1}) wavenumbers in the spectra in TFE or DMSO was associated with inverse bifurcation (two acceptor C═Os and one donor N−H).

The effects of Ca(II) on the conformation in TFE of linear and cyclic collagen sequence analogues **34** and **35** were monitored by IR and CD.[102] The bands at 1640 ± 5 and 1630 ± 5 cm^{-1} were associated with H-bonded β-turns and γ-turns, respectively. An amide I component band in the curve-fitted spectra of the cyclic peptides between 1618 and 1603 cm^{-1} was assigned to bifurcated H-bondings. Binding of Ca(II) caused significant changes in the CD spectra. In the infrared spectra, the presence of 0.5−1.5 equiv of Ca(II) gave rise to gradual shifts to lower frequencies

Chart 6

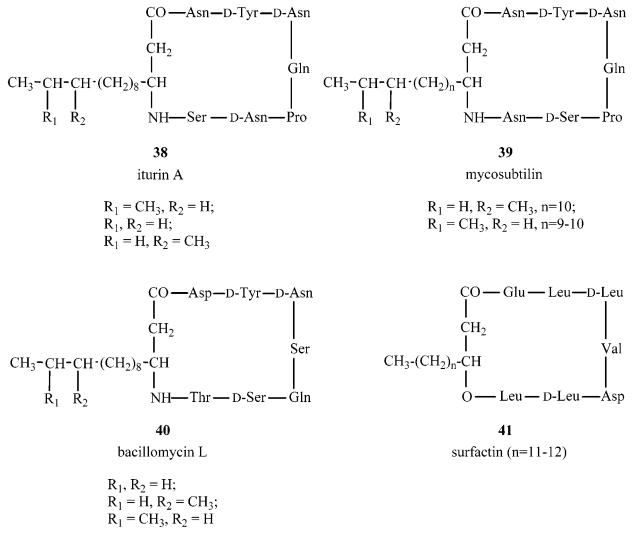

of the majority of component bands. The lack or low intensity of the component band below ~1620 cm^{-1} indicated that complexing of Ca(II) by the side chain COOH group(s) has a stabilizing effect upon β- and/or γ-turns but Ca(II) does not bind strongly to the backbone amide C═O groups.[102]

IR spectra of cyclic glycopeptides, of the general formula *cyclo*[^{1}Gly-^{2}Pro-^{3}Xxx(GlcNAc)-^{4}Gly-NH-$(CH_2)_4$−CO] **9** indicated a component band at 1642 cm^{-1}, which was assigned to the 1←4 intramolecular H-bonding of a β-turn comprising residues 1−4.[103] However, the side-chain contribution to this spectral region of the Xxx(GlcNAc) residue cannot be ruled out either.

In the IR spectrum of a cyclic peptide **36** comprising a β-Asp and γ-Abu residue, the band at 1637 cm^{-1} was associated with a βII-turn.[80d]

Turns were also identified by FTIR spectroscopy in natural cyclic lipopeptides. Iturin A **38** (Chart 6) is an antibiotic lipopeptide of *B. subtilis* with an alternating L,D sequence (^{1}Asn-D-Tyr-D-Asn-Gln-Pro-D-Asn-Ser) closed in a ring with a β-amino fatty acid (β-Afa).[104] Iturin has three Asn and one Gln residues, containing amide groups absorbing in the amide I region. The side-chain of nondeuterated Asn and Gln residues absorb significantly around 1680−1670[76] and shifted to 1648−1635 cm^{-1} upon deuteration. By comparing the infrared spectrum of iturin in dry state with the infrared spectrum of deuterated iturin (Figure 5), the side chain absorbance contributions could be estimated. In particular, the shift of the Asn C═O stretching mode from 1678 cm^{-1} (dry state) to 1648 cm^{-1} (deuterated state) and the shift of the Gln C═O vibrational stretching mode from 1670 cm^{-1} (dry state) to 1635 cm^{-1} (deuterated state) were expected and observed. After deducting the amino acid side chain absorbances, the IR spectrum of iturin in dry state indicated at least four component bands at 1692, 1665, 1654, and 1639 cm^{-1}. The 1692 cm^{-1} band likely corresponds to "free" non hydrogen-bonded C═O. Only three component bands at 1667, 1636, and 1624 cm^{-1} were observed when iturin was hydrated in deuterated water. The new band at 1624 cm^{-1} reflected strongly hydrogen bonded C═O groups involving D_2O and appeared at the expense of the nonhydrogen bonded C═O groups. Therefore, the 1667−1665 cm^{-1} and the 1639−1636 cm^{-1} bands signal the presence of β-turns in iturin, consistent with the NMR spectra indicating β-turns in iturin.

Other lipopeptides from *B. subtilis*, mycosubtilin **39**,[104b−d] bacillomycin **40**,[105] and surfactin **41**[106] were also investigated. Bacillomycin and surfactin contained β-turns, as evidenced by their NMR and IR spectra, while mycosubtilin contained γ-turns (section 7).

Isotope-edited FTIR and infrared linear dichroism (IRLD) spectroscopic studies were performed on cleromyrine **37**, a cyclic hexapeptide.[107] Cleromyrine comprises a ProGly βII-turn and a GlyPro βII′-turn according to X-ray crystallography. Single crystals of **37** were examined in the transmission mode and by the IRLD method. **37** was found to contain localized, uncoupled amide I modes by IRLD measurements. Thus, peaks in its IR spectrum correspond to individual amide carbonyl groups. Band assignments based are upon subtraction of the spectrum of unlabeled **37** from that of the ^{13}C═O labeled derivatives. The amide carbonyls of Leu and Tyr, acceptors of C_{10} IHBs, were found to absorb at 1616 and 1653 (1658) cm^{-1} in the spectrum of unlabeled **37**. The former value is too low, while the latter one is too high for a typical β-turn IHB acceptor amide group. The low wavenumber of the Leu C═O band was explained by unclear intrinsic factors. (Measurements were not performed in solution.)

In conclusion, due to their limited ability to form secondary structures such as α-helix, β-sheet, or random coil, cyclic peptides are very good models for β-turns. In addition, they deliver the best experimental evidence to support the infrared diagnosis of turns based on the high-wavenumber (1690−1660 cm^{-1}) and the low-wavenumber (1645−1635 cm^{-1}) regions, respectively, reflecting free and hydrogen-bonded amide carbonyl groups in β-turns. Their relative ratio ($I_{1690-1660}$:$I_{1645-1635}$ = 3:2−2:1) is consistent with their relative populations. Although the different types of β-turns cannot be differentiated on the basis of IR spectra alone, there is a possibility to differentiate the β-turns from γ-turns (see section 7).

5.5. Detection of β-Turns in Proteins

Generally, the detection of β-turns in proteins is based on the presence of an infrared component band in the amide I/I′ region between ~1690 and ~1660 cm^{-1} with extremes at 1693 and 1659 cm^{-1}.[14,75,76,108] This assignment originates from the seminal paper of Byler and Susi.[14a]

The infrared assignments of β-turns on over 70 proteins [109−178] are presented in Table 4. Indeed, β-turn content in native proteins in Table 4 ranges from 7% to 33% of the total secondary structures, except for wheat germ agglutinin that contains 47% β-turn. Due to the lack of more examples of proteins with relatively high proportion of β-turn, their infrared spectra must be interpreted carefully.

To better delineate problems encountered in the case of proteins, a very short overview of the assignments of secondary structures is presented since

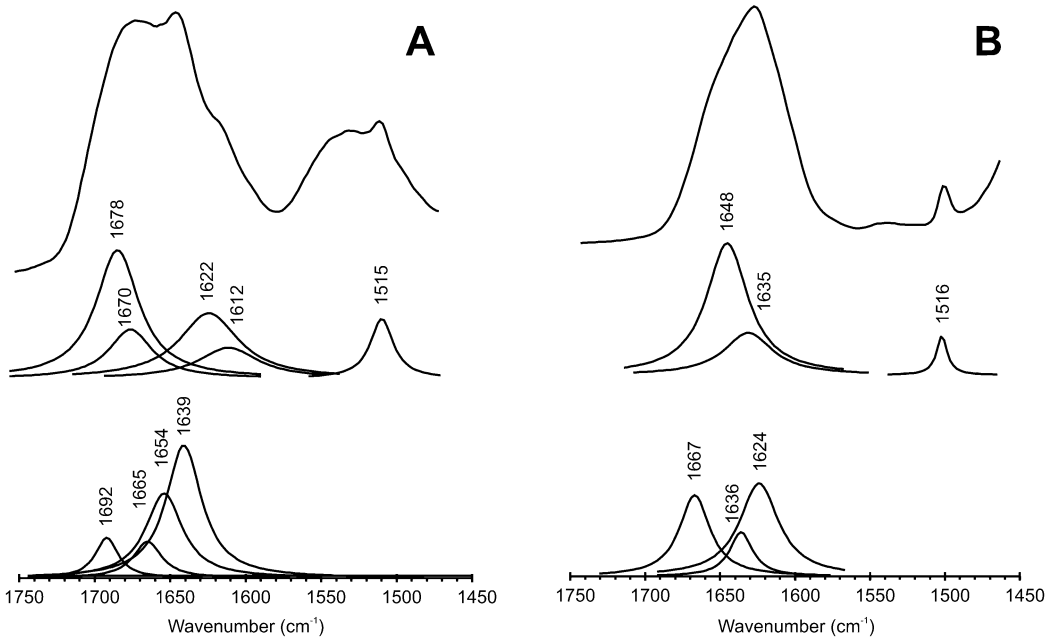

Figure 5. FTIR spectra of iturin A **38** in dry (A) and D_2O-hydrated (B) states. Top traces: original FTIR spectra. Middle traces: contribution of the Asn, Gln, and Tyr side chains. Bottom traces: estimated absorbance of peptide backbones obtained from curve-fitting analysis.

detailed reviews are available elsewhere.[14] In the case of proteins, α-helix structures absorbs at around 1662−1648 cm^{-1}, membrane-helical structures tend to be shifted to ∼1662 cm^{-1}, while hydrated hydrogen-bonded helix tend to be shifted toward 1648 cm^{-1} or even to lower-wavenumber values. β-Sheet structures present two characteristic bands located at around 1690−1670 cm^{-1} (low intensity) and at 1620−1640 cm^{-1} (high intensity).[14] Vibrational modes of carbonyl groups associated with random coil are sensitive to the deuterium exchange of the adjacent NH groups with a deuterium-labile solvent. Unordered structures absorb usually at around 1648−1640 cm^{-1} (samples in D_2O buffer) or at around 1660−1650 cm^{-1} (samples in H_2O buffer).[14]

Several authors who assigned β-turns in the 1682−1662 cm^{-1} region (Table 4) suggested that an alternate assignment such as β-sheet structures (higher-wavenumber component band) cannot be excluded.[97,109−124] The ratio of the intensities of the higher (1690−1670 cm^{-1}) wavenumber component to lower (1640−1620 cm^{-1}) wavenumber component bands characteristic of β-sheet structures is usually ∼ 1:10, while the corresponding ratio for β-turns is around 3:2−2:1 (see section 5.4). The intensity ratio can be used to distinguish between a β-sheet structure and a turn structure.[14,114] However, the intensity ratio is not always easily obtainable and is highly dependent on size and twist of the sheets. This validates the identification of turn structures on the basis of the 1690−1660 cm^{-1} component amide I band in the case of proteins. It was reported[110,127,128] that β-turns and 3_{10}-helix structures could absorb in the same region around 1666−1660 cm^{-1}, complicating the analysis of infrared spectra. Nevertheless, the occurrence of 3_{10}-helix structures in proteins is rare. Furthermore, the side-chain of amino acid residues may also absorb significantly in the amide I region,[76,129a−c] especially in the case of small cyclic peptides (see section 5.4).[129d]

It is well established that in the case of proteins containing mostly α-helix, β-sheet, and random coil structures but no turns, infrared spectroscopy is accurate in predicting β-sheet content, while CD spectroscopy is more precise than infrared spectroscopy in determining the α-helix content of proteins.[110,127,130,131] By using both spectroscopic techniques,[130] the estimation of β-sheet and α-helix structures provides reliable results.[97,117,118,132] The differences in α-helix and β-sheet content, inferred from CD or IR data, respectively, are due to overlapping-caused degeneracy rather than an incorrect conformation to band assignment. However, in the case of proteins containing turn structures, the estimation of β-turn content is more difficult and the agreement between infrared and CD spectroscopic methods are sometimes less satisfactory (Table 4). For example, in the case of a 28 kD channel protein (CHIP28), estimation of β-turn content was 14% from infrared spectra, while it was 1% from CD spectra.[133a] IR assignment and choice of soluble protein reference CD spectra may contribute to the differences in β-turn content determined by the two methods. Comparison of infrared data and X-ray diffraction results also revealed some discrepancies. Infrared data overestimated (16%) the β-turn content in α-toxin,[134] as compared to the X-ray percentage (9%). The determination of protein structures in terms of a sum of components is much too idealized and restrictive to explain the variations of infrared spectra of proteins.[135] The use of neural network methods, avoiding assumptions on band assignments, can provide more accurate secondary structure predictions.[135] Although, the neural network methods based on infrared spectra gave good estimates of α-helix content of RNAse T1, it underestimated (13−14%)

Table 4. IR Band Assignments for β-Turns and Determination of the Content of β-Turns in Proteins from IR Spectra

protein	origin	IR bands amide I	% β-turns amide I	IR bands amide I′	% β-turns amide I′	justification for β-turns	ref
adipocyte fatty acid- binding protein	recombinant protein			1674			140
aerolysin	*Aermonas hydrophila*			1662−82			141
ADP/ATP transporter	*Sacharomyces cerevisiae*	1675	5.50%				125
		1684	3.20%				
			total 8.70%				
aquaporin 1	human erythrocytes			1662−82	11−21%		142
ascut-1	*Ascaris lumbricoides*			1660	9%	CD	132a
				1667	7%		
				1683	5%		
					total 21%		
avidin	egg white			1693			109
bacteriorhodopsin	*Halobacterium salinarium*			1662−82	10−21%		142
bacteriorhodopsin	*Halobacterium salinarium*			1664			143
				1676			
				1694			
					total 13%		
bacteriorhodopsin (bleached)	*Halobacterium salinarium*	1673	5.30%	1674	3.40%		110
		1679	6.80%	1680	4.80%		
		1686	3.90%	1688	1.20%		
			total 16%		total 9.4%		
bacteriorhodopsin (purple membrane)	*Halobacterium halobium*	1693					144
basilase	*crotalus basiliscus basiliscus*	1669	8.9−9.9%				145
		1679	7.1−8.4%				
		1685	7.4−8.6%				
			total 23−27%				
Bax (fragment)	synthetic peptide			1666	12%		146
				1680	2%		
					total 14%		
botulinum neurotoxin	*Clostridium botulinum*			1668			111
				1680			
				1690			
					total 7−8%		
bovine seminal plasma protein PDC-109				1671	9%	CD	147c
				1680	6%		
					total 15%		
Ca-ATPase	rabbit back and leg muscles	1689		1680			112
Ca-ATPase	rabbit back and leg muscles	1672	10%	1669	9%	CD	113
		1684	9%	1680	5%		
			total 19%	1669	total 14%		
Ca-ATPase	rabbit back and leg muscles	1660					148
calcineurin B	recombinant protein			1666		X-ray cryst.	149
				1683			
Chip28 (aquaporin)	blood bank			1670		CD	133a
coat-protein of M13	bacteriophages M13			1634			114
				1676	7%		
coat-protein of Pf1	bacteriophages Pf1			1637			114
				1673	2%		
γ-Cro represseur	γ phage	1672				X-ray cryst.	150
				1665			
cytochrome *C* (dried film A)				1612	2%		151
				1619	14%		
				1689	17%		
					total 33%		
cytochrome *C* (dried film B)	horse heart			1619	13%		151
				1682	5%		
				1689	17%		
					total 25%		
cytochrome *C*	horse heart type VI			1661−82	24%	CD, X-ray cryst., NMR	152
cytochrome *C* (Met-80 modified)				1661−82	17%		152
cytochrome *C*	horse heart type VI			1675			139
cytochrome *C*	horse, cow and tuna			1637		X-ray cryst., NMR	138
cytochrome *C* oxidase	*Paracoccus denitrifican*	1672	11%	1674	10%		153
		1682	3%	1686	3%		
			total 14%		total 13%		
cytochrome P-450 (camphor bound)	recombinant protein			1661	2%		115
				1673	17%		
				1689	2%		
					total 21%		

Table 4. (Continued)

protein	origin	IR bands amide I	% β-turns amide I	IR bands amide I′	% β-turns amide I′	justification for β-turns	ref
cytochrome P-450 (substrate free)	recombinant protein			1673 1689	17% 1% total 18%	X-ray cryst.	115
EF edema toxin	*Bacillus anthracis*			1662−82	18%		154
factor XIII (transglutaminase)	recombinant human protein			1661 1674 1680	9.7% 12.4% 6.6% total 29%	CD	133b
fibrinogen	human			1665			127
fibroblast growth factor	recombinant protein			1666	19−23%		155
F1-ATPase	bovine heart			1667 1678 1689		X-ray cryst.	116
γ-hemolysin	*Staphylococcus aureus*			1660−70 1680−96	total 13−14%		134
G-colony-stimulating factor	recombinant protein			1677 1681−86			156
gp41 (fragment)	synthetic peptide			1670 1690			157
H, K ATPase	hog gastric fundus			1661−82	20%		158
histone C-terminal fragment	synthetic peptide			1662	25%		159
ω-gliadin	wheat	1642 1669				CD	160
β-glucosidase	recombinant protein	1667 1673 1680 1690	13% 4% 5% 3% total 25%	1657 1667 1676 1683	13% 6% 6% 2% total 27%		126
immunoglobulin G	human			1659			127
insulin	bovine pancreas			1680 1690	total 9.4%	X-ray cryst.	161
Kv1.1 potassium channel N-terminal fragment	recombinant protein			1674 1680	total 22%	CD	132b
α-lactalbumin	human			1677			128
β-lactoglobulin	bovin			1664 1677			162
lactose permease	recombinant protein			1682−84	17−22%		163
legumin	pea seed			1672			164
lentil lectin	lentil seed	1663−61 1679−78	16% 9% total 25%	1666−68 1676−79	8% 5% total 13%	X-ray cryst.	165
lens crystallin α-	calf eye			1666−72 1682	8−14% 2−3%		166
lens crystallin β-	calf eye			1669−70 1679−80	3−5% 5% total 5−10%		166
lens crystallin γ-	calf eye			1670−71 1683−84	4−5% 2−3% total 6−8%		166
low-density lipoprotein	human	1670 1683	5% 5% total 10%	1671 1680	3% 3% total 6%	CD	167
lysozyme	human			1669			127
metmyoglobin	horse heart			1673 1683	6% 2% total 8%	CD	132c
Na/Ca exchanger protein	bovine heart			1661−1681	25%		168
nicotinic acetylcholine receptor	torpedo	1691 1680		1680		CD	169
nisin		1636 1673				NMR	137
nucleoplasmin	*Xenopus laevis* oocytes and eggs			1662 1671		CD	117
manganese stabilizing protein of photosystem II	native and recombinant proteins			1661−68	native 6% denatured 37%	CD	118

Table 4. (Continued)

protein	origin	IR bands amide I	% β-turns amide I	IR bands amide I′	% β-turns amide I′	justification for β-turns	ref
panton-valentine leucidin	*Staphylococcus aureus*			1660−70 1680−96	 total 10−13%		134
phenylalanine hydrolase	recombinant protein			1677	12%		170
photosystem II reaction center	pisum sativum	1685		1683	17%		171
pneumococcal autolysin LytA Amidase	*Escherichia coli*			1663 1672 1681	10% 9% 4% total 23%	CD	132d
rhodopsin	bovine eye			1660			132e
ribonuclease A	bovine pancreas			1663 1673			172
ribonuclease A	bovine pancreas			1663 1672			173
ribonucleases A and S	bovine pancreas	1667 1682		1661			174
ribonuclease S	bovine pancreas			1674			127
Shiga toxin (C-terminus of the A1 domain)	synthetic peptide	1670−75	24%				119
spermadhesin (acidic seminal fluid protein)	porcin and bovin			1661 1679	25% 11% total 36%	CD	132 f
staphylokinase	recombinant protein	1670 1680 1688	20% 1% 4% total 25%	1664 1678	18% 8% total 26%		120
staphylococcal nuclease fragments	recombinant protein			1660 1694		CD	121
staphylococcal nuclease	recombinant protein	1673 1681	10.30% 6.30% total 16.6%	1665 1673 1684	9.70% 8.40% 1.50% total 19.6%	X-ray cryst.	122
streptomyces lividians K channel	recombinant protein			1673	10−12%		123
α-Synuclein	human			1673 1688	18.50% 2.90% total 21.4%		175
T4 gene 33 protein	recombinant protein			1659 1668	25% 9% total 34%	CD	124
α-toxin	*Staphylococcus aureus*			1660−70 1680−96	 total 16%		134
transferrin receptor	human			1679−78	14%		176
tyrosine hydrolase	human recombinant protein	1669 1679	2% 12% total 14%	1666 1677	9% 7% total 16%		177
UMP kinase	*Escherichia coli*			1669 1680	11% 7% total 18%		178
wheat germ agglutinin				1657		X-ray cryst.	136

the β-turn content as compared with X-ray measurements (24%).[135] The origins of the discrepancies between predicted values from infrared spectra and X-ray diffraction data can be explained with (i) band overlapping, (ii) infrared experimental errors in the determination of secondary structure content (between 3% and 8%), (iii) ambiguous estimation of secondary structure content from X-ray diffraction data, and (iv) infrared band assignment or choice of reference spectra.

As in the case of small and cyclic peptides, there is much experimental evidence which supports the assignment of the 1645−1635 cm^{-1} band to β-turns. On the basis of the usual assignment between 1682 and 1662 cm^{-1}, the β-turn content in wheat germ agglutinin (WGA)[136] was about 20%, in contrast to 47% as determined by X-ray diffraction. By taking into account not only the 1682−1662 cm^{-1} region, but also the 1645−1635 cm^{-1} regions, the determination of β-turn content in WGA was closer to that obtained from X-ray diffraction.[136] Nisin that does not contain any β-sheet structures absorbs at 1636 cm^{-1}. Therefore, the 1636 cm^{-1} band was tentatively assigned to β-turns.[137] On the basis of similar arguments, it was suggested in the case of cytochrome-C[138] that the 1636−1633 cm^{-1} region could be assigned to β-turns since no β-sheet structure was present in cytochrome C. Alternatively, the 1636−1633 shoulder in the spectrum of cytochrome C was associated with extended chains connecting α-helices or with helix−

Table 5. Raman Band Assignments for Small and Midsize Peptides

peptides	type of structure	amide I	amide III	evidence for β-turns	ref
(ATPAKKAA)2	β-turns	1675		CD	181d
S-benzyl-CPLG	type I β-turns	1664	1235	X-ray cryst.	183
			1261		
			1294		
cyclosporine	β-turns	1665		X-ray cryst.	181c
		1672			
echistatin (49 amino acid peptide)	β-turns	1680−60		CD, NMR	187d
GPGG	type II β-turns	1644	1257		181a
		1655	1277		
		1674			
(KTPKKAKKP)2	β-turns	1675		CD	181d
PLG	type II β-turn	1669	1260−20	X-ray cryst.	182
PLG	type II β-turns	1688	1238	X-ray cryst.	183
		1649	1266		
			1283		
RPKPGGFFGLM (substance P)	β-turns	1680		CD, IR	188b
cyclo(VPGVG)$_3$	type II β-turns	1652	1243	X-ray cryst.	179
		1676	1256		
YGGFL (Leu5-enkephalin)	type II β-turns	1665	1255		181b
			1263		
YGGFM (Met5-enkephalin)	type II β-turns	1665	1265	X-ray cryst.	181b

helix interactions.[139] For further examples of the determination of β-turn content in proteins by FTIR spectroscopy, see Table 4 and refs 140−178.

In conclusion, in the case of proteins without β-turns, infrared spectroscopy is a reliable method for assessing secondary structures, especially with a relatively high β-sheet content. The joint application of CD and IR spectroscopies can improve the prediction of secondary structure determination due to their respective different sensitivities toward α-helix and β-sheet structures. However, the prediction of β-turn content in proteins from infrared spectra is not straightforward, due to their relatively low content and to band overlapping. The assignment of the 1690−1660 cm^{-1} band to β-turn in the case of proteins is still valid, provided that the contribution of β-sheet and 3_{10}-helix structures are taken into account. Fortunately, the intensity of the 1690−1670 cm^{-1} component band associated with β-sheet content is weak, and the content of 3_{10}-helix in proteins is usually negligible. Therefore, an intense band in the 1690−1660 cm^{-1} region is highly diagnostic of turn structures. Although a strong band may indicate β-turn structures, it does not lead always to accurate secondary structure estimates. Recent results on proteins[136−138] indicate that β-turns absorb also in the 1645−1635 cm^{-1} region.[136−138] Whether the presence of both the 1690−1660 and 1645−1635 cm^{-1} bands are required for the identification of β-turns in proteins remains to be investigated further.

6. Raman Spectra of Peptides and Proteins Containing β-Turns

On the basis of the normal-mode analysis of polypeptides, it was predicted that Raman bands for β-turns should fall within the interval from ∼1690 to ∼1660 cm^{-1} (amide I) and within the ∼1320−1220 cm^{-1} region (amide III).[75a,b] It has been well established that the pure α-helix and β-sheet are relatively easily distinguished by their Raman amide I profile: the ∼1660−1645 cm^{-1} region is characteristic of α-helix, while the 1680−1665 cm^{-1} and the less intense ∼1640−1620 cm^{-1} region is associated with β-sheets.[77] The relative intensity of the 1680−1665 cm^{-1} Raman band of β-sheet structures is stronger than that of the lower-wavenumber ∼1640−1620 cm^{-1} component band,[179] in contrast to what is observed in the infrared spectra of β-sheet structures. Therefore, combination of Raman and infrared spectroscopies can improve the determination of secondary structure of proteins. The amide II band is usually weak under nonresonance condition, however, it can be observed in the UV-excited resonance Raman spectra of proteins.[77b] There are several methods to evaluate secondary structures of proteins from nonresonance Raman spectra.[77b] The predictions are usually good for the proteins containing mostly α-helix and β-sheet structures but no turns.[77b,e] Due to the overlap of the amide I bands, especially when turns and other structures could scatter in the same or nearby region, it is judicious to analyze not only the amide I but also other modes.[77e,179] To take advantage of this possibility, a new approach based on the simultaneous use of the amide I (1690-∼1610 cm^{-1}), amide II (1560-∼1530 cm^{-1}), amide III (1300-∼1200 cm^{-1}), and the $C_\alpha H$ bending band regions (∼1390 cm^{-1}) was developed and successfully applied.[180] This methodology compares very well with CD spectroscopy in the prediction of α-helix, while it is superior to CD for the determination of β-sheet and unordered structures.[180] So far, this approach has not yet been used for the estimation of β-turn structures.

Table 5 reports Raman amide I and amide III assignments for β-turns in small and midsize peptides. The presence of β-turns in almost all peptides was ascertained by X-ray crystallography, NMR, or CD spectroscopy. The band assignment may also serve for larger polypeptides and proteins. The β-turn amide I band falls around 1688−1664 cm^{-1},[181−183] as predicted by the normal-mode analysis[77] and/or around 1656−1644 cm^{-1}.[181a] The β-turn amide III band appears in the high-wavenumber region ∼1294−1283 cm^{-1}, in agreement with normal-mode analysis,[77]

Table 6. Raman Band Assignments for Proteins

proteins	type of structure	amide I	amide III	evidence for β-turns	ref
amelogenin of bovine tooth enamel	β-turns	1664	1285	CD, IR	187a
metallothionein	β-turns	1666−60	1296	CD, X-ray	187c
proteodermatan sulfate from pig skin	β-turns	1686	1264		188a
tailspike endorhamnosidase of phage P22	β-turns	1668	1235		188c
toxin γ from the venom of scorpion	β-turns	1683	1305		188d

and/or in the lower-wavenumber region[181,182] 1277−1238 cm^{-1}, which is close to another normal mode treatment.[181a] It has been recognized that the position of amide III band is sensitive to the state of hydrogen bond[77,181a] (strong H-bond shifts the amide III band toward higher wavenumber), to the side chain composition,[77] and to the ϕ and ψ dihedral angles.[184−186]

Table 6 presents Raman amide I and amide III assignments for β-turns in proteins. There is a consensus among several groups[97,187,188] that β-turn bands of proteins appear around 1686−1660 cm^{-1}, consistent with theoretical predictions[77] and experimental results on peptides.[181] However, it was observed that in this region the possible contribution of β-sheet structures[187c,188b] cannot be neglected and usually no distinction can be made among the different types of β-turns. The location of the amide III band may help to assign β-turns. As in the case of peptides, β-turn in proteins may contribute around[187c,d,188d] 1305−1285 cm^{-1} and/or around 1275−1235 cm^{-1}.[97,188a,c] Several authors estimated β-turn secondary structures from nonresonance Raman spectra.[187c,188b,c,189] Although the determination of β-turn content in proteins is not as accurate as the determination of α-helix and β-sheet structures, there will be a possibility in the future to extract the ψ dihedral angle based on the amide III band position and on the Raman enhancement of the $C_\alpha H$ bending band from UV resonance Raman spectra.[186b]

7. Infrared Spectra of Peptides and Proteins Containing γ-Turns

The second major subtype of folded polypeptide structures is γ-turns (for classification and X-ray crystallographic characterization of γ-turns, see section 4). Normal-mode calculations have been performed on turn structures by Bandekar and Krimm.[190] The model system used was CH_3CO-$(Ala)_5$-$NHCH_3$, with the Ala CH_3 groups taken as point masses. These calculations suggest that the absorptions due to C═O groups around the β-turn are very sensitive to changes in the dihedral angles. Choosing the tetrapeptide Gly-Pro-Gly-Gly as model, the normal mode vibrations of the C_7C_5 structure have also been calculated by Lagant et al.[185] The dihedral angles of trialanine in D_2O have been determined recently by FTIR and polarized visible Raman spectroscopy in combination with theoretical calculations.[191] The results showed that trialanine adopts a dominant 3_1 helical (PPII-like) conformation in D_2O for all of its three protonation states, while the C_7^{eq} (γ-turn) structure is favored in vacuo. Even assuming standard structures, the positions calculated for type I, II, and III β-turns cover the entire 1700−1640 cm^{-1} range. The wavenumber range characteristic of γ-turns is not well established.

7.1. Infrared Spectra of Diamide Models

Diamide models represent the simplest and smallest molecules capable of forming γ-turn structures. A systematic evaluation of ^1H NMR and IR spectroscopic data on the γ-turn-forming characteristics of N-acyl-proline-methylamides in CH_2Cl_2 was reported by Liang et al.[78c] At room temperature these compounds contain predominantly a trans acyl-Pro amide bond (trans/cis ratio ∼7), with the exception of the pivaloyl derivative which is present exclusively as a trans conformer. It was found that the population of trans conformers with C_7 IHBs (γ-turns) is 68% for the *N*-acetyl, 75% for the N-propionyl and N-isobutyryl, and 50% for the pivaloyl derivative. This work focused exclusively on the N−H stretching region, assigning the sharp 3448 cm^{-1} band to non-H-bonded and the broader 3325 cm^{-1} band to H-bonded structures in the spectrum of Ac-Pro-$NHCH_3$. Little enthalpic or entropic difference was found between the C_7 H-bonded and non H-bonded states.

Comparative analysis of IR spectra on diamide models of type Ac-Xxx-$NHCH_3$ (Xxx = Gly, Ala, Pro) in various solvents were performed by Vass et al.,[192] the results being published only in part. IR spectra of Ala (similar to Gly) and Pro derivatives are summarized in Table 7. The assignment of component bands to particular amide carbonyls [C═O(Ac) and C═O(Xxx), respectively] was assisted by ^{13}C labeling. The replacement of ^{12}C by ^{13}C in the acetyl group caused in general a shift of 37−40 cm^{-1} of the corresponding amide I bands.

The amide I bands related to weakly solvated ("free") C═O groups appear at ∼1671 cm^{-1}, while the bands due to TFE solvated C═O groups are located at ∼1646 cm^{-1}. The 1622 cm^{-1} band of Ac-Ala-$NHCH_3$ in TFE may arise from the C_7 H-bond acceptor carbonyl of a more or less well-defined γ-turn. The IR spectra of Ac-Pro-$NHCH_3$ and Ac-Pro-OCH_3 in CH_2Cl_2 show the $\nu_{C=O}$(Ac) band at 1624 and 1647 cm^{-1}, respectively (Figure 6). These results suggest that H-bonded γ-turns in diamides absorb at around 1622−1624 cm^{-1}, while nonbonded γ-turn structures absorbs at higher wavenumbers (greater than 1645 cm^{-1}).

7.2. Detection of γ-Turns in Cyclic Peptides

Similar to β-turns, γ-turns were first studied by vibrational spectroscopy in cyclic peptides with well-established steric structure. A selection of naturally occurring and synthetic cyclic peptides is shown in Table 3. Cyclosporin A (CSA) **42a** (Chart 7), a cyclic

Table 7. Amide I Component Bands in the Curve-Fitted Spectra of Diamide Models Ac-Xxx-NHCH$_3$ and Their ^{13}C-Labeled Derivatives in Different Solvents[a]

diamide model	derivative	solvent	$\nu_{C=O}$ (Xxx)/cm^{-1}	$\nu_{C=O}$ (Ac)/cm^{-1}
Ac-Ala-NHCH$_3$	unlabeled	D_2O	1636s[b](~1642)	(~1628)
	Ac(^{13}C)		1642s	1588s[b]
	unlabeled	TFE	1671s[b], 1646s[b]	(~1657, ~1639), 1622m
	Ac(^{13}C)		1671s, 1646s	1620m, 1602w, 1585m
	unlabeled	DMSO	1681m	1665s[b], 1641w
	Ac(^{13}C)		1677s, 1662m	1630s, 1616w
	unlabeled	CH_2Cl_2	1681s	1664s
	Ac(^{13}C)		1681s, 1667w	1648w, 1626s
Ac-Pro-NHCH$_3$	unlabeled	D_2O	1643s	1608s
	Ac(^{13}C)		1643s	1569s
	unlabeled	TFE	1671m, 1641s[b]	(~1630), 1624w, 1605s
	Ac(^{13}C)		1671m, 1645s	1593m, 1568s
	unlabeled	DMSO	1679m, 1665m	1645s
	Ac(^{13}C)		1680m, 1665m	1602s
	unlabeled	CH_2Cl_2	1676s, 1651m[b]	(~1652, ~1640), 1624m
	Ac(^{13}C)		1676s, 1654w	1615w, 1603m, 1586m

[a] Values in parentheses indicate theoretical band positions derived from the expected isotopic shifts. [b] Bands containing the contribution of two (or more) overlapping amide I component bands which could not be resolved by FSD. Abbreviations: s, strong, m, medium, w, weak.

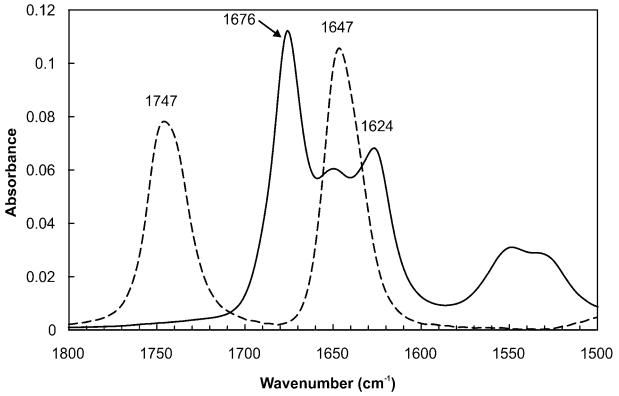

Figure 6. FTIR spectra of Ac-Pro-NHCH$_3$ (—) and Ac-Pro-OCH$_3$ (---) in CH_2Cl_2.

Chart 7

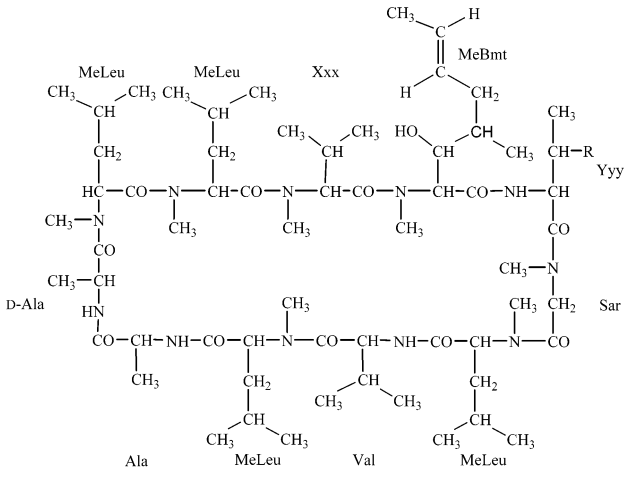

42

(**a**) cyclosporin A; Xxx = MeVal, Yyy = Abu (R = H)
(**b**) cyclosporin C; Xxx = MeVal, Yyy = Thr (R = OH)
(**c**) cyclosporin D; Xxx = MeVal, Yyy = Val (R = CH$_3$)
(**d**) cyclosporin H; Xxx = D-MeVal, Yyy = Abu (R = H)

undecapeptide has a γ-turn, centered at Ala^7, fixed by an IHB between the C═O of MeLeu^6 and N−H of D-Ala^8 as determined by X-ray, neutron diffraction, and NMR.[193] The analysis of IR spectra of four structurally related cyclosporines[193] **42** (CSA, CSC, CSD, and CSH) and their cation complexes[194] permitted indentifying γ-turn bands. The shoulder appearing at 1625 cm^{-1} in the amide I region was assigned as a superposition of the third H-bond of the dominant β-sheet and that forming the γ-turn (C^6═O←H−N^8). This band was affected by polar solvents (acetonitrile, DMSO). The CSH spectrum is unique: the band at ~1625 cm^{-1} is shifted to 1616 cm^{-1}, indicating a very strongly H-bonded C═O, likely due to strengthening of the γ-turn.[193]

Bridged cyclic peptides *cyclo*(Pro-Xxx-ϵ-Aca)$_n$ **33a**−**d** served as models for the interpretation of IR spectra of folded (β- and γ-turn) structures[100] (Table 3). In the spectrum of **33a** in acetonitrile, three component bands of comparable intensity were seen at 1648, 1631, and 1621 cm^{-1}. The 1648 cm^{-1} component was associated with weakly H-bonded or open γ-turns, while the 1621 cm^{-1} band corresponded to strongly H-bonded γ-turns. The 1631 cm^{-1} band was assigned to strongly H-bonded β-turn(s). In D_2O solution, the strongest component appears at 1674 (**33d**), 1641 (**33a**), and 1636 cm^{-1} (**33b**). In addition, the IR spectra of **33a** and **33b** exhibit a rather low-wavenumber band at 1595 and 1602 cm^{-1}, respectively. The IR spectrum of **33a** in TFE shows several amide I bands at 1673, 1641, and 1600 cm^{-1}. It was concluded that the presence of the low-wavenumber component band may be related to the strength of the solvent as H-bond donor. Another possible explanation is the formation of bifurcated H-bonds (see section 8).

IR and CD spectra of a selection of cyclic penta- and hexapeptides (**4**−**8**, section 5.4) adopting well-established β- or γ-turn conformation(s) were measured and compared (Table 3).[101a] Band assignment was assisted by conformational data inferred from NMR measurements and MD simulations.[101a,b] Due to geometric factors, cyclic pentapeptides generally form one β- and one γ-turn or two γ-turns, while cyclic hexapeptides normally adopt conformations containing two β-turns, but structures with one β- and one γ-turn or with two or more γ-turns have also been found. Consequently, roughly 40% of the total

integrated amide I area can result from intramolecular hydrogen-bonded carbonyls. However, relative band intensities cannot be interpreted quantitatively, since hydrogen-bonded and nonacceptor carbonyls have slightly different dipole moments and therefore give rise to IR absorption bands with different molar extinction. In general, the assignment of IR absorption bands appearing between 1641 and 1628 cm^{-1} to H-bonded β-turns was proposed. All D-proline-containing cyclopeptides presented an intense β-turn band, which was not significantly affected by changing the solvent from TFE to DMSO. This confirms the strong structure-inducing property of D-Pro, which leads to a βII′-turn arrangement with D-Pro in the $i + 1$ position. In contrast, in the case of compound **4b** which can theoretically form two identical H-bonded β-turns [(^{6}Ala)-C═O···H−N−(^{3}Ala) and (^{3}Ala)-C═O···H−N−(^{6}Ala)], the strong 1636 cm^{-1} band practically disappeared when TFE was replaced by DMSO, and at the same time a considerable intensity increase from 33% to 47% of the 1652−53 cm^{-1} band was observed. This indicates a lowering of the H-bond strength. A plausible explanation for this intense band can be the formation of a γ-turn incorporated in a distorted and consequently weakened β-turn in an "inverse bifurcated" manner (see section 8).

At this point an important question should be raised: which IR absorption band can be attributed to γ-turns appearing independently, that is, not incorporated into distorted β-turns? TFE spectra of many models show appreciable component bands below 1628 cm^{-1}, which can be clearly distinguished from the β-turn bands. Such low-wavenumber bands are seen even in the DMSO solution spectra, though with diminished intensities. Considering these facts, as well as similar findings previously published,[101a,193,194] it seems very likely that the region between 1625 and 1615 cm^{-1} is where strongly bound γ-turns occur. This region can reveal the presence of γ-turns in cyclic collagen sequence analogues[102] and in the cyclic lipopeptides[104−106] The amide I component bands of the cyclic lipopeptide mycosubtilin **39**, after deduction of side chain absorbances, appear at 1690−1689, 1658−1655, (the most intense), and 1613−1610 cm^{-1}. IR spectra of **39** in dry state and aqueous solution showed that the conformations are similar, suggesting that the IHBs are preserved even in solution. Hydration produced a slight intensity increase of the 1613−1610 cm^{-1} band which could be associated with a strongly hydrogen bonded amide group involved in bifurcated hydrogen bond with water and/or with the adoption of γ-turn(s) (section 8). Organic solvents such as DMSO and pyridine resulted in drastic IR changes in the spectrum of **39** that were explained by the breakage of IHBs. The remaining component band at 1638−1636 cm^{-1} corresponds to relatively strong H-bondings involving amide groups of the peptide backbone. The lowest-wavenumber amide I component band (1613−1610 cm^{-1}) in the IR spectrum of the natural antibiotic lipopeptide, mycosubtilin **39**, was assigned to the C═O group involved in an H-bonded γ-turn.[104c]

Chart 8

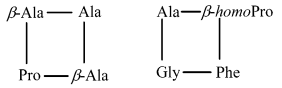

43 **44**

The best-suited models for conformational and spectroscopic characterization of γ-turns are cyclic peptides of the general formula *cyclo*(β-Ala-Xxx-β-Ala-Yyy) where Xxx and Yyy are Pro, Ala, or Gly residues. The simplest member of this series of 14-membered ring models is *cyclo*(β-Ala-Pro-β-Ala-Pro) with only two H-bond donor N−H groups. According to X-ray crystallography,[195a] both of its Pro residues are involved in inverse (γ_L^{eq}) turns with ϕ, ψ torsion angles −87.3°, 50.1° and −85.5°, 70.5°. ^{1}H and ^{13}C NMR studies confirmed the presence of two inverse γ-turns.[195] Other members of the family of cyclic tetramers are *cyclo*[Ser(O^{t}Bu)-β-Ala-Gly-β-Asp-(OMe)][196] and *cyclo*(β-Ala-Pro-β-Ala-Val).[197] The former model adopts no γ-turn conformation in the solid state, while the latter one has different conformation in the crystal and in solution (evidence of γ-turn). Chlamydocin [*cyclo*(Ala^1-Aib-Phe-D-Pro)] and its analogue Ala^4-chlamydocin[25,198] adopt inverse γ-turn conformation both in the crystal and in solution. Unfortunately, none of the above papers on cyclic tetrapeptides report IR data from the amide I spectral region.

In an attempt to understand the IR spectroscopic behavior of γ-turns in detail, we have synthesized 14- and 13-membered cyclic tetrapeptide models of γ-turns. The CD spectrum of *cyclo*(β-Ala-Ala-β-Ala-Pro) **43** (Chart 8) in acetonitrile is characterized by a positive $\pi\pi^*$ band at 193 nm and a negative nπ^* band at 228 nm, the latter being indicative of γ_L^{inv} conformations.[13] The shape of the CD spectrum is mostly unchanged in TFE, while it is somewhat different in D_2O (negative band at 217 nm with a negative shoulder at 202 nm) suggesting a mixture of conformers in the latter solvent.[199b] The CD spectra of **43** in TFE and acetonitrile[199a,b] are practically identical with those of *cyclo*(β-Ala-Pro-β-Ala-Pro) reported by Tamaki et al.[195b] suggesting that *cyclo*(β-Ala-Ala-β-Ala-Pro) is also present as a main conformer containing two H-bonded γ-turns (Figure 7).

NMR data obtained in TFE,[199c] 6-31G*/B3LYP DFT calculations,[199b,c] as well as FTIR spectroscopic data[199] are in agreement with this assumption. The amide I region of **43** shows 3−4 component bands, depending on the solvent (see Table 8 and Figure 8), from which the low-wavenumber and medium-intensity band, characteristic for H-bonded γ-turns, appears at ∼1624 cm^{-1} in aprotic solvents (acetonitrile, CH_2Cl_2, DMSO). According to the normal-mode analysis of the main conformer, the lowest-wavenumber band can be assigned to the >C═O of β-Ala^3 preceding the Pro^4 residue and forming a C_7 H-bond with the NH of β-Ala^1. This band is downshifted to 1604 and 1615 cm^{-1} in TFE and D_2O, respectively, suggesting strong solvation with formation of bifurcated H-bonds. The weak band at 1642 cm^{-1} appearing in the spectrum obtained in acetonitrile (Figure 8) can be related to the less stable γ-turn, centered at Ala^2.

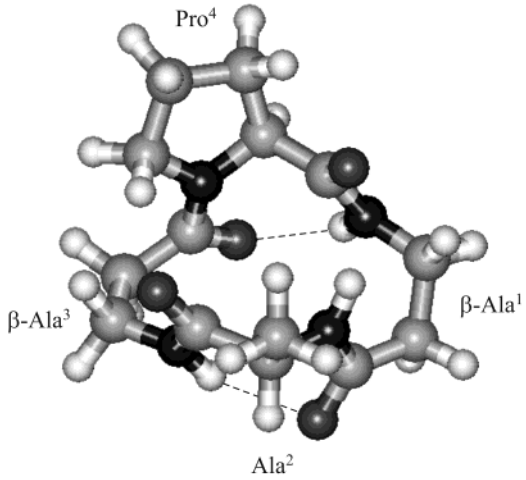

Figure 7. Steric strtucture of the main conformer of *cyclo*(*β*-Ala-Ala-*β*-Ala-Pro) **43** featuring two inverse *γ*-turns.

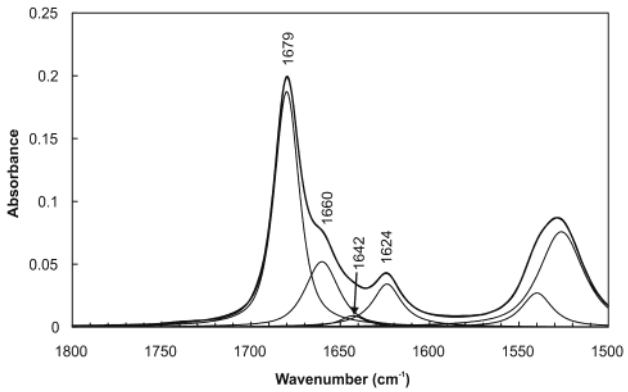

Figure 8. Curve-fitted FTIR spectrum of *cyclo*(*β*-Ala-Ala-*β*-Ala-Pro) **43** in acetonitrile.

In the 13-membered model *cyclo*(Ala-*β*-*homo*Pro-Phe-Gly) **44**, the presence of the *β*-*homo*Pro residue increases the flexibility to some extent allowing the formation of various intramolecular H-bonds. The presence of a strong amide I component band at 1636 cm^{-1} in acetonitrile and a medium-intensity band at 1622 cm^{-1} in TFE is compatible with *γ*-turn structures.[199a,b] Formation of a *pseudo*-*γ*-turn with C_8 intramolecular H-bond encompassing the *β*-*homo*Pro residue was proposed from the interpretation of IR spectrum of **44** in TFE (band at 1648 cm^{-1}) and acetonitrile (band at 1658 cm^{-1}), the position of these bands indicating weak H-bonds.

Antifreeze proteins (AFPs) from overwintering larvae of the beetle *Dendroides canadensis* (DAFPs) are among the most active AFPs known. DAFPs consist of 6- or 7-, 12-, or 13-mer repeat units with a consensus sequence of −C-T-X^3-S-X^5-X^6-C-X^8-X^9-A-X^{11}-T-X^{13}−. Nearly all of the Cys residues are in internal disulfide bridges between positions 1 and 7 within the repeats resulting in a polycyclic peptide structure.[200] The spectra measured under different conditions showed no major changes. Component bands at 1623, 1636, and 1642 cm^{-1} were associated with *β*-sheet, while other bands located at 1677 and 1684 cm^{-1} were assigned to turns. Alternatively, it is tempting to assign the 1623 cm^{-1} band to an IHB carbonyl group of *γ*-turns.

In conclusion, the amide I acceptor band of H-bonded *γ*-turns appears around 1635−1610 cm^{-1} (weak or less stable IHB *γ*-turns absorb in the 1635−1625 cm^{-1} range). Bifurcation (one acceptor C═O and two hydrogen-bond donors such as N−H groups, water, or TFE) may shift the band around 1615−1600 cm^{-1}. The less characteristic bands above 1648 cm^{-1} (1690−1647 cm^{-1}) may reflect non or weakly hydrogen-bonded carbonyl groups of *γ*-turns.

7.3. Detection of γ-Turns in Midsize Peptides and Proteins

Amide groups in *β*-pleated sheets give rise to highly diagnostic bands between approximately 1640 and 1620 cm^{-1}, although in some *β*-aggregates the "*β*-bands" are shifted even below 1620 cm^{-1}.[14] The IR spectra of midsize peptides and proteins are generally measured in water (D_2O or H_2O) or aqueous buffers. Thus, in the spectra of proteins with a substantial (>10%) *β*-sheet content, the *γ*-turn band is superimposed or overlapped by the much stronger amide I component of *β*-sheets or *β*-aggregates. In cases when, according to X-ray crystallography or NMR, *β*-sheets are not present, an amide I component near

Table 8. Characteristic Amide I Wavenumbers of Selected 14- and 13-Membered Cyclic Tetrapeptides Containing *β*-Amino Acids

peptide	FTIR approach	other methods used	type of folded structure	characteristic amide I wavenumbers/cm^{-1}	ref
cyclo(*β*-Ala-Ala-*β*-Ala-Pro) **43**	amide I (TFE, CH_3CN, CH_2Cl_2, DMSO, D_2O)	NMR (TFE), CD (TFE, CH_3CN, H_2O)	two inverse *γ*-turns centered at Pro and Ala in the main conformer	1672s, 1644s, 1604m[a] (TFE) 1679s, 1660m, 1642w, 1624m[a] (CH_3CN) 1678s, 1663m, 1624m[a] (CH_2Cl_2) 1676s, 1656m, 1623m[a] (DMSO) 1673w, 1649s, 1632m, 1615m[a] (D_2O)	199
cyclo(Ala-*β*-*homo*Pro-Phe-Gly) **44**	amide I (TFE, CH_3CN)	CD (TFE, CH_3CN)	*γ*-turn, pseudo-*γ*-turn (C_8)	1674s, 1648m, 1622m[a] (TFE) 1692s, 1672m, 1658m, 1636s[a] (CH_3CN)	199a,b

[a] Bands assigned to H-bonded *γ*-turns (C_7); in protic solvents, low wavenumbers indicate strong solvation. Abbreviations: s, strong, m, medium, w, weak.

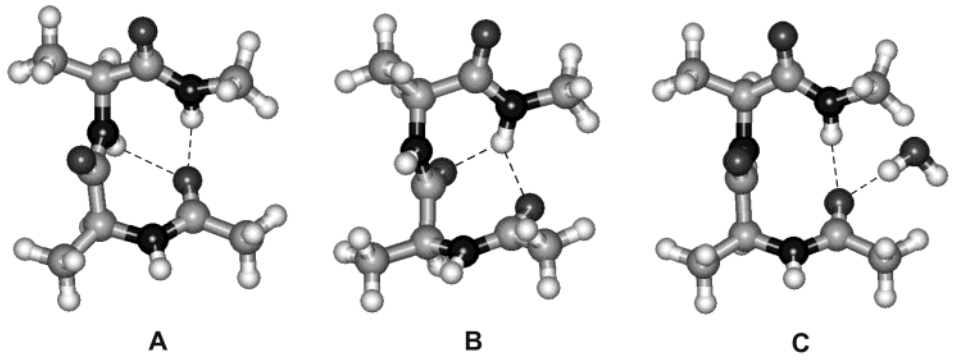

Figure 9. Turn structures with three-center (bifurcated) H-bonds. Bifurcation between two donor N−H groups and one acceptor C═O (A). Bifurcation between two acceptor C═O groups and one donor N−H ('inverse bifurcation') (B). Bifurcation with the participation of a water molecule (C).

1630 cm^{-1} or below in IR spectra may be a sign of γ-turns or their repeats.

Midsize peptides are, in general, structureless in water or aqueous buffers. Their conformational preferences are usually monitored by CD, FTIR, or NMR spectroscopy in fluorinated solvents (TFE or HFIP). These solvents are well-known to stabilize the intramolecular H-bondings of α- or 3_{10}-helices and turns[86] and break the intermolecular H-bondings of β-sheets. Consequently, amide I components in the IR spectra of midsize peptides near or below 1640 cm^{-1} are a sign of the presence of turns. A component between 1645 and 35 cm^{-1} can be associated with β-turns and those below 1635 cm^{-1} with γ-turns or turns with bifurcated H-bondings (see also sections 5 and 8). This spectral region is clearly separated from that of a typical α-helix. CD experiments in the same solvent are recommended to confirm the presence of turns and NMR measurements to localize them.

The repeating sequences of elastin are the pentapeptide VPGVG and the hexapeptide VAPGVG. Boc- and Ac-protected penta- and hexapeptide benzylesters or methylamides, their polymers and analogues comprising S-α-hydroxyisovaleric acid (Hiv) instead of the second valine **28**, have been synthesized. ^{1}H NMR, CD, and FTIR spectroscopy[92] suggested the adoption of β- and/or γ-turns comprising the Pro and Hiv residues. In the IR spectra of elastin peptides and depsipeptide analogues, the bands located between 1646 and 1634 cm^{-1} were associated with β-turns, while those between 1632 and 1628 cm^{-1} with inverse γ-turns.[92] CD spectra recorded in TFE at different temperatures and concentrations showed a negative band between 220 and 230 nm characteristic of inverse γ-turns.[25]

Active antifreeze glycopeptides (AFGPs), with a molecular mass range of 20−33 kDa, have the same basic repeat unit of Ala-Thr-Ala. Raman spectra of AFGPs were measured between 1700 and 1000 cm^{-1} in water and D_2O.[202] On the basis of a theoretical comparison, a γ-turn motif was proposed as a plausible conformation for AFGPs. The amide I bands were observed at 1684, 1667, and 1648 cm^{-1} suggesting non H-bonded γ-turn.

Although the experimental evidence is scarce in the case of proteins, the assignment of γ-turn as proposed in the case of cyclopeptides and small peptides could be also relevant for larger peptides and proteins.

8. Three-Center (Bifurcated) H-Bondings

There are two types of three-center or bifurcated H-bondings: (1) bifurcation between two H-bond donor N−H groups and one H-bond acceptor C═O group and (2) bifurcation between two H-bond acceptor C═O groups and one H-bond donor N−H group (termed "inverse bifurcation" herein) (Figure 9). Molecules of solvent may participate in bifurcated H-bondings: proton donors in the first type (bifurcation) and proton acceptors in the second one (inverse bifurcation). Water (or D_2O) may be involved in both types of three-center H-bondings.

A comparison of the temperature coefficients ($\Delta\delta/\Delta T$) of N−H protons in the ^{1}H NMR spectra and of the amide I (C═O) positions in the IR spectra may be of great help in investigating three-center H-bonded peptide structures. In DMSO solution of cyclic peptides, a low (<−2 ppb) $\Delta\delta/\Delta T$ value of the donor N−H proton in the ^{1}H NMR spectrum[24,25] and a high wavenumber (∼1650 cm^{-1}) component band of the possible acceptor amide groups is an indication of inverse bifurcation.[101a] The cyclic pentapeptide **4a** has the same conformation in DMSO and TFE on the basis of the IR spectra (Table 3). The lowest-wavenumber amide I components show up at 1648 and 1646 cm^{-1}, respectively. This indicates that no strong IHB is formed. The low value of the temperature coefficient of Ala^5 N−H in DMSO (−0.7 ppb) is due to inverse bifurcation. Contrary to this, there is a band located at 1618−15 cm^{-1} in the IR spectra of **6b**, **7**, and **8** in TFE. This band is completely missing in the spectra measured in DMSO. This observation suggests the presence of conformers with strong, but solvent-sensitive 1←3 IHB of γ-turns or bifurcated H-bonding.

The IR spectrum of *cyclo*(Pro-Ala-ϵ-Aca) **33a** in D_2O or TFE indicated a band located at around 1595 cm^{-1}, signaling a bifurcated H-bond with the participation of solvent molecules.[100]

The relative stability of three-center (bifurcated) H-bonds was monitored in the amide A region, on depsipeptide models comprising Pro and D-Lac (lactic acid) residue Ac-Gly-Pro-D-Lac-$NHCH_3$ **45a**−**c** (Chart 9).[203] The IR data (see section 9, Table 10) suggest that each of the two-centered IHBs in **45a**,**b** may be

Chart 9

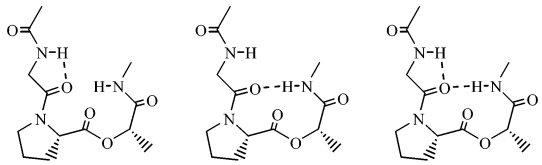

45

weakened because both of the bands assigned to H-bonded NH groups occur at significantly higher (9−16 cm^{-1}) wavenumber than the corresponding bands of the reference compounds. A van't Hoff analysis suggested that the bifurcated structure **45c** is ∼1 kcal/mol more enthalpically favorable but ∼3 eu less entropically favorable than the C_5 or C_{10} IHBs.

Bifurcated H-bondings likely play an important role in protein folding. A bifurcated H-bonding, mediating between a C_{10} H-bonded β-turn and a C_7 γ-turn, assists in opening-up of hairpin structures. By contrast, inverse bifurcation helps to replace a γ-turn by a β-turn and thereby to fold polypeptide chains. It has been proposed that the helix→coil unfolding is promoted by insertion of a water molecule into the α-helix 5→1 H-bonding via initial formation of a transient external or three-center H-bonding system.[204] This leads to the formation of a repertoire of hydrated reverse turns connecting the α- and β-regions and so might facilitate the extremely rapid α↔β "flickering", as sensed by ROA (see section 10).

9. Infrared Spectroscopy of Peptidomimetics

A great variety of biologically active peptides have been discovered and characterized during the last 30 years. They are of enormous medical interest and the number of native or modified peptides used as drugs is constantly increasing. However, the use of peptide drugs is limited by the following factors: (a) low metabolic stability toward proteolysis; (b) poor absorption after oral digestion; (c) rapid excretion through liver and kidneys; and (d) side effects caused by interaction with various receptors due to their conformational flexibility.

Peptide chemists have made great efforts to develop peptidomimetics that display more favorable pharmacological properties than their prototypes.[15] A peptidomimetic is a compound that, as the ligand of a receptor, can imitate or block the biological effect of a peptide. As the ligand of an enzyme, it can serve as substrate or inhibitor.

It is ironic that there are only a few examples [angiotensin converting enzyme (ACE) inhibitors, cholecystokinin antagonists (CCK), etc.] of peptide-based drugs which are in therapeutic use. The opioid alkaloids are classic examples of rigid nonpeptide ligands which were later discovered to be mimetics of endogenous peptides. In addition to morphine, there are many other known drugs whose peptidomimetic character has already been demonstrated.[15a]

Strategies for the synthesis of peptidomimetrics involve (i) modification of the structure and/or configuration of the amino acids, (ii) application of dipeptide analogues, lactames or oxopiperazines, (iii) bridging neighboring amino acids, and (iv) using dipeptides with cis configuration of the amide group. Another approach is the modification of the peptide backbone by (a) replacement of the amide bond by the −CH=CH−, $-CH_2-NH-$, or −CS−NH− group or application of (b) retro-inverso isomers and (c) vinilogues, etc. The most promising idea is the global restriction in the conformation of a peptide through cyclization (formation of a disulfide bridge or an amide bond between the side chains of Lys and Asp or Glu, or connecting two Lys ϵ-NH_2 groups with a succinate bridge).

A secondary structure mimetics is a building block that forces a defined secondary structure after its incorporation into a peptide. The basic requirement of such a mimetics is that the synthesis should permit the introduction of the desired side chains in a sequential and steric position that is necessary for receptor binding. Because of the limited size of the drug candidate, the best choice from peptide secondary structures is turns. The β-turn is the most frequently imitated secondary structure but there are several examples also for γ-turn mimetics.[15,205]

Another critical feature is the topography of the side chains of constituting amino acid residues, often referred to as chi (χ) space.[15b] Each side chain χ^1 torsion angle (Figure 1) (and some of the following torsion angles in longer side chains, χ^2, χ^3, etc.) can assume three low energy staggered conformations (rotamers): −60° [gauche (−), g−], +60° [gauche (+), g+]; and ±180° [trans, t]. In a chain of four or five residues, different dispositions of side chain groups in terms of χ^1 space will give rise to a great diversity of the 3D recognition surface ("pattern of key") even with a single backbone conformation. Introducing an alkyl group at the β-position or on the ring of an aromatic residue will constrain both χ^1 and χ^2, respectively. These modifications also enhance the lipophilicity of the peptide. Extra alkyl groups can thus help in overcoming blood-brain barrier or other membrane barrier problems.

Turn mimetics, in particular cyclic ones, are valuable lead structures because they are easy targets of structure-biological function studies. In linear peptides (and proteins) turns arise mainly due to the inherent tendency of the constituting amino acids to form intramolecular H-bondings. Thus, vibrational spectroscopy is the method of choice for the screening of turn mimetics and performing preliminary structure−activity investigations.

The simplest backbone-modified peptide mimetics are thiopeptides comprising thioamide (−CS−NH−) group(s) in midchain or terminal position. A great number of linear thiopeptides[206] and thionated turn mimetics has been described and characterized by IR, ^1H, ^{13}C NMR and CD spectroscopy.[207] It was found that thionated peptides can adopt highly populated thioturn conformation in $CHCl_3$ or CH_2Cl_2 solution. Thioturns may be fixed by mixed amide−thioamide or pure thioamide−thioamide IHBs. The relative strength of thioamide IHBs were characterized by the amide A wavenumbers (Table 9). These studies proved that the thioamide group is not only an

Table 9. Amide A Data on Intramolecular H-Bonds in Thiopeptides and Hydrazonopeptides

intramolecular H-bond acceptor−donor	conformation (ring size)	model	solvent	ν(NH),[a] cm^{-1}	ref
−C═O···H−N−CS−	C_5	Act-Ala-OCH_3	CCl_4	3390	207
		Act-Ala-$NHCH_3$	CH_2Cl_2	3380	
	C_7	Ac-Alat-$NHCH_3$	CH_2Cl_2	3325	
	C_{10}	Boc-Pro-Glyt-$NHCH_3$	CH_2Cl_2	3283	
		Boc-Ala-Glyt-$NHCH_3$	CH_2Cl_2	3300	
−C═S···H−N−CO−	C_5	Boc-Alat-$N(CH_3)_2$	CCl_4	3378	207a−c
	C_7	Act-Ala-$NHCH_3$	CH_2Cl_2	3355	
		Act-Pro-$NHCH_3$	CH_2Cl_2	3345	
	C_{10}	Act-Pro-Gly-$NHCH_3$	CH_2Cl_2	b	
		Act-Ala-Gly-$NHCH_3$	CH_2Cl_2	b	
−C═S···H−N−CS−	C_5	Act-Alat-$NHCH_3$	CCl_4	3390	207a−c
	C_7	Act-Alat-$NHCH_3$	CCl_4	3357	
	C_{10}	Act-Pro-Glyt-$NHCH_3$	CH_2Cl_2	3271	
		Act-Ala-Glyt-$NHCH_3$	CH_2Cl_2	3287	
−NH−N···H−N−CO	C_5 (contributed by inverse bifurcation)	**53**, $n = 3$	$CHCl_3$	3338	215
	C_6	**52**, $n = 5$	$CHCl_3$	3430 (with amide A contribution)	

[a] ν_{free}(thioamide) = 3417 cm^{-1} (CCl_4), 3400 cm^{-1} (CH_2Cl_2).[207c] For ν_{free}(amide) data, see Table 10. [b] C_7 IHBs according to NMR. Abbreviations: Act, CH_3CS, Alat, thioalanine, Glyt, thioglycine, Prot, thioproline residues.

excellent donor but also a superior acceptor group of IHBs.[207]

Ac-, Z-, and Tos-protected Pro-substituted homochiral and heterochiral diprolines proved to be good models of β-turn-forming peptidomimetics.[78e] NMR and X-ray crystallography was used in combination with IR spectroscopy. According to the ^{13}C NMR spectra, the homochiral parent peptides Ac-Pro-Pro-$NHCH_3$ and Ac-Pro-Pro-NH_2 preferred to adopt a type VI β-turn with a *cis*-amide bond between the prolines. In the FTIR spectra, IHB NH and C═O bands were seen at 3335, 3322 and 1634, 1632 cm^{-1}, respectively. As expected, the heterochiral (L−D) dipeptides adopted a major type II β-turn conformation with a 1←4 H-bonding. Amide bands were measured at 3330 and 3335 cm^{-1} and 1628 and 1634 cm^{-1}, respectively (Table 10). 2-Methyl-D-proline in the $i + 2$ position and either a *cis*- or *trans*-3-methyl-L-proline in the $i + 1$ position was found to induce the same type II β-turn conformation as that identified experimentally for the unsubstituted heterochiral models. In contrast, placement of a *cis*-3-methyl-D-proline in the $i + 1$ position of homochiral (D,D) diprolines seems to change the conformational preference, whereas *trans*-3-methyl-D-proline stabilizes the predicted type VI′ β-turn (for IR data, see Table 10).

Toniolo and co-workers reported the synthesis and conformational characterization of a great number of peptide mimetics comprising α,α-disubstituted glycine(s).[208,209] The simplest dialkylated amino acid is α-amino isobutyric acid (Aib) **46** (Chart 10). Aib oligomers show a high tendency for adopting 3_{10}-helical (or repeating type III β-turn) conformation.[17] In the IR spectrum of peptides rich in Aib, the amide I band appears near 1660 cm^{-1}.[17b] A set of terminally protected model peptides to the pentamer level, comprising (αMe)Nva **47** or Nva **48**, in combination with Ala and/or Aib, was prepared.[208] Conformational analysis based on FTIR, ^1H NMR and X-ray diffraction techniques allowed to draw the conclusion that **47** is an effective β-turn and right-handed 3_{10}-helix former. Typically, the NH stretching vibration of H-bonded structures was observed at 3360 ± 20 cm^{-1}. In a series of papers, the synthesis and conformational characterization of protected peptides rich in cycloaliphatic $C^{\alpha,\alpha}$-glycines (Ac_nc, **49**) were also reported.[209] According to FTIR and ^1H NMR spectroscopy in $CDCl_3$ solution, the preferred conformation of these constrained models is β-turn or 3_{10}-helix (IHB band between 3387 and 3350 cm^{-1} for the higher members of the series).

The molecular structures of two Z-protected peptide esters comprising $Ac_{10}c$ (**49**, $n = 10$) were determined in the crystal state using X-ray diffraction. Peptides rich in $Ac_{10}c$ were also found to preferentially adopt β-turn or 3_{10}-helix conformation. Amide A bands were seen at 3433−3426 cm^{-1} (free, solvated NH groups) and 3375−3343 cm^{-1} (H-bonded NH groups). The relative intensity of the low-wavenumber band increased markedly parallel with the increase of chain length.[209e]

Infrared spectra of protected βII turn forming C_{60}-based fulleroproline peptides[210a] and protected aza-crown-functionalized 3_{10}-helical peptides[210b] were also recorded.

X-ray crystallographic, ^1H NMR, CD, and FTIR spectroscopic studies, as well as theoretical calculations, have been performed on various di- and triamide models comprising an α,β-dehydro amino acid residue [ΔAla, (*E*)- or (*Z*)-ΔAbu, ΔVal; **50**].[78b,211] Ac-Pro-(*E*)-ΔAbu-$NHCH_3$ was found to adopt a βII turn in the crystal.[212] Previous spectroscopic studies revealed that in solution Ac-Pro-(*Z*)-ΔAbu-$NHCH_3$ and also Ac-Pro-ΔVal-$NHCH_3$ prefer a βII-turn. Instead, according to X-ray crystallography, Ac-Pro-ΔAla-$NHCH_3$ adopts an extended conformation with the ΔAla residue in a C_5 form. On the basis of ^1H NMR spectroscopic studies and ab initio (6-31G**) calculations, ΔAla has a tendency to adopt extended conformation with a C_5 IHB, in contrast to other dehydroamino acids.[213] For amide A and amide I data, see Table 10. The amide II wavenumbers of the acceptor amide group of Ac-ΔXxx-$NHCH_3$ models range between 1524 and 1518 cm^{-1}. The only excep-

Table 10. Wavenumbers (cm^{-1}) of the Donor N−H and Acceptor C=O Groups of C_n Intramolecular H−Bonds in Peptides and Peptidomimetics

model[a]	solvent	free	C_5	C_6	C_7	C_8	C_{10}	C_{12}	C_{20}	remark	ref
Ac-Ala-OCH_3	CCl_4	3454									*b*
Ac-Ala-$NHCH_3$	CCl_4		3420 1684								207c
Ac-Ala-$NHCH_3$	CH_2Cl_2	3432(1) 3449(2) 1685(2)	3413		1672(1)						213
Ac-Ala-$NHCH_3$	CH_2Cl_2	3450(2) 1681(2) 3431(1) 1675(1)	3412(1) 1667(2)		3349(2) 1664(1)						*c*
Ac-Ala-$NHCH_3$	CH_3CN	− 1684(2)	3375(1)		3402(2) 1673(1)						213
Ac-Gly-$N(CH_3)_2$	CH_2Cl_2		3406								213
Ac-Pro-$NHCH_3$	CCl_4	3454	−								*b*
Ac-Pro-$NHCH_3$	CH_2Cl_2	3454 1672 1653	−		3333 1626						78e
Ac-Pro-$NHCH_3$	CH_2Cl_2	3452−42	−		3329−10						78c
Ac-Pro-$NHCH_3$	CH_2Cl_2	3448(2) 1652(1) 1640(1) 1676(2) 1654(2)			3327(2) 1624(1)						*c*
Ac-ΔAla-$NHCH_3$	CH_2Cl_2	3466(2) 1698(1) 1674(2)	3379(1) 1663(2)								213
Ac-ΔVal-$NHCH_3$	CH_2Cl_2	3431(1) 3449(2)	3408(1) −		1634(1)						213
in well-established β-turns	CCl_4	− −					3350(2)				24a
Ac-Pro-D-Pro-$NHCH_3$	CH_2Cl_2	*d* 1661[e]					1628(1)			βII-turn	78e
Ac-ProPro-$NHCH_3$	CH_2Cl_2	3450(2) 1659					3335(2) 1634(1)			60% βVI -turn	78e
Ac-GlyPro-OEt	CH_2Cl_2		3411(1) −								203
Ac-Pro-(*S*)-Lac-$NHCH_3$	CH_2Cl_2						3334(2) −				203
Ac-GlyPro-(*S*)-Lac-$NHCH_3$ **45**	CH_2Cl_2	3451 −	3420[f] −				3360 −				203
Ac-D-Pro(2-Me)-$NHCH_3$	CH_2Cl_2	3476[e] 3461 1667[e] 1647			3301(2) 1630(1)						78e
Ac-Pro-ΔAla-$NHCH_3$	CH_2Cl_2	3465(2) 1670[e]			3364(2)[e] 1633(1)[e]						212
Ac-Pro-(*E*,Z)-ΔAbu-$NHCH_3$	CH_2Cl_2						3350(2) 1630(1)				78b, 211
Pr^iCO-*trans*-ACHC-$NHCH_3$	CH_2Cl_2	>3425 −				3357 −					217
Pr^iCO-*trans*-ACPC-$NHCH_3$	CH_2Cl_2	>3425 −				3306 −					217
H-(*cis*-ACPC)$_n$-NH_2, $n = 3, 5, 7$	CH_2Cl_2 DMSO	− >1680		1645 1670							218
dinipecotic acid peptides **58-64**	CH_2Cl_2	3454−49 (NH^3) 3425−21 ($NH^{1,2}$)									216
58								3333 (3373)[e]	3373 (3333)[e]		
60								3337 (3378)[e]	3378 (3337)[e]		
59, **61**, **63**, **64**								3342− 3337[g]	3342− 3337[g]		

[a] Numbers in parentheses indicate amide group positions: 1, N-terminal, 2, C-terminal. [b] Burgess, A. W.; Scheraga, H. A. *Biopolymers* **1973**, *12*, 2177. [c] Data based on FSD analysis of Ac(^{13}C) derivatives (see also ref 192 and Table 7). [d] Not observed. [e] Not assigned or uncertain assigment. [f] Alone or bifurcated. [g] Unresolved.

tion is Ac-ΔAla-$NHCH_3$ with an amide II component at 1536 cm^{-1}.

The temperature coefficients of amide protons, characteristic NOE patterns, restrained MD simulation and quantum chemical calculations defined a βII turn preference of azaLeu **51** (Chart 11) in the model peptide, Boc-Phe-azaLeu-Ala-OCH_3.[214] In the IR spectrum of the azatripeptide in CCl_4, an intense amide A band between 3400 and 3375 cm^{-1} was assigned to N−H(Ala) involved in C_{10} IHB. No band below

Chart 10

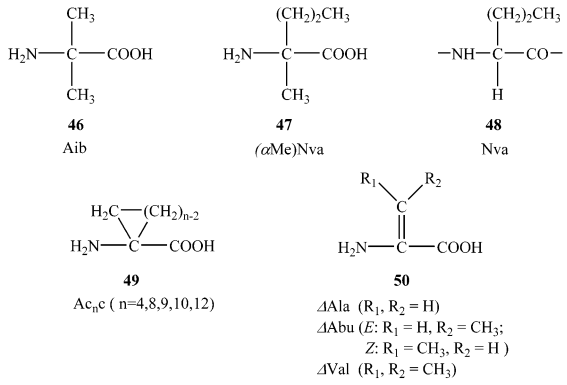

Chart 11

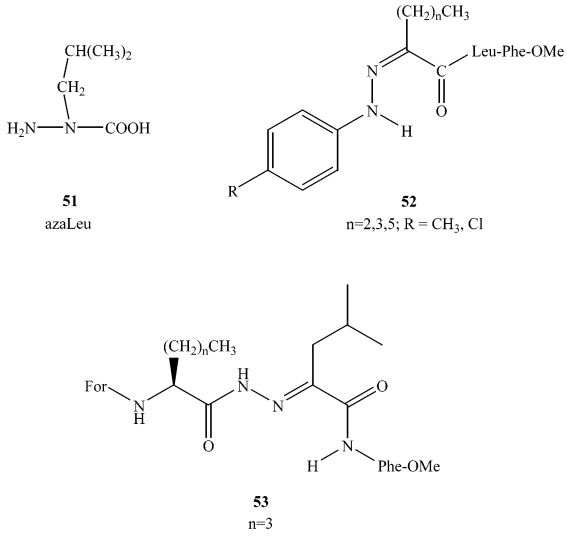

Chart 12

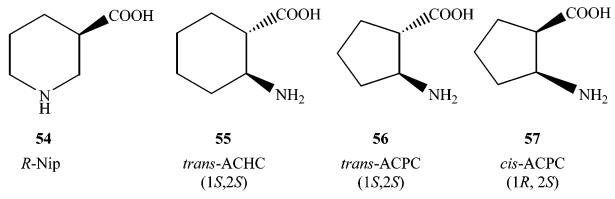

3400 cm^{-1} was observed in the spectrum of the reference tripeptide Boc-Phe-Leu-Ala-OCH$_3$. Therefore, introduction of the azaamino acid residue into the $i + 2$ position in synthetic peptides is expected to provide a stable β-formation, and this could be utilized in the design of new β-peptidomimetics.

IR data have been reported on pseudopeptides containing the 2-hydrazonoacyl fragment **52**, **53**.[215] The possible formation of C_6 (**52**) and C_5 (**53**) IHBs was suggested by ^{1}H NMR data. For IR data, see Table 9. The band at 3338 cm^{-1} can be assigned to C_5 IHB reinforced by the participation as H-bond acceptor of the preceding amide C=O (inverse bifurcation).

Gellman and co-workers have described the synthesis of a series of diastereomeric β-peptides to elucidate the effect of the configuration of piperidine-3-carboxylic acid (nipecotic acid, Nip, **54**, Chart 12).[216] Reverse turn structures with all four configurations of Nip [(*R*,*S*), (*S*,*R*) (*R*,*R*), and (*S*,*S*)] **58**−**64** (Chart 13) were prepared while the strand residues were kept constant (**58**−**62**) or replaced by β-Ala (**63**, **64**). The conformation of the tetra-β-peptides was inferred from ^{1}H NMR data and, for **62** and **63**, from X-ray crystallography. In the crystal structure of **63**, the C_{18} H-bonded "outer ring" is replaced by a C_{20} IHB like in **62**, while the size (C_{12}) of the "inner ring" is retained in all structures. Amide A band frequencies in CH_2Cl_2 of the tetra-β-peptides are listed in Table 10. According to ^{1}H NMR data (NH temperature coefficients) and relative intensities of the amide A IR bands, all tetra-β-peptides are present in CH_2Cl_2 as a mixture of open and β-hairpin conformers. The population of the C_{12} and C_{20} (or C_{18}) H-bonded β-hairpins is definitely higher in the heterochiral [(*R*, *S*) or (*S*, *R*)] structures **58**, **59**, **62**, and **63**. The heterochiral (*R*, *S*) and homochiral (*R*, *R*) structures comprising β-Ala (**63** and **64**) show quite different conformational preference. **63** features a highly populated C_{12}, C_{18} double H-bonded β-hairpin structure, while **64** experiences very little IHB. On the basis of the studies discussed above, tetra-β-peptides with a heterochiral [(*R*, *S*) or (*S*, *R*)] Nip−Nip core are superior turn-formers to the homochiral [(*R*, *R*) or (*S*, *S*)] ones.

A modified force field (AMBER*C) was elaborated to improve the treatment of the conformational preferences of *trans*-2-aminocyclohexanecarboxylic acid (*trans*-ACHC, **55**) and *trans*-2-aminocyclopentanecarboxylic acid (*trans*-ACPC, **56**).[217] Qualitative comparison of the amide A region of the IR spectra in CH_2Cl_2 of N-isobutyryl methylamide derivatives of **55** and **56** indicated that the *trans*-ACPC derivative experiences more C_8 IHB than does the *trans*-ACHC derivative. The amide A band of the C_8 H-bonded derivatives of **55** and **56** appears at 3357 and 3306 cm^{-1}, respectively, suggesting that the C=O and H−N in the ACHC model are not oriented as favorably for a strong hydrogen bond as in the ACPC derivative.

In the amide I region of the FTIR spectra of the diasteromeric *cis*-(1*R*,2*S*)-2-aminocyclopentane carboxylic acid (*cis*-ACPC, **57**) oligomers (n = 3, 5, 7), the strongest band appears at ∼1645 cm^{-1} in CH_2Cl_2.[218] In DMSO the ∼1645 cm^{-1} band is replaced by a shoulder at ∼1653 cm^{-1} in the spectrum of the pentamer (n = 3) and appears with decreased relative intensity in the spectrum of the heptamer (n = 5). DMSO is well-known to destroy weak IHBs. On the basis of its absence or decreased intensity in the FTIR spectra in DMSO, the band at ∼1645 cm^{-1} can be assigned to repeats of C_6 IHBs. The high-wavenumber (>1660 cm^{-1}) component bands in the curve-fitted spectra which appear in many cases as shoulders in the experimental spectra in CH_2Cl_2 or DMSO belong to amide CO groups not involved as acceptor in H-bonding. In the amide A (NH stretching) region of the FTIR spectra measured in CH_2Cl_2, a strong asymmetric band turns up near 3300 cm^{-1}. (Note that the ν_{NH} band of strong C_6 IHB appears at 3306 cm^{-1} in the spectrum of *trans*-ACPC models.[217]) Its position suggests that the majority of NH groups of the oligomers (n = 3, 5, 7) is involved in strong IHB. On the basis of ^{1}H NMR (TOCSY, ROESY) measure-

Chart 13

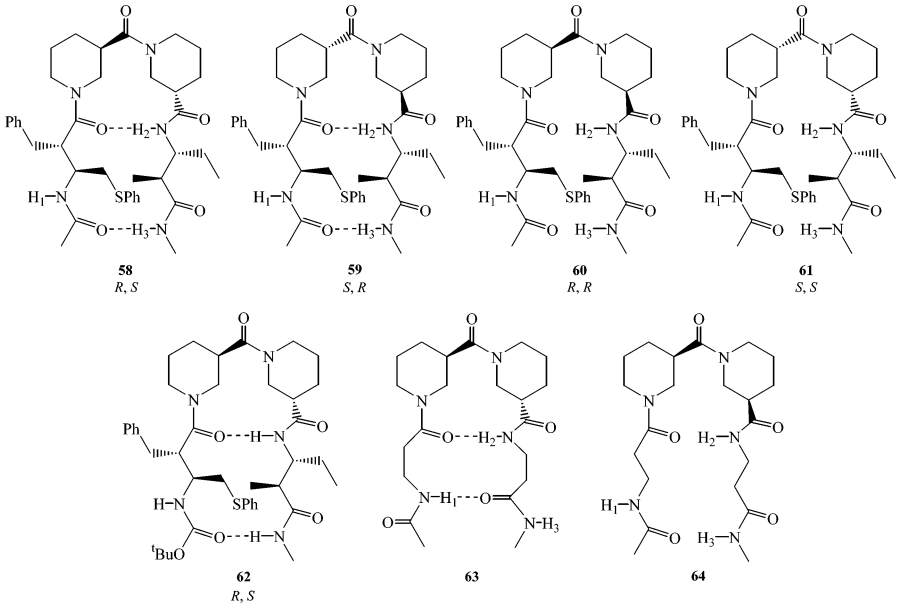

ments and restrained MD simulations, *cis*-ACPC oligomers adopt in apolar solution an extended conformation stabilized by intraresidual C_6 IHBs.

Many IR spectra of peptidomimetics were analyzed in the amide A region, providing strong experimental evidence of the presence of IHB in β-turn-forming peptidomimetics. The amide A band located around 3440−3400 cm^{-1} signals free backbone NH groups, while the band between 3400 and 3300 cm^{-1} indicates hydrogen-bonded NH groups. The amide I region, especially around 1645−1635 cm^{-1} permitted, as in the case of peptides and proteins, to detect the presence of β-turn structures.

10. Vibrational Optical Activity (VOA) of Turns

Vibrational optical activity (VOA) is due to the differential response of a molecule to left-circularly polarized (LCP) versus right-circularly polarized (RCP) radiation during a vibrational transition.[219,220] There are two principal forms of VOA, an IR form referred to as vibrational circular dichroism (VCD) and a Raman form known as Raman optical activity (ROA). ROA is measured as circularly polarized (CP) intensity differences in the incident laser radiation, the scattered radiation, or both. As with CD, VOA is zero unless the sample possesses molecular chirality. Both VCD and ROA are very sensitive to the stereochemical features of chiral molecules, and they have similar differences and advantages to their parent spectroscopies, IR absorption, and Raman scattering. In fact, neither VCD nor ROA can be successfully measured unless an excellent parent IR or Raman spectrum can first be measured. The availability of commercial instrumentation for VCD and ab initio molecular orbital software for VCD intensity calculation in Gaussian 98 from Gaussian Inc. have hastened the advance of VCD for widespread application in chemistry and biochemistry.

Perhaps the simplest application of VCD spectroscopy is the determination of the optical purity of a sample of a chiral molecule. The most promising area of application of VCD to stereochemical analysis is the determination of absolute configuration in solution.

VCD can also be used to monitor the conformation of a chiral molecule in various solution environments. For many years, VCD has been used to study the conformational properties of most classes of chiral molecules, particularly those of biological origin. In the case of biological macromolecules, the complexity of the structures of many of these molecules is currently beyond the scope of ab initio quantum methods. As a result, most of the research on biological molecules is concerned with the measurement of their spectra and the interpretation of the data using simple empirical analysis.

This section deals mainly with the application of VOA in detection of turns and related structures in proteins and peptides. For other applications and more details on the theory, practice and instrumentation of VCD and ROA, see refs 219−224.

The first attempts to measure VCD spectra of biopolypeptides dealt with synthetic α-helical homopolypeptides. The amide I band (amide I′ in D_2O) is the most characteristic and easiest way to monitor VCD spectrum of polypeptides or proteins.[225a] The characteristic feature of α-helix VCD is a positive couplet with a more intense negative lobe and an additional weak negative band (Figure 10). The amide I′ VCD spectrum for the antiparallel β-sheet shows two separated negative bands, while a negatively biased negative couplet for the unordered form. In oligo- and polypeptide examples, the β-sheet is almost always an antiparallel β-stranded conformation of low solubility. This aggregated form is most easily recognized by its characteristic, widely split amide I′ band with a major, low-wavenumber feature at ∼1620−15 cm^{-1} and a weaker one at ∼1690 cm^{-1} (Figure 10, middle). For a revised interpretation, based on ab initio calculations, of the IR and VCD spectra of β-sheet-containing proteins, see ref 225b.

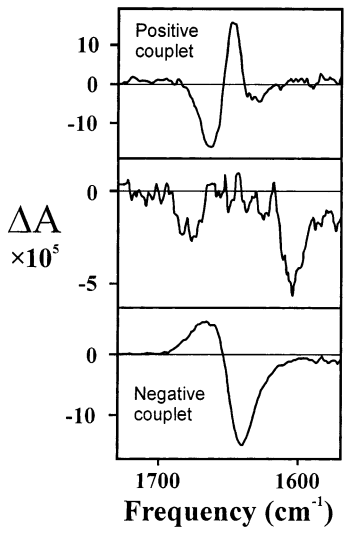

Figure 10. Amide I region of the VCD spectra of polypeptides or proteins in α-helix (top), β-sheet (middle), and unordered (bottom) conformation. (Note the differences in the absorbance scales.) Adapted from ref 225a, copyright 2000 John Wiley & Sons, Inc. Reprinted by permisson of John Wiley & Sons, Inc.

Because of the multiple transitions accessible in VCD, 3_{10}-helices and β-bend ribbons in oligomers can also be characterized on the basis of magnitude as well as band shape of amide I, II, and A bands.[83a,226] Aib-containing peptides were used for exploring the VCD characteristics of the 3_{10}-helix in nonaqueous solution. The amide I VCD couplet of the 3_{10}-helix has the same sign pattern (positive/negative) as that of the α-helix, but the amide I VCD is much weaker than the amide II VCD for the 3_{10}-helical peptides,[83,225a] while the opposite is true for the α-helix. This finding was also confirmed by ab initio density functional theory calculations of the amide I and II IR and VCD spectra for Ac-$(Ala)_4$-NH_2, Ac-$(Aib\text{-}Ala)_2$-NH_2, and Ac-$(Aib)_4$-NH_2.[83b] Peptides with the repeating $(Pro\text{-}Aib)_n$ sequence proved to be stable models for the β-bend ribbon structure[226] (see also section 5.2). VCD can also be used to characterize mixed $\alpha/3_{10}$-helical conformations.[225a]

The amide II transition can be studied in H_2O solution, giving it more utility than the amide A. There are distinct differences between the amide II VCD for α-helices (dominant negative) and that for β-sheet (negative couplet). Concerning the amide III region between ∼1350 and 1250 cm^{-1}, α-helices have mostly positive while β-sheets negative VCD.[225c] (For an analysis of amide III ROA, see the closing part of this section). The random coil form has a weaker and broader negative couplet.

Another situation in which VCD leads to improved interpretation of polypeptide structure is characterization of the unordered or random-coil form which in many cases gives rise to a large negative VCD couplet. VCD results support the early hypothesis based on ECD measurements that these structures can best be viewed as a left-handed, extended helix, that is poly(proline) II or PPII conformation.[227]

Table 11 contains the VCD characteristics of several synthetic peptides adopting different types of turn conformations. Cyclic peptides containing four to six amino acid residues are good models of β-turns and related structures. They exhibit relatively distinct VCD features, suggesting that VCD is extremely sensitive to local structures and it can distinguish between various turn conformations. Indeed, unique spectra of type I and II β-turns in cyclic peptides have been reported by Diem and co-workers[228,229] that differ from those of type III β-turns. A distinctive (−++−) pattern for the VCD of *cyclo*(Gly-Pro-Gly-D-Ala-Pro) **65** (Chart 14) was attributed to the βII-turn formed according to NMR data. The VCD spectra of a series of oxytocin analogues shows an intense negative band at ∼1630 cm^{-1} and a broad, possibly doubled weaker positive band at ∼1650 cm^{-1}. X-ray analysis indicates the adoption of a C_{10} H-bonded β-turn.[230]

Due to the relative large variety of VCD spectra in Table 11, it is difficult to suggest characteristic β-turn VCD features. However, the calculated and measured VCD amide I and amide II bands are in good agreement in the case of **65**.[231]

To take advantage of the detailed information available from VCD, it has been developed a new predictive method of secondary structures (including α-helix, β-sheet, turns and others), using statistical analysis of spectral data obtained from VCD, IR and ECD spectra. Combining IR and VCD data did not improve the prediction. However, the predictions were improved by combining both methods with ECD.[232] Although in the infancy, VCD spectroscopy combined with ab initio quantum mechanical calculation is a very promising approach to identify turns in peptides and proteins.

ROA is a very weak phenomenon, yielding small intensity differences.[233] Due to the extreme experimental difficulties and to the complexity of theoretical background, the development of ROA was concentrated in very few laboratories. However, the experimental difficulties were overcome several years ago, and high-quality ROA data can now be obtained routinely on biomolecules.[204b] A commercial ROA instrument is also available. A great advantage of Raman spectroscopy is that both H_2O and D_2O can be used as solvent.

The ROA vibrations of interest for conformational analysis of peptides and proteins are the backbone skeletal region (1150−870 cm^{-1}), the amide III region extended to at least 1340 cm^{-1} and the amide I region.[204b] (For an interpretation of amide I ROA bands, see ref 204b.)

The ROA bands in the amide III region often dominate the overall spectrum. In addition to the dominant in-phase combination of N−H deformation with the C_α−N stretch, the extended amide III region between ∼1340−1230 cm^{-1} involves mixing between the N−H and C_α−H deformations, and therefore, it is very sensitive to geometry. Indeed, characteristic ROA bands in the amide III region are described for various types of secondary structures.[234] Of particular interest is the finding that α-helical polypeptides which are intensively solvated with water show a strong positive ROA band at ∼1345−1342 cm^{-1}.[204b] Besides, α-helix also gives rise to positive ROA bands in the range ∼1297−1312 cm^{-1}. These additional

Table 11. VCD Spectroscopic Studies on Peptides Adopting Folded Conformations

peptide or protein[a]	VCD approach, solvent	other methods used	type of folded structure	frequency used for assignment, cm^{-1}	ref
Ac-Ala-$NHCH_3$, $(Ala)_3$	measurements between 1750 and 1550 cm^{-1}	−	folded str. stabilized by electrostatic interactions in A_3	coupled oscillator mechanism	230
GlyAla, AlaGly, AlaAla,$(Ala)_3$	CH-stretching pH dependence	−	C_5, C_7 structures based on the ring current mechanism	positive CH band	242
cyclo(Gly[1]ProGly-D-AlaPro)	amide I and II regions, $CDBr_3$	X-ray cryst., NMR, computations	β-turn and γ-turn	−++−[b] (s, m, m, w)[c] pattern, due to all-amide interaction	228
CysAlaCys and *cyclo*(CysAlaCys)	amide I region, $CDBr_3$/DMSO	−	γ-turn	broad negative VCD at ∼1690	229
cyclo$(ProGly)_3$	$CDBr_3$	X-ray, NMR, CD	γ-turn	strong positive couplet at ∼1642	
Cys[1]ProGlyCys	$CDBr_3$/DMSO	NMR	βII-turn	−++−(vw, m, m, s)	
cyclo(Gly[1]ProGly-D-AlaPro)	calculations using the degenerate two-state exciton approximation	X-ray cryst., NMR contact-distance calculations	calculations for 13 conformers comprising β- and/or γ-turns	agreement between calculated and measured amide I and II modes for the β- and γ-turn conformers	231
Piv(Ac)-Pro-$NHCH_3$	amide A region	−	C_7 γ^{eq}-turn	positive VCD at 3330	240
Piv-ProGly-$NHCH_3$			C_{10} βII-turn	positive VCD at 3345	
Piv(Ac)-ProGly-OCH_3			C_7C_5 conformer with bifurcated H-bond	positive VCD at 3300	
Boc-LVVpGLVV-OCH_3	Amide I		βII′-turn (β-hairpin)	negative VCD between 1659 and 43, weak positive VCD at ∼1693	241
Boc-LFVpGLFV-OCH_3					
Cys[1]ProGlyCys	measurements in different solvents, exciton-type calculations	FTIR	mixture of βI(III)- and βII-turns	∼1630 br positive in $CDBr_3$/DMSO positive couplet above 1660 in DMSO	243
Cys[1]ProPheCys	DMSO		βI(III)- and some βII-turn	∼1640 positive, positive couplet above 1670	
Cys[1]Pro-D-Phe-Cys	$CDBr_3$/DMSO		βII-turn	positive couplet with bands at ∼1640 and ∼1690	
cyclo(Gly[1]ProGly-D-Ala-Pro)	$CDBr_3$		βII-turn at P^2G^3 γ-turn at P^5	strong negative couplet at 1630−1650, positive couplet about 1660	

[a] Small letter codes mean D-amino acids. [b] From low to high wavenumbers. [c] s, strong; m, medium; w, weak; vw, very weak.

Chart 14

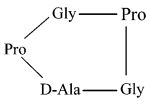

65

bands appear to be associated with α-helix in a more hydrophobic environment.[204b] The relative intensities of the positive amide III bands at ∼1340 and ∼1300 cm^{-1} reflect the ratio of the hydrated and hydrophobic variants of α-helix. (It should be mentioned here that the positive ∼1340 cm^{-1} band was earlier assigned to 3_{10}-helix). One recent suggestion is that a positive ROA band at ∼1268 cm^{-1} may be generated by 3_{10}-helix.[235] However, differences in the hydration states of 3_{10}-helix and turns (see later) may also results in distinct ROA bands in the extended amide III region.

The β-sheet amide III band appears at lower-wavenumber values. The negative ROA band at ∼1253 cm^{-1} originates in parallel β-sheet structures, while the negative band at ∼1246−44 cm^{-1} in the antiparallel β-sheet or β-strands.[204b] Some proteins containing β-sheet according to X-ray data also show a negative ROA band at ∼1220 cm^{-1}. This band appears to be a signature of a distinct variant of β-strand or sheet.[204b]

Higher-wavenumber bands (between ∼1380−1340 cm^{-1}) were suggested to originate in tight turns of the type found in β-hairpins and in up-and-down β-sheet motifs.[204b] It may be possible to distinguish parallel from antiparallel β-sheet because only the antiparallel form should show these negative ∼1380−1340 cm^{-1} ROA bands.

In the ROA spectra of disordered polypeptides or proteins an amide III band at ∼1325−1315 cm^{-1} can be assigned to hydrated PPII helical conformation[204b,233] Longer loops may also contain residues with ϕ and ψ torsion angles typical of PPII conformation. Protein X-ray crystallographic data in the PDB support the idea of the "nonrandomness" of loops.[236]

Amide III ROA bands associated with loops and turns appear in the 1295−1255 cm^{-1} range.[204b,235] A strong positive ROA band peaking at ∼1312 cm^{-1} with a broad shoulder extending to ∼1275 cm^{-1} was observed for metallothionein, a protein containing the most β-turns.[187c]

Since ROA spectra contain bands characteristic of loops and turns in addition to bands indicating periodic secondary structures, they should provide

information to deduce the motif types of supersecondary elements, or perhaps the domain superfold class from ROA band patterns, especially in the extended amide III region. The fold type and side-chain stereochemistry of major coat protein subunits of viruses may also be deduced from ROA spectra.[237] Because of its ability to detect loop and turn structures separately from periodic secondary structures, ROA is able to monitor delicate changes in protein folding. It appears to be the method of choice for revealing the structure of natively unfolded proteins,[238] which in some cases have a propensity to form the fibrils found in a number of neurodegenerative diseases.[238b,239] ROA may also be of great help in characterizing "nonnative" or "denatured" states ranging from the extended random coil to collapsed molten globules. Finally, since ROA spectra can be measured both in D_2O and H_2O solution, one of the benefits of ROA is that this method can provide information about hydrated variants of helices and turn structures.[204b]

11. Conclusions

Vibrational spectroscopy of polypeptides and proteins can reveal their overall structure and details of their local conformations resulting from the formation of hydrogen bonds or deformation of chemical bonds. The dual nature of information (global and local types)[14] obtained from IR and Raman spectroscopies allows to expand the application of vibrational spectroscopy to various chemical and biological problems but also to support the interpretation of vibrational spectra. Problems related with the contribution of turns to the vibrational spectra of polypeptides and with the estimation of turn content are discussed below.

(i) The assignment of amide vibrations of β-turn and γ-turn structures is based on the presence of different free and hydrogen bonded amide modes. β-Turn structures in small peptides and cyclopeptides can be identified on the basis of contributions in two amide I regions. The first band is located in the well-established high-wavenumber $\sim$1690−1660 cm^{-1} region (IR amide I/I′ band[14,74−76] and Raman amide I band[75a,77]). A second band may appear at 1645−1635 cm^{-1} (IR amide I/I′)[79,81] and at 1656−1644 cm^{-1} (Raman amide I band).[179,181−183] The 1690−1660 cm^{-1} band likely corresponds to the second and third free or weakely solvated amide carbonyl groups of β-turns (Figure 2), whereas the low-wavenumber band to the H-bond acceptor amide carbonyl group.[79,81] It is well-known that transition-dipole coupling induces splitting of the amide I band of antiparallel β-sheet structures,[14,75] while in the case of β-turns the origin of the two bands is probably related to the presence of free or weakly solvated and hydrogen-bonded amides.[79,81] In agreement with this, it was observed earlier that the IR intensity ratio of the 1690−1660 cm^{-1} and the low-wavenumber component bands may serve for distinguishing β-turns from β-sheet structures.[114,126] The infrared intensity ratio $I_{1690-1660}$: $I_{1645-1635}$ is often between 2:1 and 3:2 for β-turns reflecting approximately the ratio of free to hydrogen bonded amide groups involved in turns, while $I_{1690-1660}$: $I_{1640-1620}$ is usually between 1:10 and 1:8 for antiparallel β-sheet structures.[114,126] (ii) In the infrared spectra of proteins and midsize peptides with significant β-sheet content the 1645−35 cm^{-1} β-turn band is overlapped or covered by the low-wavenumber β-sheet band and the determination of the ratio is not always straightforward. Besides, its value may also depend on other factors, such as side chain contribution. However, in the case of polypeptides with low β-sheet content, it may support the assignment of vibrational bands to the different conformations. (iii) In organic solvents IR spectra of small peptides and cyclopeptides containing γ-turn structures show, in some cases, two component bands in the amide I region. The amide I band of H-bonded γ-turns appears around 1635−1610 cm^{-1} (at lower wavenumbers than that corresponding to β-turns), while non H-bonded γ-turn structures absorb at higher (>1645 cm^{-1}) wavenumbers. Bifurcation (one acceptor C═O and two hydrogen-bond donor such as N−H groups, water, or TFE) may shift the band around 1615−1600 cm^{-1}, while non-H-bonded γ-turns or structures with inverse bifurcation (two H-bond acceptor C═O groups and one H-bond donor N−H group) absorb at wavenumbers >1645 cm^{-1}. Contrary to this, vibrational spectra of proteins are mostly measured in aqueous (or D_2O) solution or buffers. Since the infrared spectroscopic evidence used for the identification of γ-turn structures in proteins is relatively scarce, this assignment is not well established and needs to be corroborated by using different spectroscopic methods.

The combined use of vibrational and CD spectroscopies can decrease the choice of putative conformers deduced from NMR spectra. This is particularly the case for small peptides and cyclopeptides which are more flexible than proteins and therefore the analysis of their NMR spectra, assisted by molecular dynamic simulations using constraints, may lead to a variety of distinct conformers and not to a predominant structural model. Small and cyclic peptides as well as peptidomimetics are not likely to contain α-helix or β-sheet structures, whereas turns can be observed in these molecules. Thus, their infrared spectra may reveal unambiguously the presence of β-turn structures since band overlapping with β-sheet structures is less likely. In certain cases, β- and γ-turns can be distinguished in cyclic peptides on the basis of the position of the low-wavenumber IR amide I/I′ component band.[100,101,103]

Another area of successful application of CD and vibrational spectroscopy is the conformational mapping of midsize peptides. The majority of peptides of biological importance comprise less than $\sim$20 amino acid residues. In aqueous (or D_2O) solution or buffers, they are present as mixtures of rapidly interconverting conformers. NMR spectroscopy is a slow method resulting in averaged parameters, the interpretation of which is of little value in terms of a single component of conformer mixtures. Traditionally, CD experiments in organic solvents such as halogenated alcohols are used for exploring the tendency of midsize peptides to adopt ordered conformations in the lower dielectric constant environment of biologi-

cal events. Examples discussed in section 5.3 and Table 2 demonstrate that FTIR spectra in different solvents, alone or in combination with CD (ECD or VCD), yield useful data on the turn forming ability of midsize peptides.

Characteristic Raman bands in the extended amide III region (1380−1250 cm^{-1}) can improve the detection of β-turn structures in small peptides and eventually lead to their dihedral angles.[114] Isotopic labeling studies on replacement or deletion analogues produced by solid-phase synthesis and site-directed mutagenesis[244] will certainly enhance the diagnostic value of vibrational spectroscopy. VCD and ROA spectroscopy supplying spectra with band shapes which are sensitive to the relative position of interacting dipoles is another tool for characterizing and quantitating secondary structures (for reviews see refs 204, 220, 221, 223, 225, 233 and 238a). Accordingly, in the case of small and cyclic peptides, the detection of β-turn structures by vibrational spectroscopy looks very promising.

In the case of larger polypeptides and proteins, the prediction of secondary structures from IR spectra is reliable (the difference between predicted and X-ray crystallography- or NMR-based secondary structure contents ranges only from 3% to 8%) for proteins containing relatively high percentage of β-sheet, random coil, and α-helix but 0% or only small amount of turns.[14] The estimation of β-sheet structures from IR spectra gives the best results, while CD spectroscopy provides more precise estimates for the α-helix. So far, the prediction of β-turn content of proteins from infrared spectra is less accurate than that obtained for other secondary structures. The main problem often evoked is the overlapping of component bands, especially with those of β-sheet structures. Recently, several authors[72,137,138] have suggested to consider not only the 1690−1660 cm^{-1} but also the 1645−1635 cm^{-1} region for the assignment of β-turn structures as in the case of midsize and small peptides (see earlier). This will certainly not solve the problem of component band overlapping but improve the diagnostic value of vibrational spectroscopy.

In summary, there are no general rules which can be applied for interpreting the vibrational spectra of all classes of polypeptides regardless of their size and amino acid composition as well as the experimental technique and conditions used. In the case of cyclic peptides and many peptidomimetics, β-turns can be detected and quantified on the basis of component bands appearing in both the high and low amide I wavenumber region of their vibrational spectra. The same principle of assignment is applicable also to small and midsize protected or free linear peptides if, under favorable conditions (e.g., in structure-promoting solvents), the population of well-defined H-bonded β-turns adopted by them is high enough. The vibrational spectra of proteins and midsize peptides are generally measured in aqueous solutions or buffers. Hydration may loosen or open up β-turns, the spectra of which do not show the low-wavenumber acceptor band. However, bands appearing in the high-wavenumber amide I region (∼1690−1660 cm^{-1}) are indicative of both H-bonded and open β-turns but the determination of their amount (percentage) meets difficulties because of the possible contribution of 3_{10}-helices and β-sheets in this spectral region. The detection of γ-turns is even more problematic. In our opinion vibrational spectroscopy can be successfully used only in the case of small peptides and in organic solvents for revealing the presence of γ-turns.

Very exciting applications of vibrational spectroscopy on larger polypeptides and proteins concern structural changes caused by physical or chemical tools. Such structural changes[74,245,246] can be induced during protein folding/unfolding or protein aggregation (e.g., in stop-flow systems, etc). Structural changes initiated by photochemical (caged substrates or caged enzymes, etc.) or electrochemical triggers (in electron-transfer proteins or redox-coupled enzymes) as well as the rate of H/D exchange[247] can also be followed by vibrational spectroscopy. These applications do not rely extensively on the prediction of overall structure from vibrational spectra, especially when the 3D structure of the protein is known but, rather, on the alteration of a part of the overall secondary structure of proteins. New experimental approaches, such as 2D IR spectroscopy, can improve the resolution by spreading the overlapped peaks on one plane instead of one line. Nonlinear-infrared spectroscopy[248] and external changes[249−252] can produce ps and larger time range relaxation phenomena permitting to generate 2D IR spectra that can be better interpreted. IR attenuated total reflectance[253−257] and external reflectance[258−260] on biomembrane monolayers can reveal details of the molecular structures of lipids and of proteins. In conclusion, vibration spectroscopy and its new developments, combined with NMR and CD is a useful tool to probe secondary structures and their changes in peptides, peptidomimetics and proteins.

12. Acknowledgments

This work was supported by the "Balaton" Project (No. 98040) and the Hungarian Research Fund (OTKA Grants T 034866, T 037719, and F 026632). CNRS (UMR 5013) support is gratefully acknowledged.

13. Abbreviations

Abu	α-amino butyric acid
Ac	acetyl
Aca	δ-amino caproic acid
Afa	amino fatty acid
Aib	α-amino isobutyric acid
β-Ala	β-alanine

L-Amino Acids

Ala (A)	alanine
Asx (B)	asparagine or aspartic acid
Cys (C)	cysteine
Asp (D)	aspartic acid
Glu (E)	glutamic acid
Phe (F)	phenylalanine
Gly (G)	glycine
His (H)	histidine
Ile (I)	isoleucine
Lys (K)	lysine

Leu (L)	leucine
Met (M)	methionine
Asn (N)	asparagine
Pro (P)	proline
Gln (Q)	glutamine
Arg (R)	arginine
Ser (S)	serine
Thr (T)	threonine
Val (V)	valine
Trp (W)	tryptophan
Tyr (Y)	tyrosine
Glx (Z)	glutamine or glutamic acid

D-Amino Acid Residues

small one-letter and three-letter symbols or the usage of D (e.g. D-Ala)

Other Abbreviations

Boc	*tert*-butyloxycarbonyl
Cbz	benzyloxycarbonyl
CD	circular dichroism
DMSO	dimethyl sulfoxide
FOD	frequently occurring domain
For	formyl
FTIR	Fourier transform infrared
GlcNAc	2-acetylamino-2-deoxy β-D-glucopyranosyl
IHB	intramolecular H-bond(ed)
IR	infrared
Lac	lactic acid
MD	molecular dynamics
MM	molecular mechanics
β-*homo*Pro	(*S*)-2-pyrrolidinyl acetic acid
PDB	Brookhaven Protein Data Bank
ROA	Raman optical activity
TFA	trifluoroacetic acid
TFE	trifluoroethanol
Tos	tosyl, *p*-toluenesulfonyl
VCD	vibrational circular dichroism
VOA	vibrational optical activity
Z	see Cbz

14. References

(1) Orengo, C. A.; Todd, A. E.; Thorton, J. M. *Curr. Opin. Struct. Biol.* **1999**, *9*, 374.
(2) Gerstein, M.; Jansen, R. *Curr. Opin. Struct. Biol.* **2000**, *10*, 574.
(3) (a) Jaenicke, R. *Biochemistry* **1991**, *30*, 3147. Orengo, C. A.; Michine, A. D.; Jones, S.; Jones, D. T.; Swindells, M. B.; Thorton, J. M. *Structure* **1997**, *5*, 1093.
(4) Fasman, G. D. In *Prediction of Protein Structure and the Principles of Protein Conformation*; Fasman, G. D., Ed.; Plenum Press: New York, 1986; pp 193−316.
(5) Sternberg, M. F. E.; Bates, P. A.; Kelley, L. A.; MacCallum, R. M. *Curr. Opin. Struct. Biol.* **1999**, *9*, 368.
(6) (a) Koehl, R.; Levitt, M. *Nat. Struct. Biol.* **1999**, *6*, 108. (b) Jones, D. T.; Taylor, W. R.; Thorton, J. M. *Nature* **1992**, *358*, 86.
(7) Richardson, J. S. *Adv. Protein Chem.* **1981**, *34*, 167.
(8) (a) Milner-White, E. J. *J. Mol. Biol.* **1990**, *216*, 385. (b) Milner-White, E. J.; Ross, B. M.; Ismail, R.; Belhadj-Mostefa, K.; Poet, R. *J. Mol. Biol.* **1988**, *204*, 777.
(9) (a) Pavone, V.; Gaeta, A. L.; Nastri, F.; Maglio, O.; Isernia, C.; Saviano, M. *Biopolymers* **1996**, *38*, 705. (b) Chou, K.-C. *Biopolymers* **1997**, *42*, 837.
(10) (a) Li, W.; Liu, Z.; Lai, L. *Biopolymers* **1999**, *49*, 481. (b) Fiser, A.; Kinh Gian Do, R.; Šali, A. *Protein Sci.* **2000**, *9*, 1753. (c) Galaktionov, S.; Nikiforovich, G. V.; Marshall, G. R. *Biopolym. (Peptide Sci.)* **2001**, *60*, 153.
(11) Sreerama, N.; Woody, R. W. In *Circular Dichroism*; Berova, N., Nakanishi, K., Woody, R. W., Eds.; Wiley-VCH: New York, 2000; Chapter 21, pp 601−620.
(12) Venyaminov, S. Yu.; Vassilenko, K. S. *Anal. Biochem.* **1994**, *222*, 176.
(13) Perczel, A.; Hollósi, M. *Circular Dichroism and the Conformational Analysis of Biomolecules*; Fasman, G. D., Ed.; Plenum Publishing Co.: New York, 1996; Chapter 9, pp 285−380.
(14) (a) Byler, M. D.; Susi, H. *Biopolymers* **1986**, *25*, 469. (b) Susi, H.; Byler, D. M. *Methods Enzymol.* **1986**, *130*, 290−311. (c) Surewicz, W. K.; Mantsch, H. H.; Chapman, D. *Biochim. Biophys. Acta* **1988**, *952*, 115. (d) Haris, P. I.; Chapman, D. *Trends Biochem. Sci.* **1992**, *17*, 328. (e) Arrondo, J. L. R.; Muga, A.; Castresana, J.; Goñi, F. M. *Prog. Biophys. Mol. Biol.* **1993**, *59*, 23. (f) Haris, P. I.; Chapman, D. *Biopolymers* **1995**, *37*, 251. (g) Jackson, M.; Mantsch, H. H. *Crit. Rev. Biochem. Mol. Biol.* **1995**, *30*, 95.
(15) (a) Giannis, A.; Kolter, T. *Angew. Chem., Int. Ed. Engl.* **1993**, *32*, 1244. (b) Hruby, V. J.; Balse, P. M. *Curr. Med. Chem.* **2000**, *7*, 945.
(16) Burley, S. K.; Almo, S. C.; Bonanno, J. B.; Capel, M.; Chance, M. R.; Gaasterland, T.; Lin, D.; Sali, A.; Studier, F. W.; Swaminathan, S. *Nat. Genet.* **1999**, *23*, 151.
(17) (a) Prasad, B. V. V.; Balaram, P. *CRC Crit. Rev. Biochem.* **1984**, *16*, 307. (b) Kennedy, D. F.; Crisma, M.; Toniolo, C.; Chapman, D. *Biochemistry* **1991**, *30*, 6541.
(18) Chou, P.; Fasman, G. G. *J. Mol. Biol.* **1977**, *115*, 135.
(19) Dukor, R. K.; Keiderling, T. A. *Biopolymers* **1991**, *31*, 1747.
(20) Levitt, M.; Greer, J. *J. Mol. Biol.* **1977**, *114*, 181.
(21) Kabsh, W.; Sander, C. *Biopolymers* **1983**, *22*, 2577.
(22) Hutchinson, E. G.; Thornton, J. M. *Protein Sci.* **1994**, *3*, 2207.
(23) Guruprasad, K.; Prasad, M. S.; Kumar, G. R. *J. Peptide Res.* **2001**, *57*, 292.
(24) (a) Smith, J. A.; Pease, L. G. *CRC Crit. Rev. Biochem.* **1980**, *8*, 315. (b) Gierasch, L. M.; Deber, C. M.; Madison, V.; Niu, C. H.; Blout, E. R. *Biochemistry* **1981**, *20*, 4730.
(25) Rose, G. D.; Gierasch, L. M.; Smith, J. A. *Adv. Protein Chem.* **1985**, *37*, 1.
(26) (a) Woody, R. W. in *The Peptides*; Hruby, V. J., Ed.; Academic Press: New York, 1985; Vol. 7, pp 15−114. (b) Yang, J. T.; Wu, C.-S. C.; Martinez, H. M. *Methods Enzymol.* **1986**, *130*, 208. (c) Johnson, W. C., Jr. *Proteins: Struct. Funct. Genet.* **1990**, *7*, 214.
(27) Greenfield, N.; Fasman, G. D. *Biochemistry* **1969**, *8*, 4108.
(28) Woody, R. W. In *Peptides, Polypeptides and Proteins*; Blout, E. R., Bovey, F. A., Lotan, N., Goodman, M. Eds.; Wiley: New York, 1974; pp 338−350.
(29) Bandekar, J.; Evans, D. J.; Krimm, S.; Leach, S. J.; Lee, S.; Mcquie, J. R.; Minisian, E.; Nemethy, G.; Pottle, M. S.; Scherega, H. A.; Stimson, E. R.; Woody, R. W. *Int. J. Pept. Protein Res.* **1982**, *19*, 187.
(30) (a) Hollósi, M.; Kövér, K. E.; Holly, S.; Fasman, G. D. *Biopolymers* **1987**, *26*, 1527. (b) Hollósi, M.; Kövér, K. E.; Holly, S.; Radics, L.; Fasman, G. D. *Biopolymers* **1987**, *26*, 1555. (c) Perczel, A.; Hollósi, M.; Foxman, B. M.; Fasman, G. D. *J. Am. Chem. Soc.* **1991**, *113*, 9772.
(31) Sathyanarayana, B. K.; Applequist, J. *Int. J. Pept. Protein Res.* **1986**, *27*, 86.
(32) Brahms, S.; Brahms, J.; Soach, G.; Brack, A. *Proc. Natl. Acad. Sci. U.S.A.* **1977**, *74*, 3208.
(33) Provencher, S. W.; Glöckner, J. *Biochemistry* **1981**, *20*, 33.
(34) Chang, C. T.; Wu, C.-S. C.; Yang, J. T. *Anal. Biochem.* **1978**, *91*, 13.
(35) Ealick, S. E.; Walter, R. L. *Curr. Opin. Stuct. Biol.* **1993**, *3*, 725.
(36) Nave, C. *Acta Crystallogr., Sect. D* **1999**, *55*, 1663.
(37) Stubbs, G. *Curr. Opin. Struct. Biol.* **1999**, *9*, 615.
(38) Byrne, B.; Iwata, S. *Curr. Opin. Stuct. Biol.* **2002**, *12*, 239.
(39) Faigel, G.; Tegze, M. *Rep. Prog. Phys.* **1999**, *62*, 355.
(40) Nave, C. *Radiat. Phys. Chem.* **1995**, *45*, 483.
(41) Marraud, M.; Aubry, A. *Biopolymers* **1996**, *40*, 45.
(42) Kay, L. E.; Gardner, K. H. *Curr. Opin. Struct. Biol.* **1997**, *7*, 722.
(43) Dötsch, V.; Wagner, G. *Curr. Opin. Struct. Biol.* **1998**, *8*, 619.
(44) Wider, G.; Wütrich, K. *Curr. Opin. Struct. Biol.* **1999**, *9*, 594.
(45) Moseley, H. N. B.; Montelione, G. T. *Curr. Opin. Struct. Biol.* **1999**, *9*, 635.
(46) Palmer, A. G., III *Curr. Opin. Struct. Biol.* **1997**, *7*, 732.
(47) Case, D. A. *Curr. Opin. Struct. Biol.* **1998**, *8*, 624.
(48) Marassi, F. M.; Opella, S. J. *Curr. Opin. Struct. Biol.* **1998**, *8*, 640.
(49) De Groot, H. J. M. *Curr. Opin. Struct. Biol.* **2000**, *10*, 593.
(50) Rossum, B. J.; Förster, H.; de Groor, H. J. M. *J. Magn. Reson.* **1997**, *124*, 516.
(51) Bruch, M. D.; Rizo, J.; Gierash, L. M. *Biopolymers* **1992**, *32*, 1741.
(52) Kessler, M.; Gehrke, M.; Griesinger, C. *Angew. Chem.* **1988**, *100*, 507.
(53) (a) Auer, M.; Scarborough, G. A.; Kühlbrand, W. *Nature* **1998**, *392*, 840. (b) Shi, D.; Lewis, M. R.; Youg, H. S.; Stokes, D. L. *J. Mol. Biol.* **1998**, *284*, 1547. (c) Stowell, M. H. B.; Miyazawa, A.; Unwin, N. *Curr. Opin. Struct. Biol.* **1998**, *8*, 595.
(54) Kimura, Y.; Vassylyev, D. G.; Miyazawa, A.; Kidera, A.; Matsushima, M.; Mitsuoka, K.; Murata, K.; Hirai, T.; Fujiyoshi, Y. *Nature* **1997**, *389*, 206.
(55) Trewhella, J. *Curr. Opin. Struct. Biol.* **1997**, *7*, 702.
(56) Bustamante, C.; Rivetti, C.; Keller, D. J. *Curr. Opin. Struct. Biol.* **1997**, *7*, 709.
(57) Fleming, G. R.; van Grondelle, R. *Curr. Opin. Struct. Biol.* **1997**, *7*, 738.

(58) Hubbell, W. L.; Gross, A.; Langen, R.; Lietzow, M. A. *Curr. Opin. Struct. Biol.* **1998**, *8*, 649.
(59) Niimura, N.; Minezaki, Y.; Nonaka, T.; Castana, J. C.; Cipriani, F.; Hoghoj, P.; Lehmann, M. S.; Wilkinson, C. *Nat. Struct. Biol.* **1997**, *4*, 909.
(60) Gustaffsson, M. G. L. *Curr. Opin. Struct. Biol.* **1999**, *9*, 627.
(61) Chalikian, T. V.; Breslauer, K. J. *Curr. Opin. Struct. Biol.* **1998**, *8*, 657.
(62) (a) Grantcharova, V.; Alm, E. J.; Baker, D.; Horwich, A. L. *Curr. Opin. Struct. Biol.* **2001**, *11*, 70. (b) Ternstrom, T.; Mayor, U.; Akke, M.; Oliveberg, M. *Proc. Natl. Acad. Sci. U.S.A.* **1999**, *96*, 14854. (c) Roder, H.; Ramachandra Shastry, M. C. *Curr. Opin. Struct. Biol.* **1999**, *9*, 620.
(63) Kuntz, I. D. *J. Am. Chem. Soc.* **1972**, *94*, 4009.
(64) (a) Wilmot, C. M.; Thornton, J. M. *J. Mol. Biol.* **1988**, *203*, 221. (b) Wilmot, C. M.; Thornton, J. M. *Protein Eng.* **1990**, *3*, 479.
(65) Venkatachalam, M. *Biopolymers* **1968**, *6*, 1425.
(66) Lewis, P. N.; Momany, F. A.; Scheraga, H. A. *Biochim. Biophys. Acta* **1973**, *303*, 211.
(67) Némethy, G.; Printz, M. P. *Macromolecules* **1972**, *5*, 755.
(68) Levitt, M. *Biochemistry* **1978**, *17*, 4277.
(69) Ball, J. B.; Andrews, P. R.; Alewood, P. F.; Hughes, R. A. *FEBS Lett.* **1990**, *273*, 15.
(70) Perczel. A.; McAllister, M. A.; Császár, P.; Csizmadia, I. G. *J. Am. Chem. Soc.* **1993**, *115*, 4849.
(71) Matthews, B. W. *Macromolecules* **1972**, *5*, 818.
(72) Miyazawa, T. in *Poly-α-Amino Acids*; Fasman, G. D., Ed.; Marcel Dekker: New York, 1967; pp 69−103.
(73) Braiman, M. S.; Rotschild, K. J. *Annu. Rev. Biophys. Chem.* **1988**, *17*, 541.
(74) Fabian, H.; Mäntele, W. In *Handbook of Vibrational Spectroscopy*; Chalmers, J. M., Griffiths, P. R., Eds; John Wiley & Sons: Chichester, 2002; pp 1−27.
(75) (a) Krimm, S.; Bandekar, J. *Adv. Prot. Chem.* **1986**, *38*, 181. (b) Bandekar, J. *Biochim. Biophys. Acta* **1992**, *1120*, 123. (c) Bandekar, J.; Krimm, S. *Biopolymers* **1980**, *19*, 31.
(76) (a) Goormaghtigh, E.; Cabiaux, V.; Ruysschaert, J. M. *Eur J. Biochem.* **1990**, *193*, 409. (b) Goormaghtigh, E.; Cabiaux, V.; Ruysschaert, J. M. in *Physical Methods in the Study of Biomembranes*; Hilderson, H. J., Ralston, G. B., Eds; Plenum Press: New York, 1994; Vol. 23, pp 329−362.
(77) (a) Wharton, C. W. *Biochem. J.* **1986**, *233*, 25. (b) Carey, P. R. In *Modern Physical Methods in Biochemistry, Part B*; Neuberger, A., Van Deenen, L. L. M., Eds.; Elsevier Science Publishers: Dordrecht, The Netherlands, 1988; pp 27−64. (c) Miura, T.; Thomas, G. J., Jr. *Subcell Biochem.* **1995**, *24*, 55. (d) Peticolas, W. L. *Methods Enzymol.* **1995**, *246*, 389. (e) Williams, R. W. *Methods Enzymol.* **1986**, *130*, 311.
(78) (a) Marraud, M.; Aubry, A. *Int. J. Pept. Protein Res.* **1984**, *23*, 123. (b) Pietrzynski, G.; Rzeszotarska, B.; Kubica, Z. *Int. J. Pept. Protein Res.* **1992**, *6*, 524. (c) Liang, G.-B.; Rito, C. J.; Gellman, S. H. *Biopolymers* **1992**, *32*, 293.(d) Takeda, N.; Kato, M.; Taniguchi, Y. *Biochemistry* **1995**, *34*, 5980. (e) Baures, P. W.; Ojala, W. H.; Gleason, W. B.; Johnson, R. L. *J. Pept. Res.* **1997**, *50*, 1.
(79) Hollósi, M.; Majer, Zs.; Rónai, A. Z.; Magyar, A.; Medzihradszky, K.; Holly, S.; Perczel, A.; Fasman, G. D. *Biopolymers* **1994**, *34*, 177.
(80) (a) Di Bello, C.; Simonetti, M.; Dettin, M.; Paolillo, L.; D'Aurla, G.; Falcigno, L.; Saviano, M.; Scatturin, A.; Vertuani, G.; Cohen, P. *J. Pept. Sci.* **1995**, *1*, 251. (b) Simonetti, M.; Di Bello, C. *Biopolym. (Biospectrosc.)* **2001**, *62*, 95. (c) Simonetti, M.; Di Bello, C. *Biopolym. (Biospectrosc.)* **2001**, *62*, 109. (d) Dettin, M.; Falcigno, L.; Campanile, T.; Scarinci, C. D.; Auria, G.; Cusin, M.; Paolillo, L.; Di Bello, C. *J. Pept. Sci.* **2001**, *7*, 358. (e) Carpenter, K. A.; Schmidt, R.; von Mentzer, B.; Haglund, K.; Roberts, E.; Walpole, C. *Biochemistry* **2001**, *40*, 8317. (f) Gerothanassis, I. P.; Birlirakis, N.; Karayannis, T.; Sakarellos-Daitsiotis, M.; Sakarellos, C.; Vitoux, B.; Marraud, M. *Eur. J. Biochem.* **1992**, *210*, 693.
(81) Mantsch, H. H.; Perczel. A.; Hollósi, M.; Fasman, G. D. *Biopolymers* **1993**, *33*, 201.
(82) Dwivedi, A. M.; Krimm, S.; Malcolm, B. R. *Biopolymers* **1984**, *23*, 2025.
(83) (a) Yoder, G.; Keiderling, T. A.; Formaggio, F.; Crisma, M.; Toniolo, C. *Biopolymers* **1995**, *35*, 103. (b) Kubelka, J.; Silva, R. A. G. D.; Keiderling, T. A. *J. Am. Chem. Soc.* **2002**, *124*, 5325.
(84) (a) Miick, S. M.; Martinez, G. V.; Fiori, W. R.; Todd, A. P.; Millhauser, G. L. *Nature* **1992**, *359*, 653. (b) Martinez, G. V.; Millhauser, G. L. *J. Struct. Biol.* **1995,** *114*, 23. (c) Williams, S.; Causgrove, T. P.; Gilmanshin, R.; Fang, K. S.; Callender, R. H.; Woodruff, W. H.; Dyer, R. B. *Biochemistry* **1996**, *35*, 691. (d) Yoder, G.; Pancoska, P.; Keiderling, T. A. *Biochemistry* **1997**, *36*, 15123.
(85) Surewicz, W. K.; Mantsch, H. H.; Chapman, D. *Biochemistry* **1993**, *32*, 389.
(86) (a) Nelson, J. W.; Kallenbach, N. R. *Proteins* **1986**, *2*, 211. (b) Jackson, M.; Mantsch, H. H. *Biochim. Biophys. Acta* **1992**, *1118*, 139.
(87) (a) Hollósi, M.; Kajtár, M.; Gráf, L. *FEBS Lett.* **1977**, *74*, 185. (b) Hollósi, M.; Kawai, M.; Fasman, G. D. *Biopolymers* **1985**, *24*, 211. (c) Hollósi, M.; Ürge, L.; Perczel, A.; Kajtár, J.; Teplán, I.; Ötvös, L., Jr.; Fasman, G. D. *J. Mol. Biol.* **1992**, *223*, 673. (d) Hollósi, M.; Ötvös, L., Jr.; Ürge, L.; Kajtár, J.; Perczel, A.; Laczkó, I.; Vadász, Zs.; Fasman, G. D. *Biopolymers* **1993**, *33*, 497. (e) Perczel, A.; Hollósi, M.; Sándor, P.; Fasman, G. D. *Int. J. Pept. Protein Res.* **1993**, *41*, 223. (f) Hollósi, M.; Shen, Z. M.; Perczel, A.; Fasman, G. D. *Proc. Natl. Acad. Sci. U.S.A.* **1994**, *91*, 4902.
(88) (a) Laczkó, I.; Hollósi, M.; Ürge, L.; Mantsch, H. H.; Thurin, J.; Ötvös, L., Jr. *Biochemistry* **1992**, *31*, 4282. (b) Perczel, A.; Kollát, E.; Hollósi, M.; Fasman, G. D. *Biopolymers* **1993**, *33*, 665. (c) Horvat, S.; Jakas, A.; Vass, E.; Samu, J.; Hollósi, M. *J. Chem. Soc., Perkin Trans.* **1997**, *2*, 1523. (d) Vass, E.; Hollósi, M.; Kveder, M.; Kojic-Prodic, B.; Cudic, M.; Horvat, S. *Spectrochim. Acta, Part A* **2000**, *56*, 2479.
(89) (a) Holly, S.; Laczkó, I.; Fasman, G. D.; Hollósi, M. *Biochem. Biophys. Res. Commun.* **1993**, *197*, 755. (b) Tóth, G. K.; Laczkó, I.; Hegedüs, Z.; Vass, e.; Hollósi, M.; Janáky, T.; Váradi, Gy.; Penke, B.; Monostori, É. *Pept. Immunol.* **1996**, 223. (c) Laczkó, I.; Hollósi, M.; Vass, E.; Hegedûs, Z.; Monostori, É.; Tóth, G. K. *Biochem. Biophys. Res. Commun.* **1998**, *242*, 474.
(90) (a) Hollósi, M.; Ismail, A. A.; Mantsch, H. H.; Penke, B.; Váradi, I. Gy.; Tóth, G. K.; Laczkó, I.; Kurucz, I.; Nagy, Z.; Fasman, G. D.; Rajnavölgyi, É. *Eur. J. Biochem.* **1992**, *206*, 421. (b) laczkó, I.; Hollósi, M.; Ürge, L.; Mantsch, H. H.; Thurin, J.; Ötvös, L., Jr. *Biochemistry* **1992**, *31*, 4282. (c) Holly, S.; Majer. Zs.; Tóth, G. K.; Váradi, Gy; Rajnavölgyi, É.; Laczkó, I.; Hollósi, M. *Biochem. Biophys. Res. Commun.* **1993**, *193*, 1247. (d) Laczkó, I.; Holly, S.; Kónya, Z.; Soós, K.; Varga, J. L.; Hollósi, M.; Penke, B. *Biochem. Biophys. Res. Commun.* **1994**, *205*, 120. (e) Majer, Zs.; Holly, S.; Tóth, G. K.; Váradi, Gy.; Nagy, Z.; Horváth, A.; Rajnavölgyi, É.; Laczkó, I.; Hollósi, M. *Arch. Biochem. Biophys.* **1995**, *322*, 112. (f) Laczkó, I.; Vass, E.; Soós, K.; Varga, J. L.; Száraz, S.; Hollósi, M.; Penke, B. *Arch. Biochem. Biophys.* **1996**, *335*, 381.
(91) Uray, K.; Kajtár, J.; Vass, E.; Price, M. R.; Hollósi, M.; Hudecz, F. *Arch. Biochem. Biophys.* **1999**, *361*, 65.
(92) Arad, O.; Goodman, M. *Biopolymers* **1990**, *29*, 1651.
(93) Gray, R. A.; Vander Velde, D. G.; Burke, C. J.; Manning, M. C.; Middaugh, C. R.; Borchard, R. T. *Biochemistry* **1994**, *33*, 1323.
(94) Wennerberg, A. B. A.; Jackson, M.; Öhman, A.; Gräslund, A.; Langel, Ü.; Bartfai, T.; Rigler, R.; Mantsch, H. H. *Nat. Res. Council Can.* **1994**, *72*, 1495.
(95) Szendrei, Gy. I.; Fabian, H.; Mantsch, H. H.; Lovas, S.; Nyéki, O.; Schön, I.; Ötvös, L., Jr. *Eur. J. Biochem.* **1994**, *226*, 917.
(96) Mimeault, M.; De Léan, A.; Lafleur, M.; Bonenfant, D.; Fournier, A. *Biochemistry* **1995**, *34*, 955.
(97) Saudek, V.; Atkinson, R. A.; Lepage, P.; Pelton, J. T. *Eur. J. Biochem.* **1991**, *202*, 329.
(98) Lamthanh, H.; Léonetti, M.; Nabedryk, E.; Ménez, A. *Biochim. Biophys. Acta* **1993**, *1203*, 191.
(99) Wei, J.; Xie, L.; Lin, Y.-Z.; Tson, C.-L. *Biochim. Biophys. Acta* **1992**, *1110*, 69.
(100) Shaw, R. A.; Perczel, A.; Mantsch, H. H.; Fasman, G. D. *J. Mol. Struct.* **1994**, *324*, 143.
(101) (a) Vass, E.; Kurz, M.; Konat, R. K.; Hollósi, M. *Spectrochim. Acta. Part A* **1998**, *54*, 773. (b) Kurz, M. Ph.D. Thesis Technical University of Munich, Munich, Germany, 1992.
(102) Likó, Zs.; Botyánszki, J.; Bódi, J.; Vass, E.; Majer, Zs.; Hollósi, M.; süli-Vargha, H. *Biochem. Biophys. Res. Commun.* **1996**, *227*, 351.
(103) Vass, E.; Láng, E.; Samu, J.; Majer, Zs.: Kajtár-Peredy, M.; Mák, M.; Radics, L.; hollósi, M. *J. Mol. Struct.* **1997**, *440*, 59.
(104) (a) Besson, F.; Raimbault, C.; Hourdou, M. L.; Buchet, R. *Spectrochim. Acta* **1996** *52*, 793. (b) Peypoux, F.; Pommier, M. T.; Marion, D.; Ptak, M.; Das, B. C.; Michel, G. *J. Antibiot.* **1986**, *39*, 636. (c) Besson, F.; Buchet, R. *Spectrochim. Acta* **1997**, *53*, 1913. (d) Genest, M.; Marion, D.; Caille, A.; Ptak, M. *Eur. J. Biochem.* **1987**, *169*, 389.
(105) (a) Besson, F. *Spectrochim. Acta* **1998** *54*, 1007. (b) Volpon, L.; Besson, F.; Lancelin, J.-M. *Eur. J. Biochem.* **1999** *264*, 200.
(106) Vass, E.; Besson, F.; Majer, Zs.; Volpon, L.; Hollósi, M. *Biochem. Biophys. Res. Commun.* **2001**, *282*, 361.
(107) Anderson, T. S.; Hellgeth, J.; Lansbury, P. T., Jr. *J. Am. Chem. Soc.* **1996**, *118*, 6540.
(108) (a) Kalnin, I. A.; Baikalov, I. A.; Venyaminov, S. Y. *Biopolymers* **1990**, *30*, 1273. (b) Prestrelski, S. J.; Byler, D. M.; Thompson, M. P. *Int. J. Pept. Protein Res.* **1991**, *37*, 508. (c) Prestrelski, S. J.; Byler, D. M.; Liebman, M. M. *Proteins: Struct. Funct. Genet.* **1992**, 14450.
(109) Swamy, M. J.; Heimburg, T.; Marsh, D. *Biophys. J.* **1996**, *71*, 840.
(110) Cladera, J.; Torres, J.; Padrós, E. *Biophys. J.* **1996**, *70*, 2882.
(111) Encinar, J. A.; Fernández, A.; Ferragut, J. A.; Gonzáles-Ros, J. M.; DasGupta, B. R.; Montal, M.; Ferrer-Montiel, A. *FEBS Lett.* **1998**, *429*, 78.

(112) (a) Barth, A.; Kreutz, W.; Mäntele, W. *Biochim. Biophys. Acta* **1994**, *1194*, 75. (b) Barth, A.; Mäntele, W. *Biophys. J.* **1998**, *75*, 538.
(113) Echabe, I.; Dornberger, U.; Prado, A.; Goñi, F. M.; Arrondo, J. L. *Protein Sci.* **1998**, *7*, 1172.
(114) Wolkers, W. F.; Haris, P. I.; Pistorius, A. M. A.; Chapman, D.; Hemminga, M. A. *Biochemistry* **1995**, *34*, 7825.
(115) Mouro, C.; Jung, C.; Bondon, A.; Simonneaux, G. *Biochemistry* **1997**, *36*, 8125.
(116) Cladera, J.; Villaverde, J.; Hartog, A. F.; Padros, E.; Berden, J. A.; Rigaud, J.-L.; Dunach, M. *FEBS Lett.* **1995**, *371*, 115.
(117) Hierro, A.; Arizmendi, J. M.; De La Rivas, J.; Urbaneja, M. A.; Prado, A.; Muga, A. *Eur. J. Biochem.* **2001**, *268*, 1739.
(118) Lydakis-Simantiris, N.; Hutchison, R. S.; Betts, S. D.; Barry, B. A.; Yocum, C. F. *Biochemistry* **1999**, *38*, 404.
(119) Menikh, A.; Saleh, M. T.; Gariépy, J.; Boggs, J. M. *Biochemistry* **1997**, *36*, 15865.
(120) Dornberger, U.; Fandrei, D.; Backmann, J.; Hübner, W.; Rahmelow, K.; Gührs, K.-H.; Hartmann, M.; Schott, B.; Fritzsche, H. *Biochim. Biophys. Acta* **1996**, *1294*, 168.
(121) Tian, K.; Zhou, B.; Geng, F.; Jing G. *Int. J. Biol. Macromol.* **1998**, *23*, 199.
(122) From, N. B.; Bowler, B. E. *Biochemistry* **1998**, *37*, 1623.
(123) Tatulian, S. A.; Marien Cortes, D.; Perozo, E. *FEBS Lett.* **1998**, *423*, 205.
(124) Shao, W.; Kearns, D. R.; Sanders, G. M. *Int. J. Biol. Macromol.* **1997**, *20*, 115.
(125) Lorenz, V. A.; Villaverde, J.; Trézéguet, V.; Lauquin, G. J.-M.; Brandolin, G. Padros, E. *Biochemistry* **2001**, *40*, 8821.
(126) Perez-Pons, J. A.; Padros, E.; Querol, E. *Biochem. J.* **1999**, *308*, 791.
(127) van Stokkum, I. H. M.; Linsdell, H.; Hadden, J. M.; Haris, P. I.; Chapman, D.; Bloemendal, M. *Biochemistry* **1995**, *34*, 10508.
(128) Banuelos, S.; Muga, A. *Biochemistry* **1996**, *35*, 3892.
(129) (a) Chirgadze, Y. N.; Fedorov, O. V.; Trushina, N. P. *Biopolymers* **1975**, *14*, 679. (b) Venyaminov, S. Y.; Kalnin, N. N. *Biopolymers* **1990**, *30*, 1243. (c) Barth, A. *Progr. Biophys. Mol. Biol.* **2000**, *74*, 141. (d) Besson, F.; Buchet, R. *Spectrochim. Acta, Part A* **1997**, *53*, 1913.
(130) (a) Sarver, R. W.; Krueger, W. C. *Biochemistry* **1991**, *30*, 89. (b) Pribic, R.; van Stokkum, I. H. M.; Chapman, D.; Haris, P. T.; Bloemenda, M. **1993**, *214*, 366. (c) Baumruk, V.; Pancoska, P.; Keiderling, T. A. *J. Mol. Biol.* **1996**, *259*, 774.
(131) (a) LaBrake, C. C.; Wang, L.; Keiderling T. A.; Fung, W. M. *Biochemistry* **1993**, *32*, 10296. (b) Guijarro, J. I.; Jackson, M.; Chaffotte, A. F.; Delepierre, M.; Mantsch, H. H.; Goldberg, M. E. *Biochemistry* **1995**, *34*, 2998. (c) Raimbault, C.; Couthon, F.; Vial, C.; Buchet, R. *Eur. J. Biochem.* **1995**, *234*, 570. (d) De La Fournière-Bessueille, L.; Grange, D.; Buchet, R. *Eur. J. Biochem.* **1997**, *250*, 705. (e) Venyaminov, S. Y., Yang, J. T., Fasman, G. D., Eds. Plenum Press: New York, 1996; pp 69−107.
(132) (a) D'Auria, S.; Rossi, M.; Tanfani, F.; Bertoli, E.; Parise, E.; Bazzicalupo, P. *Eur. J. Biochem.* **1998**, *255*, 588. (b) Abbott, G. W.; Bloemendal, M.; van Stokkum, I. H. M.; Mercer, E. A. J.; Miller, R. T.; Sewing, S.; Wolters, M.; Pongs, O.; Srai, S. K. S. *Biochim. Biophys. Acta* **1997**, *1341*, 71. (c) Glandières, J.-M.; Calmettes, P.; Martel, P.; Zentz, C.; Massat, A.; Ramstein, J.; Alpert, B. *Eur. J. Biochem.* **1995**, *227*, 241. (d) Medrano, F. J.; Gasset, M.; López-Zúmel, C.; Usobiaga, P.; García, J. L.; Menéndez, M. *J. Biol. Chem.* **1996**, *271*, 29152. (e) Garcia-Quintana, D.; Francesch, A.; Garriga, P.; de Lera, A. R.; Manyosa, E. *Biophys. J.* **1995**, *69*, 1077. (f) Menéndez, M.; Gasset, M.; Laynez, J.; López-Zumel, C.; Usobiaga, P.; Töpfer-Petersen, E.; Calvette, J. J. *Eur. J. Biochem.* **1995**, *234*, 887.
(133) (a) Haris, P. I.; Chapman, D.; Bengha, G. *Eur. J. Biochem.* **1995**, *233*, 659. (b) Dong, A.; Kendrick, B.; Kreilgard, L.; Matsuura, J.; Manning, M. C.; Carpenter, J. F. *Arch. Biochem. Biophys.* **1997**, *347*, 213.
(134) Ferreras, M.; Höper, F.; Dalla Serra, M.; Colin, D. A.; Prévost, G.; Menestrina, G. *Biochim. Biophys. Acta* **1998**, *1414*, 108.
(135) Pancoska, P.; Fabian, H.; Yoder, G.; Baumruk, V.; Keiderling, T. A. *Biochemistry* **1996**, *35*, 13094.
(136) Bonnin, S.; Besson, F.; Gelhausen, M.; Chierci, S.; Roux, B. *FEBS Lett.* **1999**, *456*, 361.
(137) El-Jastimi, R.; Lafleur, M. *Biophys. Biochim. Acta* **1997**, *1324*, 151.
(138) Filosa, A.; Wang, Y.; Ismail, A. A.; English, A. M. *Biochemistry* **2001**, *40*, 8256.
(139) Paquet, M.-J.; Laviolette, M.; Pézolet, M.; Auger, M. *Biophys. J.* **2001**, *81*, 305.
(140) Gericke, A.; Smith, E. R.; Moore, D. J.; Mendelsohn, R.; Storch, J. *Biochemistry* **1997**, *36*, 8311.
(141) Cabiaux, V.; Buckley, T.; Wattiez, R.; Ruysschaert, J. M.; Parker, M. W.; van der Goot, F. *Biochemistry* **1997**, *36*, 15224.
(142) Cabiaux, V.; Oberg, K. A.; Pancoska, P.; Walz, T.; Agre, P.; Engel, A. *Biophys. J.* **1997**, *73*, 406.
(143) Azuaga, A. I.; Sepulcre, F.; Padrós, E.; Mateo, P. L. *Biochemistry* **1996**, *35*, 16328.
(144) Barnett, S. M.; Dracheva, S.; Hendler, R. W.; Levin, I. W. *Biochemistry* **1996**, *35*, 4558.
(145) Datta, G.; Dong, A.; Witt, J.; Tu, A. T. *Arch. Biochem. Biophys.* **1995**, *317*, 365.
(146) Martinez-Senac, M. M.; Corbalan-Garcia, S.; Gomez-Fernandez, J. C. *Biochemistry* **2001**, *40*, 9983.
(147) Gasset, M.; Saiz, J. L.; Laynez, J.; Gentzel, M.; Töpfer-Petersen, E.; Calvete, J. J. *Eur. J. Biochem.* **1997**, *250*, 735.
(148) Trouiller, A.; Gerwert, K.; Dupont, Y. *Biophys. J.* **1996**, *71*, 2970.
(149) Gallagher, S. C.; Gao, Z.-H.; Li, S.; Dyer, B.; Trewhella, J.; Klee, C. B. *Biochemistry* **2001**, *40*, 12094.
(150) Fabian, H.; Fälber, K.; Gast, K.; Reinstädler, D.; Rogov, V. V.; Naumann, D.; Zamyatkin, D. F.; Filimonov, V. V. *Biochemistry* **1999**, *38*, 5633.
(151) Bramanti, E.; Benedetti, E.; Nicolini, C.; Berzina, T.; Erokhin, V.; D'Alessio, V.; Benedetti, E. *Biopolymers* **1997**, *43*, 227.
(152) De Jongh, H. H.; Goormaghtigh, E.; Ruysschaert, J.-M. *Biochemistry* **1995**, *34*, 172.
(153) Echabe, I.; Haltia T.; Freire, E.; Goni, F. M.; Arrondo, J. L. R. *Biochemistry* **1995**, *34*, 13565.
(154) Wang, X.-M.; Wattiez, R.; Mock, M.; Falmagne, P.; Ruysschaert, J.-M.; Cabiaux; V. *Biochemistry* **1997**, *36*, 14906.
(155) Guzman-Casado, M.; Cardenete, A.; Gimenez-Gallego, G.; Parody-Morreale, A. *Int. J. Biol. Macromol.* **2001**, *28*, 305.
(156) Li, T.; Horan, T.; Osslund, T.; Stearns, G.; Arakawa, T. *Biochemistry* **1997**, *36*, 8849.
(157) Contreras, L. M.; Aranda, F. J.; Gavilanes, F.; Gonzalez-Ros, J. M.; Villalain, J. *Biochemistry* **2001**, *40*, 3196.
(158) Raussens, V.; Ruysschaert, J.-M.; Goormaghtigh, E. *J. Biol. Chem.* **1997,** *272*, 262.
(159) Vila, R.; Ponte, I.; Collado, M.; Arrondo, J. L. R.; Suau, P. *J. Biol. Chem.* **2001**, *276*, 30898.
(160) Wellner, N.; Belton, P. S.; Tatham, A. S. *Biochem. J.* **1996**, *319*, 741.
(161) Vecchio, G.; Bossi, A.; Pasta, P.; Carrea, G. *Int. J. Pept. Protein Res.* **1996**, *48*, 113.
(162) Panick, G.; Malessa, R.; Winter, R. *Biochemistry* **1999**, *38*, 6512.
(163) Patzlaff, J. S.; Moeller, J. A.; Barry, B. A.; Brooker, R. J. *Biochemistry* **1998**, *37*, 15363.
(164) Subirade, M.; Guegen, J.; Pézolet, M.; *Biochim. Biophys. Acta* **1994**, *1205*, 239.
(165) Chehín, R.; Iloro, I.; Marcos, M. J.; Villar, E.; Shnyrov, V. L.; Arrondo, J. L. R. *Biochemistry* **1999**, *38*, 1525.
(166) Liang, J. J.-N.; Chakrabarti, B. *Biochem. Biophys. Res. Commun.* **1998**, *246*, 441.
(167) Bañuelos, S.; Arrondo, J. L. R.; Goñi, F. M.; Pifat, G. *J. Biol. Chem.* **1995**, *270*, 9192.
(168) Saba, R. I.; Goormaghtigh, E.; Ruysschaert, J. M.; Herchuelz, A. *Biochemistry* **2001**, *40*, 3324.
(169) Baezinger, J. E.; Méthot, N. *J. Biol. Chem.* **1995**, *270*, 29129.
(170) Chehín, R.; Thorolfsson M.; Knappskog, P. M.; Martínez, A.; Flatmark, T.; Arrondo, J. L. R.; Muga, A. *FEBS Lett.* **1998**, *422*, 225.
(171) De Las Rivas, J.; Barber, J. *Biochemistry* **1997**, *36*, 8897.
(172) Takeda, N.; Kato, M.; Taniguchi, Y. *Biochemistry* **1995**, *34*, 5980.
(173) Panick, G.; Winter, R. *Biochemistry* **2000**, *39*, 1862.
(174) Dong, A.; Hyslop, R. M.; Pringle, D. L. *Arch. Biochem. Biophys.* **1996**, *333*, 275.
(175) Li, J.; Uversky, V. N.; Fink, A. L. *Biochemistry* **2001**, *40*, 11604.
(176) Hadden, J. M.; Bloemendal, M.; Haris, P. I.; van Stokkum, I. H. M.; Chapman, D.; Drai, S. K. S. *FEBS Lett.* **1994**, *350*, 235.
(177) Martínez, A.; Haavik, J.; Flatmark, T.; Arrondo, J. L.; Muga, A. *J. Biol. Chem.* **1996**, *271*, 19737.
(178) Serina, L.; Bucurenci, N.; Gilles, A.-M.; Surewicz, W. K.; Fabian, H.; Mantsch, H. H.; Takahashi, M.; Petrescu, I.; Batelier, G.; Bârzu, O. *Biochemistry* **1996**, *35*, 7003.
(179) Thomas, G. J., Jr.; Prescott, B.; Urry, U. W. *Biopolymers* **1987**, *26*, 921.
(180) Chi, Z.; Chen, X. G.; Holtz, J. S.; Asher, S. A. *Biochemistry* **1998**, *37*, 2854.
(181) (a) Lagant, P.; Vergoten, G.; Fleury, G.; Loucheux-Lefebvre M. H. *Eur. J. Biochem.* **1984**, *139*, 137. (b) Renugopalakrishnan, V.; Rapaka, R. S.; Collette, T. W.; Carreira, L. A.; Bhatnagar, R. S. *Biochem. Biophys. Res. Commun.* **1985**, *26*, 1029. (c) O'Leary, T. J.; Ross, P. D.; Lieber, M. R.; Levin, I. W. *Biophys. J.* **1986**, *49*, 795. (d) Erard, M.; Lakhdar-Ghazal, F.; Amalric, F. *Eur. J. Biochem.* **1990**, *191*, 19.
(182) Hseu, T. H.; Chang, H. *Biochim. Biophys. Acta* **1980**, *624*, 340.
(183) Fox, J. A.; Tu, A. T.; Hruby, V. J.; Mosberg, H. I. *Arch. Biochem. Biophys.* **1981**, *211*, 628.
(184) Lord, R. C. *Appl. Spectrosc.* **1977**, *31*, 187.
(185) Lagant, P.; Vergoten, G.; Fleury, G.; Loucheux-Lefebvre, M. H. *Int. J. Pept. Protein Res.* **1984**, *24*, 543.
(186) (a) Ianoul, A.; Boyden, M. N.; Asher, S. A. *J. Am. Chem. Soc.* **2001**, *123*, 7433. (b) Asher, S. A.; Ianoul, A.; Mix, G.; Boyden, M. N.; Karnoup, A.; Diem, M.; Schweitzer-Stenner, R. *J. Am. Chem. Soc.* **2001**, *123*, 11775.
(187) (a) Zheng, S.; Tu, A. T.; Renugopalakrishnan, V.; Strawich, E.; Glimcher, M. J. *Biopolymers* **1987**, *10*, 1809. (b) Holtz, J. S.;

Lednev, I. K.; Asher, S. A. *Biopolymers* **2000**, *57*, 55. (c) Pande, J.; Pande, C.; Gilg, D.; Vasak, M.; Callender, R.; Kagi, J. H. *Biochemistry* **1986**, *25*, 5526. (d) Saudek, V.; Atkinson, R. A.; Lepage, P.; Pelton, J. T. *Eur. J. Biochem.* **1991**, *202*, 329.
(188) (a) Renugopalakrishnan, V.; Zheng, S.; Tu, A. T.; Damle, S. P. *Biopolymers* **1989**, *28*, 1935. (b) Williams, R. W.; Weaver, J. L. *J. Biol. Chem.* **1990**, *265*, 2505. (c) Sargent, D.; Benevides, J. M.; Yu, M. H.; King, J.; Thomas, G. J., Jr. *J. Mol. Biol.* **1988**, *199*, 491. (d) Areas, E. P.; Giglio, J. R.; Arantes, E. C.; Kawano, Y. *Biochim. Biophys. Acta* **1987**, *915*, 292.
(189) (a) Williams, R. W.; Beeler, T. J. *J. Biol. Chem.* **1986**, *261*, 12408. (b) Vogel, H.; Jahnig, F. *J. Mol. Biol.* **1986**, *190*, 191. (c) DeGrazia, H.; Harman, J. G.; Tan, G. S.; Wartell, R. M. *Biochemistry* **1990**, *29*, 3557. (d) Aslanian, D.; Grof, P.; Galzi, J.-L.; Changeux, J.-P. *Biochim. Biophys. Acta* **1993**, *1148*, 291.
(190) (a) Bandekar, J.; Krimm, S. *Int. J. Pept. Protein Res.* **1985**, *26*, 158. (b) Bandekar, J. *Vibr. Spectrosc.* **1993**, *5*, 143.
(191) Schweitzer-Stenner, R.; Eker, F.; Huang, Q.; Griebenow, K. *J. Am. Chem. Soc.* **2001**, *123*, 9628.
(192) (a) Vass, E.; Holly, S.; Majer, Zs.; Samu, J.; Laczkó, I.; Hollósi, M. *J. Mol. Struct.* **1997**, *408/409*, 47. (b) Vass, E.; Samu, J.; Majer, Zs.; Hollósi, M. *J. Mol. Struct.* **1997**, *408/409*, 207. (c) Vass, E.; Holly, S.; Hollósi, M. *Mikrochim. Acta [Suppl.]* **1997**, *14*, 239.
(193) Shaw, R. A.; Mantsch, H. H.; Chowdhry, B. Z. *Can. J. Chem.* **1993**, *71*, 1334.
(194) Shaw, R. A.; Mantsch, H. H.; Chowdhry, B. Z. *Int. J. Macromol.* **1994**, *16*, 143.
(195) (a) Pavone, V.; Lombardi, A.; D'Auria, G.; Saviano, M.; Nastri, F.; Paolillo, L.; Di Blasio, B.; Pedone, C. *Biopolymers* **1992**, *32*, 173. (b) Tamaki, M.; Akabori, S., Muramatsu, I. *Biopolymers* **1996**, *39*, 129.
(196) Spatola, A. F.; Anwer, M. K.; Rockwell, A. L.; Gierasch, L. M. *J. Am. Chem. Soc.* **1986**, *108*, 825.
(197) Di Blasio, B.; Lombardi, A.; D'Auria, G.; Saviano, M.; Isernia, C.; Maglio, O.; Paolillo, L.; Pedone, C.; Pavone, V. *Biopolymers* **1993**, *33*, 621.
(198) Rich, D. H.; Kawai, M.; Jasensky, R. D. *Int. J. Pept. Protein Res.* **1983**, *21*, 35.
(199) (a) Majer, Zs.; Vass, E.; Malesevic, M.; Sewald, N.; Hollósi, M. Proceedings of the *8th International Conference on Circular Dichroism*, Sendai, Japan, September 23−28, 2001; Poster P46. (b) Vass, E.; Majer, Zs.; Sewald, N.; Hollósi, M. Proceedings of the *XXVI European Congress on Molecular Spectroscopy*, Villeneuve d'Ascq, France, September 1−6, 2002; Poster P1.7. (c) Pálfi, V. K.; Gáspári, Z.; Vass, E.; Perczel, A. *J. Pept. Sci.* **2002**, *8* (Suppl.), S197.
(200) Li, N.; Kendrick, B. S.; Manning, M. C.; Carpenter, J. F.; Duman, J. G. *Arch. Biochem. Biophys.* **1998**, *360*, 25.
(201) (a) Clark, A. H.; Saunderson, D. H. P.; Suggett, A. *Int. J. Pept. Res.* **1981**, *17*, 353. (b) Casal, H. L.; Köhler, U.; Mantsch, H. H. *Biochim. Biophys. Acta* **1988**, *957*, 11. (c) Yang, P. W.; Mantsch, H. H.; Arrondo, J. L. R.; Saint-Girons, I.; Guillou, Y.; Cohen, G. N.; Bârzu, O. *Biochemistry* **1987**, *26*, 2706.
(202) Drewes, J. A.; Rowlen, K. L. *Biophys. J.* **1993**, *65*, 985.
(203) Yang, J.; Christianson, L. A.; Gellman, S. *Org. Lett. D* **1999**, *1*, 11.
(204) (a) Barron, L. D.; Hecht, L.; Wilson, G. *Biochemistry* **1997**, *36*, 13143. (b) Barron, L. D.; Hecht, L.; Blanch, E. W.; Bell, A. F. *Progr. Biophys. Mol. Biol.* **2000**, *73*, 1.
(205) Gante, J. *Angew. Chem., Int. Ed. Engl.* **1994**, *33*, 1699.
(206) (a) Kajtár, M.; Hollósi, M.; Kajtár, J.; Majer, Zs.; Kövér, K. E. *Tetrahedron* **1986**, *42*, 3931. (b) Majer, Zs.; Zewdu, M.; Hollósi, M.; Seprödi, J.; Vadász, Zs.; Teplán, i. *Biochem. Biophys. Res. Commun.* **1988**, *150*, 1017.
(207) (a) Hollósi, M.; Majer, Zs.; Zewdu, M.; Ruff, F.; Kajtár, M.; Kövér, K. E. *Tetrahedron* **1988**, *44*, 195. (b) Hollósi, M.; Kollát, E.; Kajtár, J.; Kajtár, M.; Fasman, G. D. *Biopolymers* **1990**, *30*, 1061. (c) Hollósi, M.; Zewdu, M.; Kollát, E.; Majer, Zs.; Kajtár, M.; Batta, G.; Kövér, K.; Sándor, P. *Int. J. Pept. Protein Res.* **1990**, *36*, 173. (d) Czugler, M.; Kálmán, A.; Kajtár-Peredy, M.; Kollát, E.; Kajtár, J.; Majer, Zs.; Farkas, Ö.; Hollósi, M. *Tetrahedron* **1993**, *49*, 6661. (e) Shaw, R. A.; Kollát, E.; Hollósi, M.; Mantsch, H. H. *Spectrochim. Acta, Part A* **1995**, *51*, 1399.
(208) (a) Moretto, A.; Peggion, C.; Formaggio, F.; Crisma, M.; Toniolo, C.; Piazza, C.; Kaptein, B.; Broxterman, Q. B.; Ruiz, I.; Díaz-de-Villegas, M. D.; Galvez, J. A.; Cativiela, C. *J. Pept. Res.* **2000**, *56*, 283. (b) Pispisa, B.; Mazzuca, C.; Palleschi, A.; Stella, L.; Venanzi, M.; Formaggio, F.; Polese, A.; Toniolo, C. *Biopolym. (Pept. Sci.)* **2000**, *55*, 425.
(209) (a) Gatos, M.; Formaggio, F.; Crisma, M.; Toniolo, C.; Bonora, G. M.; Benedetti, Z.; Di Blasio, B.; Iacovino, R.; Santini, A.; Saviano, M.; Kamphuis, J. *J. Pept. Sci.* **1997**, *3*, 110. (b) Moretto, V.; Formaggio, F.; Crisma, M.; Bonora, G. M.; Toniolo, C.; Benedetti, E.; Santini, A.; Saviano, M.; Di Blasio, B.; Pedone, C. *J. Pept. Sci.* **1996**, *2*, 14. (c) Gatos, M.; Formaggio, F.; Crisma, M.; Valle, G.; Toniolo, C.; Bonora, G. M.; Saviano, M.; Iacovino, R.; Menchise, V.; Galdiero, S.; Pedone, C.; Benedetti, E. *J. Pept. Sci.* **1997**, *3*, 367. (d) Saviano, M.; Iacovino, R.; Menchise, V.; Benedetti, E.; Bonora, G. M.; Gatos, M.; Graci, L.; Formaggio, F.; Crisma, M.; Toniolo, C. *Biopolymers* **2000**, *53*, 200. (e) Moretto, A.; Formaggio, F.; Crisma, M.; Toniolo, C.; Saviano, M.; Iacovino, R.; Vitala, R. M.; Benedetti, E. *J. Pept. Res.* **2001**, *57*, 307.
(210) (a) Bianco, A.; Bertolini, T.; Crisma, M.; Valle, G.; Toniolo, C.; Maggini, M.; Scorrano, G.; Prato, M. *J. Pept. Res.* **1997**, *50*, 159. (b) Rossi, P.; Felluga, F.; Tecilla, P.; Formaggio, F.; Crisma, M.; Toniolo, C.; Scrimin, P. *Biopolymers* **2000**, *55*, 496.
(211) (a) Rzeszotarska, B.; Karolak-Wojciechowska, J.; Broda, M. A.; Galdecki, Z.; Trezwinska, B.; Koziol, A. E. *Int. J. Pept. Protein Res.* **1994**, *44*, 313. (b) Pietrzynski, G.; Rzeszotarska, B.; Ciszak, E.; Losowski, M. *Pol. J. Chem.* **1994**, *68*, 1014.
(212) Pietrzynski, G.; Rzeszotarska, B.; Ciszak, E.; Lisowski, M.; Kubica, Z.; Boussard, G. *Int. J. Pept. Protein Res.* **1996**, *48*, 347.
(213) Broda, M. A.; Rzeszotarska, B.; Smelka, L.; Rospenk, M. *J. Pept. Res.* **1997**, *50*, 342.
(214) Lee, H.-J.; Ahn, I.-A.; Ro, S.; Choi, K.-H.; Choi, Y.-S.; Lee, K.-B. *J. Pept.. Res.* **2000**, *56*, 36.
(215) Torrini, I.; Nalli, M.; Paglialunga Paradisi, M.; Pagani Zecchini, G.; Lucente, G.; Spisani, S. *J. Pept. Res.* **2001**, *58*, 56.
(216) Chung, Y. J.; Huck, B. R.; Christianson, L. A.; Stanger, H. E.; Krauthäuser, S.; Powell, D. R.; Gellman, S. H. *J. Am. Chem. Soc.* **2000**, *122*, 3995.
(217) Christianson, L. A.; Lucero, M. J.; Appella, D. H.; Klein, D. A.; Gellman, S. H. *J. Comput. Chem.* **2000**, *21*, 763.
(218) Martinek, T. A.; Tóth, G. K.; Vass, E.; Hollósi, M.; Fülöp, F. *Angew. Chem., Int. Ed. Engl.* **2002**, *41*, 1718.
(219) Nafie, L. A.; Freedman, T. B. *Enantiomer* **1998**, *3*, 283.
(220) Dukor, R. K.; Nafie, L. A. In *Encyclopedia of Analytical Chemistry*; Meyers, R. A., Ed.; John Wiley & Sons: Chiscester, U.K., 2000; pp 1−15.
(221) Nafie, L. A. *Annu. Rev. Phys. Chem.* **1997**, *48*, 357.
(222) Nafie, L. A. *Appl. Spectrosc.* **1996**, *50*, 14A.
(223) Hug, W. In *Raman Spectroscopy*; Lascombe. J., Huong, P. V., Eds.; John Wiley & Sons: New York, 1982; pp 3−12.
(224) Nafie, L. A.; Cheng, J. C.; Stephens, P. J. *J. Am. Chem. Soc.* **1975**, *97*, 3842.
(225) (a) Keiderling, T. A. In *Circular Dichroism. Principles and Applications*; Berova, N., Nakanishi, K., Woody, R. W., Eds.; Wiley-VCH: New York, 2000; pp 621−666. (b) Hilario, J.; Kubelka, J.; Syud, A. F.; Gellman, S. H.; Keiderling, T. A. *Biopolymers* **2002**, *67*, 233. (c) Baello, B. I.; Pancoska, P.; Keiderling, T. A. *Anal. Biochem.* **1997**, *250*, 212.
(226) Yoder, G.; Polese, A.; Silva, R. A. G. D.; Formaggio, F.; Crisma, M.; Broxterman, Q. B.; Kamphuis, J.; Toniolo, C.; Keiderling, T. A. *J. Am. Chem. Soc.* **1997**, *119*, 10278.
(227) Dukor, R. K.; Keiderling, T. A. *Biopolymers* **1991**, *31*, 1747.
(228) Wyssbrod, H. R.; Diem, M. *Biopolymers* **1992**, *31*, 1237.
(229) Xie, P.; Zhou, Q.; Diem, M. *Faraday Discuss.* **1994**, *99*, 233.
(230) Lee, O.; Roberts, G. H.; Diem, M. *Biopolymers* **1989**, *28*, 1759.
(231) Ito, H. *Biospectroscopy* **1996**, *2*, 17.
(232) Baumruk, V.; Pancoska, P.; Keiderling, T. A. *J. Mol. Biol.* **1996**, *259*, 774.
(233) Barron, L. D.; Hecht, L. In *Circular Dichroism. Principles and Applications*; Berova, N., Nakanishi, K., Woody, R. W., Eds.; Wiley-VCH: New York, **2000**, pp 667−701.
(234) Smyth, E.; Syme, C. D.; Blanch, E. D.; Hecht, L.; Vašák, M.; Barron, L. D. *Biopolymers* **2001**, *58*, 138.
(235) Blanch, E. W.; Hecht, L.; Barron, L. D. *Protein Sci.* **1999**, *8*, 1362.
(236) (a) Donate, L. E.; Rufino, S. D.; Canard, L. H. J.; Blundell, T. L. *Protein Sci.* **1996**, *5*, 2600. (b) Geetha, V.; Munson, P. J. *Protein Sci.* **1997**, *6*, 2538.
(237) (a) Blanch, E. W.; Robinson, D. J.; Hecht, L.; Syme, C. D.; Nielsen, K.; Barron, L. D. *J. Gen. Virol.* **2002**, *83*, 241. (b) Blanch, E. W.; Hecht, L.; Syme, C. D.; Volpetti, V.; Lomonossoff, G. P.; Nielsen, K.; Barron, L. D. *J. Gen. Virol.* **2002**, *83*, 2593. (c) Blanch, E. W.; Hecht, L.; Day, L. A.; Pederson, D. M.; Barron, L. D. *J. Am. Chem. Soc.* **2001**, *123*, 4863.
(238) (a) Barron, L. D.; Blanch, E. W.; Hecht, L. *Adv. Protein Chem.* **2002**, *62*, 51. (b) Syme, C. D.; Blanch, E. W.; Holt, C.; Jakes, R.; Goedert, M.; Hecht, L.; Barron, L. D. *Eur. J. Biochem.* **2002**, *269*, 148.
(239) Blanch, E. W.; Morozova-Roche, L. A.; Cochran, D. A. E.; Doig, A. J.; Hecht, L.; Barron, L. D. *J. Mol. Biol.* **2000**, *301*, 553.
(240) Miyazawa, M.; Inouye, K.; Hayakawa, T.; Kyogoku, Y.; Sugeta, H. *Appl. Spectrosc.* **1996**, *50*, 644.
(241) Zhao, C. X.; Polavarapu, P. L.; Das, C.; Balaram, P. *J. Am. Chem. Soc.* **2000**, *122*, 8228.
(242) Zuk, W. M.; Freedman, T. B.; Nafie, L. A. *Biopolymers* **1989**, *28*, 2025.
(243) Xie, P.; Zhou, Q.; Diem, M. *J. Am. Chem. Soc.* **1995**, *117*, 9502.
(244) (a) Ludlam, C. F. C.; Sonar, S.; Lee, C. P.; Coleman, M.; Herzfeld, J.; Rajbhanary, U. L.; Rothschild, K. J. *Biochemistry* **1995**, *34*, 2. (b) Ludman, C. F. C.; Arkin, I. T.; Liu, X.; Rothman, M. S.; Rath. P.; Aimoto, S. O.; Engelman, D. M.; Rothschild, K. J. *Biophys. J.* **1996**, *70*, 1728.
(245) Zscherp, C.; Barth, A. *Biochemistry* **2001**, *40*, 1875.

(246) Cepus, V.; Ulbrich, C.; Allin, C.; Trouiller, A.; Gerwert, K. *Methods Enzymol.* **1998**, *291*, 223.
(247) Jongh, H. H. J.; Goormaghtigh, E.; Ruysschaert, J.-M. *Biochemistry* **1997**, *36*, 13603.
(248) Hamm, P.; Lim, M.; DeGrado W. F.; Hochstrasser, R. M. *Proc. Natl. Acad. Sci. U.S.A.* **1999**, *96*, 2036.
(249) Noda, I. *J. Am. Chem. Soc.* **1989**, *111*, 8116.
(250) Szabó, Z.; Klement, É.; Jost, K.; Zarándi, M.; Soós, K.; Penke, B. *Biochem. Biophys. Res. Commun.* **1999**, *120*, 885.
(251) Murayama, K.; Ozaki, Y. *Biopolymers.* **2002**, *67*, 394.
(252) Fabian, H.; Mantsch, H. H.; Schultz, C. P. *Proc. Natl. Acad. Sci. U.S.A.* **1999**, *96*, 13153.
(253) Fringeli, U. P. *Chimia* **1992**, *46*, 200.
(254) Goormaghtigh, E.; Raussens, V.; Ruysschaert, J. M. *Biochim. Biophys. Acta* **1999**, *1422*, 105.
(255) Tamm, L.; Tatulian, S. A. *Biochemistry* **1993**, *32*, 7720.
(256) Smith, S. O.; Jonas, R.; Braiman, M. *Biochemistry* **1994**, *33*, 6334.
(257) Nabet, A.; Boggs, J.; Pézolet, M. *Biochemistry* **1994**, *33*, 14792.
(258) Dluhy, R. A.; Stephens, S. M.; Widayati, S.; Williams, A. D. *Spectrochim. Acta, Part A* **1995**, *51*, 1413.
(259) Flach, C. R.; Brauner, J. W.; Taylor, J. W.; Baldwin, R. C.; Mendelsohn, R. *Biophys. J.* **1994**, *67*, 402.
(260) Cornut, I.; Desbat, B.; Turlet, J. M.; Dufourcq, J. *Biophys. J.* **1996**, *70*, 305.

CR000100N